Démographie des espèces animales sociales

Lorena Mansilla

THÈSE POUR OBTENIR LE GRADE DE DOCTEUR DE L'UNIVERSITÉ DE MONTPELLIER

En Biostatistique

École doctorale Information, Structures et Systèmes

Unité de recherche Centre d'Écologie Fonctionnelle et Évolutive

Démographie des espèces animales sociales

Présentée par Lorena MANSILLA
Le 25 novembre 2019

Sous la direction de Roger PRADEL
et Olivier GIMENEZ

Devant le jury composé de

Jean-Noël Bacro, Institut Montpelliérain Alexandre Grothendieck, Montpellier	Président du jury
Emmanuelle Cam, Laboratoire des Sciences de l'Environnement Marin, Brest	Rapportrice
Rachel McCrea, School of Mathematics, Statistics and Actuarial Science, University of Kent, Canterbury (Angleterre)	Rapportrice
Marie Nevoux, Écologie et Santé des Écosystèmes, Rennes	Examinatrice
Roger Pradel, Centre d'Écologie Fonctionnelle et Évolutive, Montpellier	Directeur de thèse
Olivier Gimenez, Centre d'Écologie Fonctionnelle et Évolutive, Montpellier	Co-directeur de thèse

UNIVERSITÉ DE MONTPELLIER

Agradecimientos

Mis agradecimientos a R. Pradel y O. Giménez por ser los directores de esta tesis, a quienes nos prestaron los datos y colaboraron con nosotros para el desarrollo de los diferentes capítulos de esta tesis y que son autores y coautores de los artículos que lo componen. También agradezco a CONICYT (PFCHA 2016) por el financiamiento que me permitió realizar mi tesis, a mi familia por el apoyo durante estos tres años. Y por último, gracias a mi D' amado, *HaKadosh Baruj Hu* que hace posible todo.

Remerciements

Mes remerciements à R. Pradel et O. Gimenez pour être les directeurs de cette thèse, à ceux qui nous ont prêté les données et collaboré avec nous pour le développement des différents chapitres de cette thèse et qui sont auteurs et co-auteurs des articles qui la composent. Mes remerciements aussi à CONICYT (PFCHA 2016) pour le financement pour développer ma thèse, à ma famille pour le soutien pendant ces trois années. Et enfin merci à mon D' bien aimé *HaKadosh Baruj Hu* qui rend tout possible.

Résumé

Cette thèse est centrée sur l'étude de la dynamique des populations animales, avec comme principal objectif d'inclure des aspects de socialité dans les modèles démographiques. On qualifie des animaux de sociaux lorsque des individus s'associent à d'autres individus de la même espèce pas exclusivement pour se reproduire. Certains aspects de la socialité sont importants au cours des différentes étapes de la vie d'un individu, par exemple des événements de toilettage, d'agressivité, d'allaitement, etc. et d'autres aspects jouent à l'échelle de la population, comme le nombre et la taille des groupes par exemple pour le cas des animaux avec structure hiérarchique, le nombre de petits et la taille des harems, ou encore le temps d'association pour les cas des agrégations d'animaux. Dans cette thèse, j'étudie les composantes de la socialité et ses effets sur la dynamique des populations à travers, entre autres, des modèles de capture-recapture (CR) qui permettent d'estimer les principaux paramètres démographiques en conditions naturelles. On s'intéresse à trois espèces avec des structures sociales différentes. Pour une première espèce, le loup (*Canis lupus*), on développe une approche pour estimer la taille et le nombre de meutes grâce à une combinaison de modèles de capture-recapture spatialement explicites et de méthodes de hiérarchisation. Pour une deuxième espèce, l'éléphant de mer du sud (*Mirounga leonina*), on analyse l'influence de la structure sociale sur la dynamique des populations dans un cadre de modélisation intégrée. Sur un troisième cas d'étude, le dauphin de Commerson (*Cephalorhynchus commersonii*), nous modélisons le réseau social des animaux et estimons les principales caractéristiques de ce réseau (e.g., degré, centralité) grâce à une formulation à espace d'état des modèles de CR. Globalement, mes travaux illustrent le potentiel des méthodes modernes de dynamique des populations pour l'étude de la démographie des espèces sociales en conditions naturelles.

Mots-clés: Ecologie statistique, dynamique des populations, démographie, modèle de capture-recapture, socialité, structure social.

Abstract

This thesis focuses on the study of social animal populations, with the main objective of including aspects of sociality in demographic models. Animals are termed social when individuals associate with other individuals of the same species not exclusively for reproduction. Some aspects of sociality are important in the different events of an individual's life, such as grooming, aggression, breastfeeding, etc. and other aspects at the population level, such as the number and size of groups, for example, in the case of animals with hierarchical structure, the number of cubs and the size of the harems, or the duration of association for cases of aggregations of animals. In this thesis, I study the components of sociality and its effects on population dynamics through capture-recapture (CR) models, which make it possible to estimate the main demographic parameters under natural conditions. We are interested in three species with different social structures. For a first species, the wolf (*Canis lupus*), an approach is developed to estimate the size and number of packs through a combination of spatially explicit capture-recapture models and hierarchical methods. For a second species, the Southern elephant seal (*Mirounga leonina*), we analyze the influence of the social structure on population dynamics in an integrated modeling framework. On a third case study, the Commerson's dolphin (*Cephalorhynchus commersonii*), we model the social network of animals and estimate the main characteristics of this network (e.g., degree, centrality) thanks to a state space formulation of CR models. Overall, my work illustrates the potential of modern population dynamics methods for studying the demography of social species under natural conditions.

Keywords: Statistical ecology, population dynamics, demography, capture-recapture model, sociality, social structure.

Contents

Chapter 1: Introduction

1.1 Qu'est-ce qu'un animal social?

Un animal social est an animal membre d'une société. Ces animaux sont liés à des individus de la même espèce de façon coopérative pendant tout ou partie de sa vie.
Tout comme les principales caractéristiques des systèmes vivants, le comportement coopératif est une propriété émergente (Wilson 1998). La société est formée par des unités fonctionnelles elles-mêmes formées par des membres de cette société en colonies, conglomérats, groupes ou harems. On trouve dans la littérature différentes terminologies liées à un système social, comme l'organisation sociale, la structure sociale et l'accouplement social, considérées comme des composants de ce système (e.g. Kappeler & van Schaik, 2002). Dans d'autres cas, et par simplicité, ces concepts sont présentés sans aucune distinction (e.g. Whitehead 2008).

1.2 Pourquoi est-il nécessaire de considérer la socialité en démographie?

Ignorer l'information sur le comportement animal dans les études de démographie des populations peut causer des erreurs dans les résultats et les prédictions, et mener à des politiques de gestion inadaptées pour la conservation. Nous allons voir en détail comment.
Le comportement des membres d'une société détermine les caractéristiques de la structure sociale, par exemple la taille des groupes, la cohésion, la perméabilité, la différenciation des rôles, le flux d'information, ou encore la fraction de temps consacré au comportement social (Wilson 1998).
Le comportement social, par exemple, est un élément critique qui doit être pris en compte dans les modèles de dynamique des populations d'espèces à structure sociale car il peut affecter la survie et la reproduction (Zeigler & Walters 2014).
Les fortes associations entre épaulards (*Orcinus orca*) à l'île de Crozet leur permet d'améliorer leurs performances individuelles (valeur sélective ou "fitness" en anglais), via l'augmentation du succès de la recherche de nourriture et la résilience face à des événements de mortalité par les activités humaines (Busson et al. 2019).
Des études ont montré que le risque d'extinction pour des espèce sociales comme le loup gris (*Canis lupus*), le chien sauvage africain (*Lycaon pictus*) et le pic à queue rouge (*Picoides borealis*) est corrélé négativement au nombre de groupes sociaux dans la population (Vucetich et al. 1997, Walters et al. 2002, Somers et al. 2008, cité par Zeigler et Walters 2014).
Incorporer les aspects de socialité en démographie permet d'améliorer la compréhension et les estimations des patrons de risque d'extinction, par exemple, à travers l'analyse de viabilité de population lié au comportement de sélection d'habitat (González-Suárez & Gerber 2008), et d'identifier des comportements signes d'une population en déclin (Gerber 2006). Cela permet aussi de prévoir de façon plus réaliste le devenir des populations en prenant en compte dans les taux démographiques des événements liés à la stochasticité démographique ou environnementale. On citera comme exemple le loup qui produit un faible nombre de petits par an, et sur lequel donc la stochasticité peut restreindre le nombre d'individus reproducteurs et augmenter le taux de

risque d'extinction (cité par Vucetich et al. 1997). Un autre exemple est la hyène tachetée: pour cette espèce, la probabilité de contagion d'un agent pathogène et de guérison des individus sont fortement dépendantes de la structure sociale hiérarchique (Benhaiem et al. 2018), et le statut social des individus permet d'expliquer la variation de ces paramètres clés (Marescot et al. 2018). Wiliams & Lusseau (2006) signalent l'importance de modéliser l'hétérogénéité des individus des épaulards pour pouvoir prendre des décisions de gestion en conformité avec l'organisation et les besoins des agrégations, et également de la nécessité de considérer les effets de la probabilité de recapture différente entre individus sur l'identification des liens sociaux.

1.3 La difficulté de lier la socialité à la démographie

Prendre en compte les aspects du comportement dans les modèles démographiques n'est pas trivial. Les études démographiques sur les espèces sociales sont relativement rares, alors que ces espèces sont fréquentes. Cela est dû principalement à la difficulté sur le terrain d'observer le comportement des animaux et à accumuler des données sur un temps relativement long pour pouvoir étudier la démographie (Caro 1998). Cette difficulté est directement en lien avec le problème de détectabilité imparfaite, autrement dit l'impossibilité de voir ou capturer avec certitude les individus d'une population (et a fortiori leur comportement) à tout moment (Gimenez et al. 2008). Ce problème d'une probabilité de détection inférieure à 1 constitue la principale motivation qui a mené aux développements méthodologiques proposés dans ma thèse.
En outre, les animaux ne se comportent pas tous de la même façon dans une population. Alors, comme l'écrit González-Suárez (2014), il convient de déterminer dans quelles situations on devrait prendre en compte les variations individuelles car il est crucial de comprendre comment les différentes composantes du comportement affectent les taux vitaux que sont la survie et la reproduction. En résumé, il est difficile de faire se parler dynamique des populations et écologie du comportement. Or ce lien est vital pour déterminer le statut de conservation des espèces sociales. Dans sa revue des études liant biologie de la conservation et comportement des animaux, Sutherland (1998) note que les journaux d'écologie du comportement incluaient peu ou pas les thèmes de la biologie de la conservation, et vice-versa.

1.4 Objectifs de thèse

Les objectives de cette thèse sont les trois suivants: i) estimer le nombre de meutes dans des populations de loups avec des modèles de capture-recapture spatialement explicites et des méthodes de partitionnement; ii) estimer les paramètres démographiques des espèces sociales. Étude de cas sur les éléphants de mer; ii) décrire et quantifier les réseaux sociaux animaux quand la détectabilité est imparfaite.
Chacun d'eux est développé dans les trois chapitres ci-dessous, avec formats d'articles. Ci-dessous je définis les structures sociales des populations que j'ai étudié, quelques aspects généraux de ces populations, et les modèles qui ont été utilisés tout au long de l'élaboration des mes trois objectifs.

1.5 Différentes structures sociales pour différentes espèces animales

Nous donnons ici les définitions des structures sociales abordées dans cette thèse (source : Wilson 1998).

Groupes: un ensemble d'organismes appartenant à la même espèce qui restent ensemble durant certaines périodes de temps tandis qu'ils interagissent les uns avec les autres à un plus haut degré qu'avec d'autres conspécifiques. Le vocable groupe est utilisé pour se référer à une agrégation, à un type de société ou à un sous-ensemble d'une société. Il est utilisé spécialement dans les descriptions de certaines sociétés de primates dans lesquelles il existe un niveau d'organisation hiérarchique construit par des sous-ensembles d'individus appartenant à la même grande et unique congrégation.

Harem: un groupe de femelles gardées par un mâle qui empêche les autres mâles de s'accoupler avec elles.

Agrégation: un groupe d'individus de la même espèce, formé par un peu plus qu'une paire ou une famille, réunis dans le même endroit; cette structure n'a toutefois pas une organisation interne ou un comportement coopératif. Cette structure peut fournir une protection pour ses membres.

1.6 Les espèces dans nos études de cas

Loups

Socialité et territorialité: Les loups (*Canis lupus*) sont des animaux sociaux qui vivent en meutes avec une structure sociale hiérarchique, formées par un couple reproductif dominant dit alpha, et des individus qui restent dans l'état non reproducteur, qui sont généralement la progéniture de l'année du couple alpha (Mech & Boitani, 2003). Lorsque les juvéniles atteignent la maturité sexuelle, entre un et trois ans, ils dispersent et quittent la meute pour former d'autres meutes (Mech & Boitani, 2003). La taille de meute est généralement de cinq à six chiots (Mech, 1970). Le territoire et le domaine vital d'une meute de loups sont les mêmes. Puisque le territoire est le domaine vital défendu (Mech & Boitani, 2003).

Nourriture: Ils sont carnivores, et se nourrissent principalement d'ongulés en Europe (Mech & Boitani, 2003).

Distribution: L'espèce s'étend dans l'hémisphère nord, sur le continent européen, américain et asiatique.

Densité et population: Caniglia et al. (2012) signale une taille moyenne de population entre 117 et 233 par les années entre 2003 et 2007 respectivement. Cette population a une tendance constant de augmente à excepté 2003 et 2008.

Apollonio et al. (2004) ont étudié des cas locaux, avec 3 à 5 groupes, ils ont décrit une moyenne de taille de groupes de 4.2 ± 0.9 loups. Aussi ils ont estimé une densité général pour le domaine de 4.7 individus par 100 km^2 avec une distance moyenne de groupes adyacents de 11.1 km, sur données du nord des Apennins dans la péninsule italique, entre les anneés 1993 à 2000.

Éléphants de mer
Socialité et territorialité: Les éléphants de mer (*Mirounga leonina*) sont les plus grands pinnipèdes et ont un dimorphisme sexuel significatif (Oosthuizen et al. 2019), les mâles adultes ont entre 3000 à 4000 kg, tandis que des femelles adultes ont entre 400 à 900 kg (Laws, 1953). Ils se rassemblent sur terre en des harems pendant la saison de reproduction (Oosthuizen et al. 2019). Les femelles ont un petit par an. Le mâle dominant arrive avant les femelles pour protéger son territoire.
Nourriture: Leurs proies principales sont les céphalopodes (Daneri et al, 2000, Hindell et al. 2003) et les poissons (Daneri et Carlini, 2002).
Distribution: Ils ont une distribution circumpolaire antarctique (Le Boeuf & Laws 1994).
Population: La population des éléphants de mer de l'Ile Marion a diminué de 83% entre 1951 et 1994 (Laws, 1994), point à partir de quelle la population reste relativement stable (Pistorius et al. 2011), aujourd'hui environ 550 femelles reproductrices (Oosthuizen et al. 2019). Ils sont aujourd'hui catalogués comme une espèce en état global stable (UICN, 2014).

Dauphins de Commerson (*Cephalorhynchus commersonii*)
Socialité et territorialité: Les individus sont sociaux et sont rassemblés en agrégations.
Distribution: Il y a des observations de dauphins de Commerson (Cephalorhynchus commersonii) dans les océans de l'hémisphère sud, près des côtes d'Amérique du Sud, les Iles Falkland, et Austral à la Péninsule Antarctique, le Détroit de Magellan, la Terre de Feu, et l'océan Indien du sud (Goodall et al. 1988).
Populations: Des publications ont documenté des observations de groupes de 20 à 100 individus (Goodall et al. 1988, Iñíguez & Tossenberger, 2010). Ils sont catalogués comme une espèce en état global non connu (UICN 2017)

1.7 Probabilité conditionnelle et règle de Bayes

On part de l'idée que l'on a des quantités connues, les données D, et des quantités inconnues qui dans cette thèse correspondront à des paramètres, θ. Les deux quantités, D et θ sont liées à partir d'une distribution de probabilité conditionnelle:

$$p(D|\theta) = p(D, \theta)/p(D),$$

nous multiplions les deux côté par $p(D)$, nous arrivons à $p(D|\theta) \cdot p(D) = p(D, \theta)$. Nous faisons la même procédure par $p(\theta|D)$, et nous écrions la égalité

$$p(D|\theta) \cdot p(D) = p(\theta|D) \cdot p(\theta)$$

nous divisons les deux côtés par $p(D)$ et obtenons

$$p(\theta|D) = \frac{p(\theta) \cdot p(D|\theta)}{p(D)}$$

où $p(D|\theta)$ est la vraisemblance $L(\theta|D)$, et $p(D) = \int_\theta p(D) \cdot L(\theta|D)d\theta$ qui ne dépend pas de θ.

Ainsi on peut écrire la fonction de distribution a posteriori comme:

$$\pi(\theta, D) \propto p(\theta) \cdot L(\theta|D) \tag{1.1}$$

qui est la règle de Bayes. Cette expression traduite en mots dit que:

Probabilité a posteriori des paramètres $\propto$ probabilité a priori des paramètres $\cdot$ vraisemblance de θ sachant les données D (Kruschke, 2010).

1.8 Modèle hiérarchique de probabilité

Dans l'équation au-dessus, on a le cas particulier d'une seule information à priori à propos des données. S'il y a plus d'information à considérer, on a un ensemble de paramètres de dimension r, $\boldsymbol{\theta} = (\theta_1, \theta_2, ..., \theta_r)$ avec une densité a priori $p(\boldsymbol{\theta})$ et les observations $\boldsymbol{x}$ qui ont une densité $p(\boldsymbol{x}|\boldsymbol{\theta})$. Les paramètres $\boldsymbol{\theta}$ sont déterminés par d'autres paramètres, η qu'on appelle *hyperparamètres*. Ceux-ci peuvent être connus ou inconnus. Lorsque ces paramètres ne sont pas connus, ils ont eux-mêmes une distribution a priori *hyperpriori* $p(\eta)$, et dans ce cas on parle de *prior hiérarchique*.

1.9 Des modèles structurés de population

Dans cette thèse, on a fait appel à trois types de modèles structurés de population pour analyser les données de capture-recapture : un modèle à espace d'état pour les dauphins, un modèle à espace d'état pour les loups et un modèle intégré de population dont la composante capture-recapture est un modèle de Markov caché pour les éléphants de mer.

1.9.1 Le modèle de Capture-Recapture spatialement explicite

Notre base de données de capture-recapture sur lequelle nous avons appliqué le modèle SECR, corresponde à registres de individus de une population de loups italiens qui ont été reconnus par ADN prélevé sur crottes, poils (voir Caniglia et al. 2014 pour plus détailles).

Un modèle de capture recapture peut être vu comme un modèle hiérarchique de probabilité. Capture-recapture est un terme générique qui fait référence à certains protocoles de surveillance des animaux dans la vie sauvage y compris des pièges et marquage des animaux pour les identifier. Il s'agit en général des données dont l'analyse permet d'estimer la survie, la dispersion et l'abondance avec une probabilité inférieure de détection à un (Gimenez et al. 2012). La méthode de capture-recapture spatialement explicite (SECR en anglais pour "spatially-explicit capture-recapture") considére la position géographique de l'individu échantillonné, rendant possible l'estimation du centre des domaines vitaux des animaux, ou centres d'activité. Nous avons utilisé les SECR pour l'étude des loups et de leur structure sociale.
La structure du modèle SECR considère les composantes suivantes:
- un ensemble d'individus indexés par $i = \{1, 2, ..., n\}$,
- K occasions de capture,
- un ensemble de pièges indexées par $j = \{1, 2, ..., J\}$,

- un tableau $\mathbf{S}_{i,latitude,longitude}$ qui contient les positions des individus échantillonnés,
- un tableau $\mathbf{X}_{i,j,1:2}$ de dimension $n \times J \times 2$ des positions des pièges, c'est-à-dire, une matrice pour les coordonnées,
- une matrice des distances $\mathbf{D}_{i,t} = \{d_{i,j}\}$, où $d_{i,j}$ est la distance euclidienne entre les pièges et les positions des individus échantillonnés,
- une variable aléatoire latente Z_i de présence et absence de l'individu dans le domaine d'étude,
- des distributions des paramètres à priori non informatives,
- l'équation du modèle d'observation de l'individu i par le piège j, $Y_{i,j}$ qui dépend des éléments décrits au-dessus.

Dans notre cas, notre base des données ne provient pas de pièges, nous avons ajouté des pièges fictifs pour pouvoir applique le modèle SECR.

1.9.2 Modèle à espace d'état

Les modèles à espace d'état (SSM pour "state-space models" en anglais) sont composés de deux séries temporelles qui évoluent en parallèle : d'un côté une série capture la dynamique des vrais états (latents) et de l'autre une série correspond à des observations qui sont faites à partir des états sous-jacents et éventuellement inconnus (Gimenez et al. 2012). Nous avons utilisé un SSM pour les dauphins et l'étude d'une population fermée structurée en dyades.

Nous décrivons l'architecture des SSM à partir de l'article de Buckland et al. (2003).

- Un processus d'état $\mathbf{n}_t$, avec $t = 0, 1, ..., T$ est un vecteur non observable.
- Le processus d'observation $\mathbf{y}_t$, avec $t = 1, ..., T$ est un vecteur observable complètement, fonction du processus d'état.
- Soient g et f des functions de densité (ou masse) de probabilité $\mathbf{n}_t$ et $\mathbf{y}_t$ respectivement, la structure d'un SSM peut être décrite en considérant les composantes suivantes:
- la distribution d'état initial $g_0(\mathbf{n}_0; \Theta)$, la distribution du processus d'état $g_t(\mathbf{n}_t|\mathbf{n}_{t-1}; \Theta)$, associée à une matrice de transition des états, où l'état actuel est dépendant de l'état précédent (dans notre cas c'est un processus Markovien de premier ordre), la distribution du processus d'observation $f_t(\mathbf{y}_t|\mathbf{n}_t; \Theta)$, fonction de l'état actuel, où $t = 1, ..., T$ et Θ est le vector de paramètres.

1.9.3 Modèle de Markov caché

Les modèles de Markov cachés (HMM pour "hidden Markov models" en anglais) sont un cas particulier de SSM dans lequel les états sont Markoviens, i.e. l'état suivant (futur) dépend uniquement de l'état immédiatement précédent (présent) (Gimenez et al. 2012). Nous avons utilisé les HMM dans le cas des éléphants de mer pour représenter un cycle de vie relativement complexe.

Selon Rabiner (1989) nous pouvons reconnaître 5 composantes dans les HMM :

- un ensemble $S = \{S_1, S_2, \ldots, S_N\}$, des N états (cachés), nous appelons q_t l'état au temps t, - un ensemble $V = \{v_1, v_2, \ldots, v_M\}$, des M différents observables,
- une matrice des distributions de probabilité de transition entre états, $A = \{a_{ij}\}$, où $a_{ij} = P(q_{t+1} = S_j|q_t = S_i)$ est la probabilité d'être dans l'état q_{t+1} quand nous sommes dans l'état q_t au temps t, avec $1 \leq i, j \leq N$, $\sum_{j=1}^{N} a_{ij} = 1$ et $a_{ij} \geq 0$,

- un ensemble des distributions de probabilité des observables pour chaque état $B = \{b_j(v_k)\}$, où $b_j(k)$, est la probabilité d'observation de v_k quand l'état est q: $b_j(k) = P(v_{kt}|q_t = S_j)$, $\forall j \in \{1, 2, \ldots, N\}$, $\forall k \in \{1, 2, \ldots, M\}$,
- la distribution des états initiaux $\pi = \{\pi_i\}$, où π_i est la probabilité que le modèle soit dans l'état S_i au temps initial $t = 0$, avec $\pi_i = P(q_1 = S_i)$, $\forall i \in \{1, 2, \ldots, N\}$.

Ces trois familles de modèles (SECR, SSM et HMM) permettent l'analyse des données de capture-recapture.
Comme nous le verrons plus tard dans le développement des chapitres, il existe des différences entre ces modèles qui permettent une grande flexibilité dans la modélisation des processus biologiques. Pour le cas des loups par exemple, nous sommes interessés à estimer le nombre de groupes présents dans le domaine d'étude, sans inclure la dimension temporelle, contrairement aux autres modèles utilisés dans lesquels les transitions des états sont considérés. Dans le modèle HMM nous considérons des transitions entre des états (partiellement) cachés, et chaque état futur dépend nécessairement de son état actuel, par exemple, la probabilité qu'une femelle d'éléphant de mer, en état de procréer, reste reproductrice d'une année sur l'autre dépend de son état reproducteur l'année courante et non du fait qu'elle était reproductrice l'année précédente.

1.10 Méthodes de Monte Carlo par chaînes de Markov et algorithme de Gibbs

Nous cherchons, à partir des données $\boldsymbol{x}$, à inférer la distribution a posteriori des paramètres du modèle en générant des échantillons simulés et en inférant les paramètres de la population, à partir de la règle de Bayes (voir au-dessus).
JAGS est un programme informatique qui implémente des méthodes de Monte Carlo (pour l'intégration) par chaînes de Markov (MCMC), et l'algorithme de Gibbs en particulier. Nous suivons King et al. (2010) et Lee (2012) pour présenter ces méthodes.

1.10.1 L'intégration Monte Carlo

Il s'agit d'une méthode d'intégration numérique pour estimer un paramètre θ qui est l'espérance d'une fonction ψ. Si les observations $\boldsymbol{x}$ sont données, on a:

$$\mathbb{E}_\pi[\psi(\theta)] = \int \psi(\theta)\pi(\theta|\boldsymbol{x})d\theta$$

et nous utilisons la technique de simulation Monte Carlo. Nous calculons l'intégrale en la variable d'intérêt. Nous disons, pour les observations $\theta^{(1)}, ..., \theta^{(n)} \sim \pi(\theta|\boldsymbol{x})$, que l'espérance de la fonction ψ évalué en θ est défini par l'intégrale

$$\mathbb{E}_\pi[\psi(\theta)] = \int \psi(\theta)\pi(\theta|\boldsymbol{x})d\boldsymbol{x}$$

que nous pouvons approcher par
$\overline{\psi}_n = \frac{1}{n}\sum_{i=1}^{n} \psi(\theta^{(i)})$.

En d'autres termes, nous tirons des échantillons $\theta^1, ..., \theta^T$ dans la distribution à posteriori, puis nous calculons la moyenne de l'échantillon. Si les échantillons sont indépendants, par la Loi des Grands Nombres, $\overline{\psi}_n \to \mathbb{E}_\pi[\psi(\theta)]$ quand $n \to \infty$.

1.10.2 Chaîne de Markov

Une chaîne de Markov du premier ordre est une séquence de variables aléatoires $\theta^{(0)}, \theta^{(1)}, ..., \theta^{(n)}$, où la valeur de $\theta^{(0)}$ vient d'une distribution initiale arbitraire. Simuler une chaîne de Markov consiste à générer un nouvel état de la chaîne $\theta^{(k+1)}$ avec distribution de densité de noyau de transition $\mathcal{K}$ pour la chaîne et qui dépend seulement de $\theta^{(k)}$:

$$\theta^{(k+1)} \sim \mathcal{K}(\theta^{(k)}, \theta)(\equiv \mathcal{K}(\theta|\theta^{(k)})).$$

En supposant que nous avons une chaîne de Markov avec distribution stationnaire $\pi(\theta) \equiv \pi(\theta|\boldsymbol{x})$, le théorème ergodique des états nous donne que, si les échantillons sont indépendants, $\overline{\psi}_n \to \mathbb{E}_\pi[\psi(\theta)]$, quand $n \to \infty$.

1.10.3 L'échantillonneur de Gibbs

L'échantillonneur de Gibbs travaille à partir de l'ensemble complet des distributions conditionnelles de π, pour échantillonner indirectement depuis les distributions marginales. Nous supposons qu'il y a r paramètres $\boldsymbol{\theta} = (\theta_1, \theta_2, ..., \theta_p) \in \mathbb{R}^p$ avec distribution de probabilité $\pi(\boldsymbol{\theta})$, notons $\pi(\theta_i|\boldsymbol{\theta}_{(i)})$ la distribution contionnelle complète induite de θ_i étant donné les valeurs des autres composantes $\boldsymbol{\theta}_{(i)} = (\theta_1, ..., \theta_{i-1}, \theta_{t+1}, ..., \theta_r)$, $i = 1, ..., r$, $1 < r \leq p$. Alors, étant donné l'état de la chaîne de Markov à l'itération k, $\boldsymbol{\theta}^k = (\theta_1^{(k)}, \theta_2^{(k)}, ..., \theta_p^{(k)})$, l'échantillonneur de Gibbs effectue successivement les tirages aléatoires à partir de la distribution conditionnelle postérieure complète comme suit:

$\theta_1^{(k+1)}$ est échantillonné depuis $\pi(\theta_1^{k+1}|\boldsymbol{\theta}_{\mathbf{(1)}}^{\boldsymbol{(k)}}, \boldsymbol{x})$;
$\theta_2^{(k+1)}$ est échantillonné depuis $\pi(\theta_2|\theta_1^{(k+1)}, \theta_3^{(k)}, ..., \theta_r^{(k)}, \boldsymbol{x})$;
$\vdots$
$\theta_i^{(k+1)}$ est échantillonné depuis $\pi(\theta_i|\theta_1^{(k+1)}, ..., \theta_{i-1}^{(k)}, ..., \theta_{i+1}^{(k+1)}, ..., \theta_r^k, \boldsymbol{x})$;
$\vdots$
$\theta_p^{(k+1)}$ est échantillonné depuis $\pi(\theta_r^{k+1}|\boldsymbol{\theta}_{(r)}^{(k+1)}, \mathbf{x})$.

Cela complète la transition à partir de $\boldsymbol{\theta}^{(k)}$ jusque $\boldsymbol{\theta}^{(k+1)}$, et la probabilité de cette transition est donnée par:
$\mathcal{K}_G\big(\boldsymbol{\theta}^{\boldsymbol{(k)}}, \boldsymbol{\theta}^{\boldsymbol{(k+1)}}\big) = \prod_{l=1}^r \pi(\theta_l^{k+1}|\theta_j^{k+1}), \quad j < l \quad \text{et} \quad \theta_j^{(k)}, \quad j > l$
avec comme distribution stationnaire π.
Plus on d'échantillons, plus les valeurs estimées des paramètres sont proches des vraies valeurs des paramètres.

Chapter 2: OBJECTIF 1

Estimer le nombre de meutes dans des populations de loups avec des modèles de capture-recapture spatialement explicites et des méthodes de partitionnement

.

2.1 ARTICLE 1. Estimating the number of packs in wolf populations using spatially-explicit capture-recapture models and "clustering" methods

Résumé

Pour la gestion et la conservation des animaux qui passent la plupart de leur vie en groupes, il est important de pouvoir caractériser la population en termes liés à la socialité comme le nombre et la taille de groupes. Toutefois, cette caractérisation est souvent difficile à faire en conditions naturelles car les animaux ne sont pas observables de manière exhaustive à tout moment – on parle d'une détectabilité imparfaite.

Ici, on propose une approche en deux temps dans laquelle i) on utilise un modèle de capture-recapture spatialement explicite (SECR) pour estimer où sont les centres d'activité de chaque individu en tenant compte de la détectabilité imparfaite, et ii) on applique la méthode de partitionnement de Ward pour identifier le nombre et la taille des groupes. Nous présentons une étude de simulation pour valider la méthode, ainsi qu'un cas d'étude sur une population de loups italiens (*Canis lupus*) comme cas d'étude pour illustrer l'approche.

Notre travail montre comment obtenir de l'information sur la socialité des animaux à partir de données imparfaites en combinant deux méthodes bien connues des écologues.

Mots-clés: Espèces sociales, socialité, SECR, partitionnement de Ward.

Estimating the number of packs in wolf populations using spatially-explicit capture-recapture models and clustering methods

Lorena Mansilla[1], Roger Pradel[1], Romolo Caniglia[2], and Olivier Gimenez[1]

[1]*CEFE, CNRS, University of Montpellier, University Paul Valéry Montpellier 3, EPHE, IRD, Montpellier, France*

[2]*Department of Biology, Geology and Environmental Sciences, University of Bologna, Via Selmi 3, 40126 Bologna, Italy*

Abstract.− For the management and conservation of animals that spend most of their lives in groups, it is important to be able to characterize the population in terms of sociality such as the number and size of groups. However, this characterization is often difficult to do in natural conditions because the animals are not observable exhaustively at any time - we speak of imperfect detectability. Here, a two-step approach is proposed in which i) a spatially explicit capture-recapture model (SECR) is used to estimate where each individual's activity centers are, taking into account imperfect detectability, and ii) clustering methods are used to identify the number and size of groups. We present a simulation study to validate the method, as well as a case study on a population of Italian wolves (*Canis lupus*) as a case study to illustrate the approach.

Our work shows how to obtain information on animal sociality from imperfect data by combining two methods well known to ecologists.

Key words.− Social species, sociality, SECR, Ward and K−mean clustering methods.

1 Introduction

Estimating animal population density is a key step in providing sound conservation and management strategies for wildlife (Williams et al. 2002). For many large carnivores however, estimating density is difficult because these species tend to be elusive and wide-ranging, resulting in low detection rates.

To deal with these issues, non-invasive techniques, such as camera trapping and DNA sampling, are increasingly used. These non-invasive techniques generate data that can be analyzed with capture-recapture

methods to estimate densities (Royle et al. 2014). Spatial capture-recapture (SCR; Royle et al. 2014) models explicitly incorporate spatial locations of detections, therefore accounting for individual heterogeneity on the detection due to spatial variation in the distance of home ranges to the traps. Examples of the use of SCR methods and non-invasive methods for large carnivores include, without pretending to exhastivity, mountain lions (Russell et al. 2012), Grizzly bears (Whittington et al. 2015), black bears (Sollmann et al. 2012, Sun et al. 2014), Eurasian lynx (Gimenez et al. 2019) and gray wolves (Lopez-Bao et al. 2018).

In addition to the issue of imperfect and heterogeneous detection probability, large carnivores are often social species structured in groups of associated individuals. While this particular biological organisation may violate the assumption of independence between individuals, the social structure of such species may be the object of ecological investigation. For example, in the management of wolves, the number of packs is often the focus of interest to assess population dynamics at a relevant biological scale (Marucco et al. 2010, Chapron et al. 2016).

There has been several attempts to account for species social structure while estimating population abundance and density. Cubaynes et al. (2010) used mixture capture-recapture models to estimate wolf abundance while accounting for the dominance status. Martin et al. (2011) formally accounted for dependent detections when estimating abundance of manatees. Byrne et al. (2014) estimated badger social-group abundance using cross-validated species distribution modelling. Marnewick et al. (2014) estimated abundance of wild dogs and cheetahs by considering captures and recaptures of packs instead of individuals. Belant et al. (2016) estimated abundance of lions using N-mixture models incorporating group-specific detectability. Hickey and Sollmann (2018) proposed a two-step mark-recapture approach to estimate abundance of of mountain gorillas.

To the best of our knowledge, however, these studies have not considered estimating the number of groups in a social species (e.g. the number of packs in wolf). Here, we aimed at estimating population abundance and density of species that exhibits a social structure. To do so, we develop a two-step approach: first, we use SECR models to estimate the activity centers of individuals; second, we use hierarchical clustering to determine the number of groups. To accommodate and propagate uncertainty in these two steps, as well as estimate latent variables we adopt a Bayesian approach. We performed a simulation study to formally validate the performance of our approach. In addition, we illustrate our approach using capture-recapture data on wolf (*Canis lupus*) in Italy for which we also had information on the relatedness between individuals, therefore allowing an empirical validation of our approach.

2 Material and methods

2.1 Statistical approach

The statistical approach we propose to estimate the number of groups in a social species (e.g., the number of packs in a wolf population) is a two-step process. First, we use spatially-explicit capture-recapture (SECR) models to estimation the individual activity (or home range) centers. Second, we employ hierarchical clustering on the individual activity centers to determine the number of groups. Below we go through each step in details.

2.1.1 Estimation of individual activity centers

We used SECR models to estimate the individual activity centers and their coordinates (Royle et al. 2014). SECR models use the spatial locations of captures to infer the activity center (or home range) of each individual. In technical terms, we consider an observation process that describes the relationship between individual i detection probability at trap j and the Euclidean distance d_{ij} between trap j and the activity center of individual i. In details, the distance is $d_{ij} = \|x_j - s_i\|$ where x_j is a vector of positions for trap j and s_i is a vector of positions for the activity center of individual i which is considered as a latent variable to be estimated. We assumed that the detection probability of an individual i at trap j decreased as the distance (d_{ij}) from its activity center according to a detection function. We assumed that y_{ij} the number of times individual i is detected at trap j is Poisson distributed with mean λ_{ij}. We used the standard half-normal detection function:

$$\lambda_{ij} \quad = \quad \lambda_0 \cdot \exp\left(\frac{-d_{ij}^2}{2\sigma^2}\right). \tag{1}$$

where in Eq. (1) parameter λ_0 is the expected number of detections at the activity center of individual i and parameter σ is the spatial scale (or movement) parameter that controls the shape of the detection function and can be directly linked to home range size (Royle et al. 2014).

2.1.2 Clustering individual activity centers

To estimate the numbers of packs present in the area, we group the individuals using hierarchical clustering, namely the Ward's method. The Ward's method looks at cluster analysis as an analysis of variance problem. We start with say n clusters of size 1. In the first step, $n - 1$ clusters are formed, one of size two and the remaining of size 1. The pair of activity centers that yield the smallest error sum of squares forms the first cluster (we minimize the within-cluster variance). The smaller is the error sum of squares, the closer the activity centers are to their cluster means, and the more similar these units are within that

particular cluster. Then, in the second step of the algorithm, $n-2$ clusters are formed from that $n-1$ clusters defined in the previous step, and the error sum of squares is minimized. And so on, at each step of the algorithm, clusters or activity centers are combined in such a way as to minimize the error sum of squares. The algorithm stops when all sample units are combined into a single large cluster of size n. To determine the group (or pack) membership, we cut the tree at a value obtained from the distribution of all distances between estimated activity centers.

2.1.3 Model fitting

Estimating the latent positions of the individual activity centers is challenging. When one is only interested in the population density, i.e. to estimate the number of activity centers, marginalization can be used and the latent positions will be integrated over. Here, our interest was precisely on estimating the latent positions of the individual activity centers, therefore we resorted to a Bayesian approach using Monte Carlo Markov chain (MCMC). We used the data augmentation algorithm (Royle et al. 2014). We augment our observed sample of size n individuals with $M-n$ individuals (where $M > n$) that have 0's encounter histories. We define a latent variable z_i that takes value 1 if individual i ($i = 1, \cdots, M$) belongs to the sampled population and 0 otherwise; we assumed $z_i \sim \text{Bernoulli}(\psi)$ with $\psi \sim U(0,1)$ usually referred to as the inclusion probability. An estimate for population size is then $\hat{N} = \sum_{i=1}^{M} I_{\{z_i=1\}}$.

2.2 Wolf case study

To illustrate our approach, we used a case study on gray wolf (Canis lupus) in Italy. The data were obtained from identifying the individuals applying non-invasive genetic methods on feces and hair samples (see Caniglia et al. 2014 for more information).

We had data on 94 individuals that were captured and recaptured 251 times between October 1, 2006 and March 31, 2007 in the Emilia Romagna and Tuscany Apennines (between 566615 and 743917 Easting, and 4843299 and 4949916 Northing, in UTM32-WGS84). These data were pooled in six 1-month capture occasions.

In contrast with standard camera-trap studies, the data were collected through a search-effort protocol that does not require fixed traps (Royle et al. 2011, Russell et al. 2012). We built a grid cell layer and assigned all genotyped samples to a cell in which we defined the centroid as the detector location (or a trap). We ended up with 150 cells with a distance between each cell that was determined following recommendation by Solmann et al. (2012). Precisely, we considered a distance between traps at least equal to $2 \times \sigma$ and checked that the size of a cell was smaller than the home range of a wolf. We found

that a distance of 13km was appropriate[1].

Regarding parameter estimation, we augmented the sample with 100 individuals so that $M = 294$. We used the following priors on parameters: $\sigma^2 \sim U(0, 20)$, $\lambda_0 \sim \Gamma(0.1, 0.1)$, $\psi \sim U(0, 1)$. We used 2 MCMC chains with 1,000 iterations as a burnin and 2,000 iterations for final inference. To check for convergence, we visually inspected the MCMC chains for parameters of interest, and calculated the Gelman-Rubin statistic.

2.3 Simulation study

To validate our approach, we performed a simulation study by mimicking the characteristics of the wolf case study.

2.3.1 Spatial distribution of individuals

Wolves have a home range, in which they realize the activities for their survival. The center of the home range is what we call the activity center. Here, we will refer to space occupied by one group as "disc", and to central position of a group as "center of disc", and we will assume that the home ranges are circular. In Figure 1 we represent the movement of an individual in an area and its activity center S_i. Two individuals are also represented that share a space because their movement trajectories are overlapping, therefore these individuals are considered belonging to same group P with central position S_P.

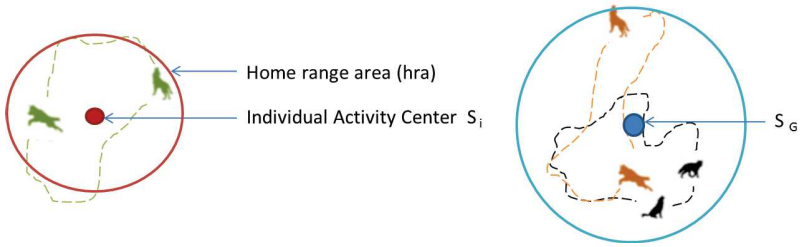

Figure 1: Home range area (hra) of an individual i, individual activity center S_i, center of disc S_P used for the pack P.

Now to simulate groups of individuals, we used a Poisson point process. We think of groups of points that represent groups of individuals, and these groups of points are disposed in circular areas similar to circular home ranges areas. We make the distinction between these two groups of points: we have the center points of discs that are called *point patterns* - which are moving in the space - and we have the points that represent the positions of individuals in the circular areas, *point sons*. Below, we explain how

[1]We determined σ that allows generating the 95% home range area (hra) of an individual as given in Caniglia et al. (2014), where $\sigma = \sqrt{(hra/\pi)}/\sqrt{\tilde{\chi}^2_{(0.95,2)}}$

we create the disc centers and then the points that represent the individual activity centers.

2.3.2 Central position of groups and movement (point patterns)

We generated the positions of the centers of discs and their movements in several steps. First, the number of groups a in the space is simulated from a Poisson distribution with mean 19. Second, the centers of groups P are spatially disposed with uniform distribution in an area of 19,171 km^2 (as in the real case study). P has dimension $a \times 2$ corresponding to x (that represent Easting coordinates) and y (Northing coordinates) (see example in Royle et al. 2014, pp. 309 and definitions in Baddeley et al. 2016, pp. 129). Third, we use these central points as initial points to generate a bidirectional Wiener process W_t, with W_t^1 and W_t^2 both stationary processes in discrete time with correlation parameters $\rho_1 = \rho_2 = 0$, which is used to capture the movement of groups over time. We provide an example in Figure 2 $a = 11$ groups and 5 repetitions.

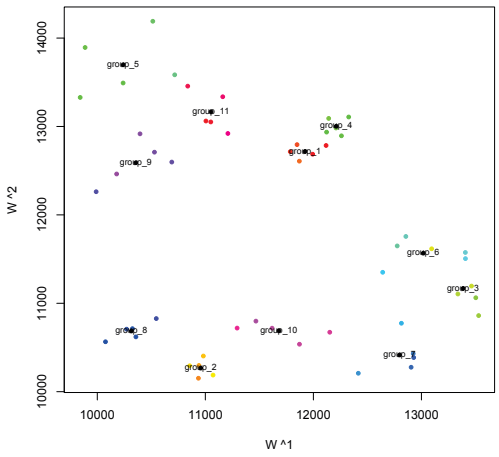

Figure 2: Five positions for $a = 11$ groups, with their center in black.

2.3.3 Positions of individuals (points sons)

The points that represent the positions of individuals are generated from a truncated multivariate normal distribution, for which we need to specify the size of groups (or packs), correlation parameter and point of truncating. The size of groups is drawn from a Poisson distribution with mean 4. We select arbitrarily the correlation parameter between the axes x and y and say $\rho = 0$. We use the ratio r_{hra} as the truncating parameter. By doing so, the points sons around of a point pattern are less than r_{hra} farther away from

the central point. Regarding the latter, the vector of mean is the matrix of coordinates P of the centers of groups over time.

Our vector of coordinates for all individual i, $i = 1, 2, ..., N$ (where N is the size of simulated population) is contained in the vector of positions XY generated from the truncated multivariate normal distribution with mean the vector of means W_t of coordinates over time, and covariance the matrix Σ such that:

$$\Sigma = \begin{pmatrix} {r_x}^2 & \rho r_x r_y r_{hra} \\ \rho r_y r_x r_{hra} & {r_y}^2 \end{pmatrix}$$

where ${r_x}^2$ is the variance in the axis x, ${r_y}^2$ is the variance in the axis y ($r_y = r_x$ here), $XY \sim N(P, \Sigma)$ and r_{hra} is the parameter of truncating. A example of a realization from the truncated multivariate normal distribution is shown in Figure 3.

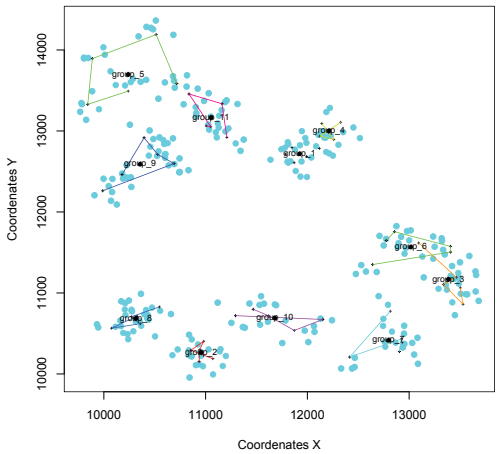

Figure 3: All groups of individuals are represented for color cyan, and generated from a truncated multivariate normal distribution with parameters mean P and Σ already defined. The positions of centers of discs for 5 times are represent little stars and the displacement of centers disc is showed with lines for each group.

2.3.4 Detection process

To obtain the individual capture-recapture histories, we apply the Poisson distribution with the detection function as in the wolf case study.

2.3.5 MCMC details and performance assessment

To simulate the data, we used parameter values $\sigma^2 = 5$, $\psi = 0.8$ and 100 individuals as the actual population size. To estimate the model parameters, we used two MCMC chains of 2,000 iterations with a burnin of 1,000 iterations and 100 augmented individuals.

To assess the performance of our approach, we generated 100 datasets and estimated the bias and root square error mean (RMSE) of the estimate $\hat{a}$ of the number of groups a.

3 Results

3.1 Wolf case study

We ended up with a grid made of 150 cells that was overlapped on the study area; the data are displayed in Figure 4 with respect to the traps and the individuals.

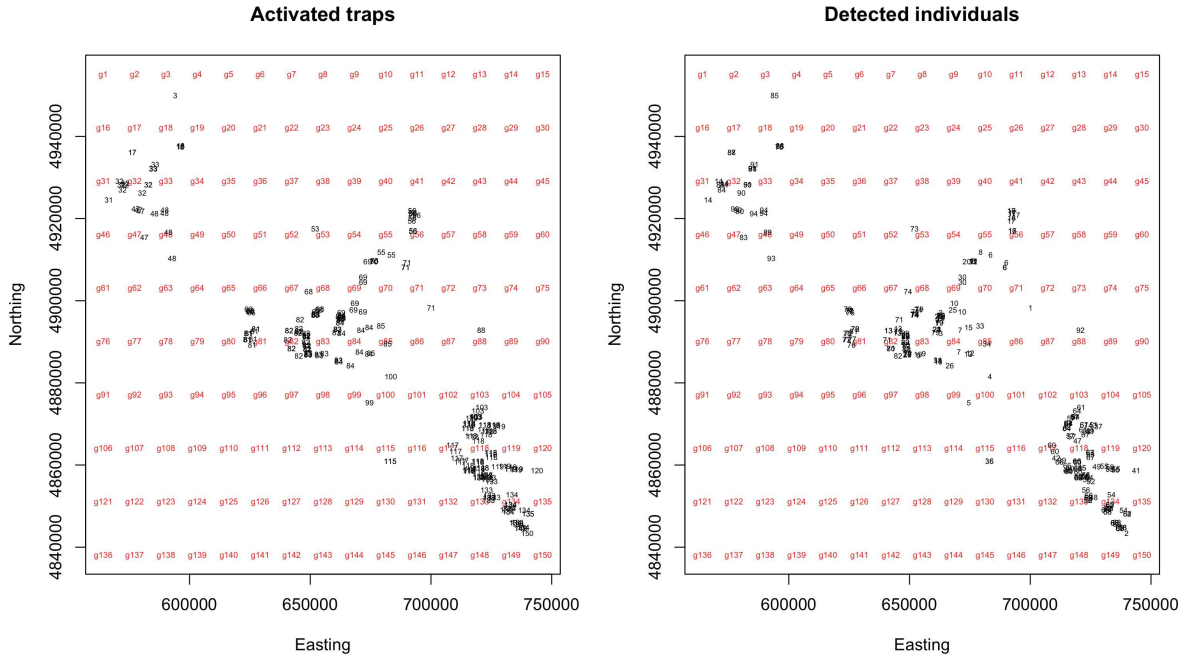

Figure 4: Wolf observations in the study area labeled by name (a number) of activated trap (left) or of detected individual (right).

Numerical summaries of parameter estimates are given in Table 1, while posterior distributions are displayed in Figure 5. We estimated 130 wolves in total (95% credible interval [116, 130]) for 94 individuals actually observed at least once.

Parameter	mean	sd	2.5%	median	97.5%
λ_0	0.12	0.02	0.09	0.12	0.15
σ^2	0.37	0.03	0.31	0.37	0.44
N	130.52	7.77	116.00	130.00	147.00

Table 1: Wolf posterior estimates for the spatially-explicit capture-recapture model. We provide the posterior mean and median, standard deviation (sd), lower (2.5%) and upper (97.5%) bounds of the credible interval.

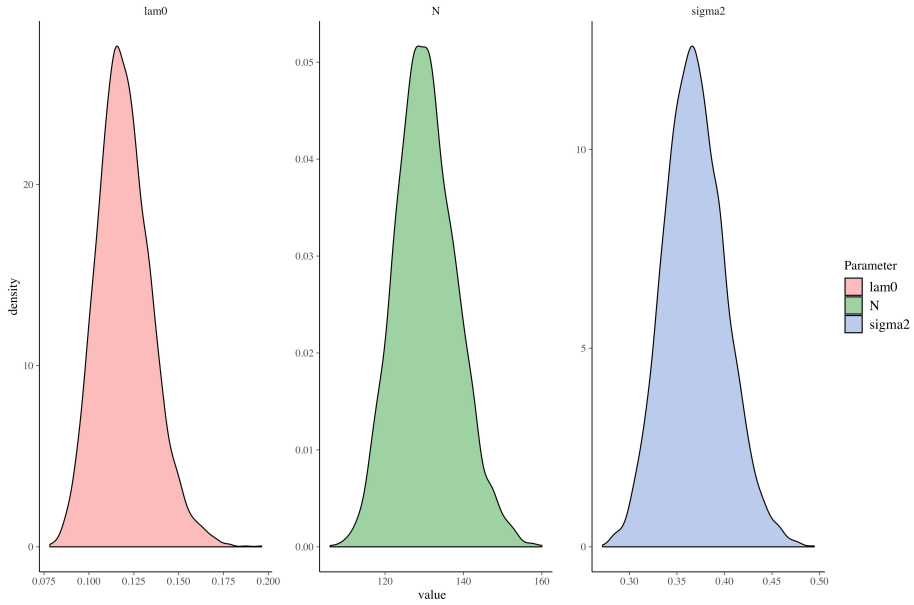

Figure 5: The map of density based on the estimates of the positions of sampled individuals. We have applied the mask that filters the positions and selects only those that belong to the favorable area.

The individual activity centers were grouped with the Ward's method using $h = 40,000^2$. We found that the number of packs varied between 8 and 14 with a posterior mean at 11.2 and standard deviation at 1.0 (Figure 6). The number of individuals per pack ranged from 6.7 to 11.8 with a posterior mean of 8.5 and standard deviation of 0.8.

We obtained 4,371 possible dyads total, from these, 50 dyads are present more of 90% of times, forming 12 groups (Figure 7).

3.2 Simulations

We obtained 100 simulated datasets, which characteristics are summarized in Table 2.

We obtained 100 simulated datasets, which characteristics are summarized in .

The bias in the number of groups and population size estimators was negligible (see Table 3, and it was of similar magnitude whatever the interval for the number of groups.

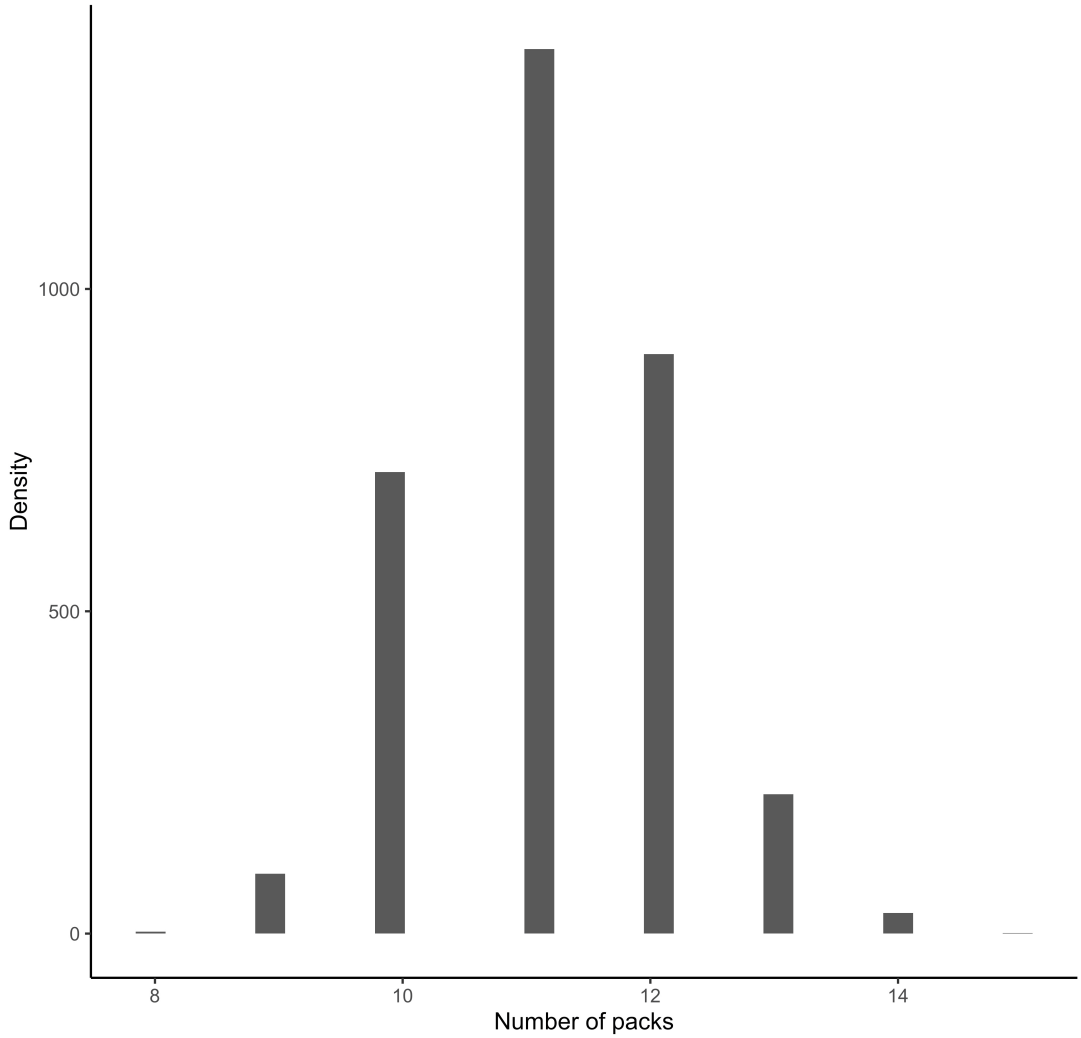

Figure 6: Histogram of the number of wolf packs.

4 Discussion

In the ecological literature, the complex structure of social species is at best acknowledged but often ignored when estimating abundance and density (Hacky and Sollmann 2018). Several attempts have been made to accommodate dependence of individuals when inferring population dynamics. However, to date, no method exists to reliably estimate the number of groups in a population of a social species. We proposed a two-step approach combining SECR models and hierarchical clustering to estimate the number of packs in a wolf population. Our proposal has several appealing advantages. First, ignoring imperfect and possibly heterogeneous detection may lead to biased inference about population abundance and density. Our approach provides a robust method to estimate the number of clusters in a population. Second, our

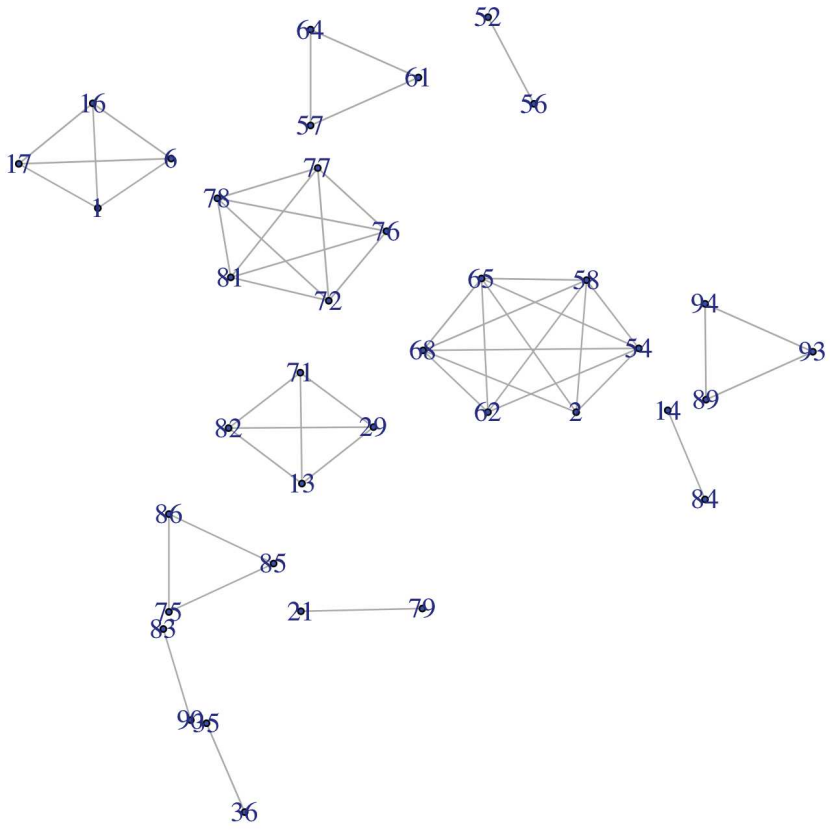

Figure 7: Network of associations between wolves with proportion of associations $> 90\%$.

approach allows the quantification and propagation of uncertainty associated with the unknown latent position of activity centers into the estimation of the number of clusters. If we think of clusters as packs, this is particularly important when the number of packs quantity is converted into population size beyond the study area using some conversion factor (e.g. Chapron et al. 2016). Last, the position of the clusters can be visualised in space. Again, if we think of the position of packs in the wolf case study, our approach provides a tool for assessing potential conflicts like depredation on livestock.

Regarding the wolf case study, we found 11 packs on average. This figure underestimates the 17 packs known to be present in the study area on the period we considered. Despite our efforts, we cannot explain this discrepancy. Reassuringly, the results of the simulation study which characteristics were chosen to mimic the wolf case study suggest little bias in the number of groups estimator.

	Mean	SD of mean	2.5%	50%	97.5%
N Simulated	92.68	33.10	-	-	-
$\tilde{N}$	94.77	20.70	82.31	96.14	100.37
$\tilde{\lambda_0}$	0.016	0.027	0.006	0.015	0.033
$\tilde{\sigma_2}$	2.68	1.94	0.77	2.26	6.40
$\tilde{\psi}$	0.930	0.055	0.785	0.945	0.998
Number of simulated groups	10.230	3.623	-	-	-
Number of estimated groups	13.194	6.885	10.83	13.125	15.691
Average pack size	4.864	2.552	-	-	-
Distance between simulated packs	1764.988	267.925	-	-	-
Distance between estimated packs	1522.778	722.035	-	-	-
Distance between activity centers	759.425	225.355	-	-	-
Distance h	1081.736	353.798	-	-	-

Table 2: Main characteristics of the simulation scenario.

	$\forall a$	$a \leq 8$	$8 < a \leq 14$	$15 < a$
Bias $(\hat{a}, a)$	1.29	0.29	0.29	0.30
RMSE $(\hat{a})$	6.23	5.88	6.56	5.20
Bias $(\hat{N}, N)$	1.02	0.16	0.04	-0.29
RMSE $(\hat{N})$	14.65	16.94	8.84	28.21

Table 3: Performance of the estimation method for various intervals of number of groups. Bias and root mean square error are provided for both the number of groups a and population size N.

Our proposal relies on assumptions that need to be discussed. The main assumption we made is that of closed populations. However, birth and death or immigration and emigration events obviously occur in animal populations over long periods of time. The extension of our model to open populations is feasible by using open SECR models (Gardner et al., 2010). This extension would allow accounting for the fate of individuals and, as a by-product, the dynamics of the number of groups or clusters. A challenge will be to track individuals changing groups (e.g., Cubaynes et al. 2010), which would permit studying fission-fusion societies like cetaceans or primates in natural conditions. Another extension would be to handle the dependence in the individual activity centers directly in the model instead of inferring clusters of estimated quantities. A promising avenue would be to adopt the framework proposed by Reich and Gardner (2014) and use an inhomogeneous point process for the individual activity centers instead of a homogeneous Poisson point process. A possible candidate is the Neyman-Scott point process that allows clustering (Baddeley et al. 2016).

5 References

Baddeley A., E. Rubak E. and R. Turner (2016). Spatial Point Patterns, Methodology and applications with R. CRC Press.

Caniglia R., E. Fabri, M. Galaverni, P. Milanesi and E. Randi (2014). Noninvasive sampling and genetic variability, pack, structure, and dynamics in an expanding wolf population. *Journal of Mammology* 95:41-59.

Chapron, G., C. Wikenros, O. Liberg, P. Wabakken, Ø. Flagstad, C. Milleret, J. Månsson, L. Svensson, B. Zimmermann, M. Åkesson and H. Sand 2016. Estimating wolf (Canis lupus) population size from number of packs and an individual based model. *Ecological Modelling* 339: 33-44.

Cubaynes, S. Pradel, R. Choquet, R. Duchamp, C. Gaillard, J.-M., Lebreton, J.-D., Marboutin, E., Miquel, C., Reboulet, A.-M., Poillot, C., Taberlet, P. and O. Gimenez (2010). Importance of accounting for detection heterogeneity when estimating abundance: the case of French wolves. *Conservation Biology* 24: 621-626.

Gardner B., J. Reppucci, M. Lucherini and J.A. Royle (2010). Spatially explicit inference for open populations: Estimating demographic parameters from camera-trap studies. *Ecology* 91: 3376-3383.

Gimenez, O., S. Gatti, C. Duchamp, E. Germain, A. Laurent, F. Zimmermann and E. Marboutin (2019). Spatial density estimates of Eurasian lynx (Lynx lynx) in the French Jura and Vosges Mountains. bioRxiv 600015.

Hickey J.R. and R. Sollmann (2018). A new mark-recapture approach for abundance estimation of social species. *PLoS ONE* 13(12): e0208726.

López-Bao, J.V., R. Godinho, C. Pacheco, F.J. Lema, E. García, L. Llaneza, V. Palacios and J. Jiménez (2018) Toward reliable population estimates of wolves by combining spatial capture-recapture models and non-invasive DNA monitoring. *Scientific Reports* 8(1):2177.

Martin, J., J.A. Royle, D.I. Mackenzie, H.H. Edwards, M. Kéry, and B. Gardner (2011). Accounting for non-independent detection when estimating abundance of organisms with a Bayesian approach. *Methods in Ecology and Evolution* 2: 595-601.

Marucco, F. and E.J. McIntire (2010). Predicting spatio-temporal recolonization of large carnivore populations and livestock depredation risk: wolves in the Italian Alps. *Journal of Applied Ecology* 47: 789-798.

Mattioli, L., A. Canu, D. Passilongo, M. Scandura, and M. Apollonio 2018. Estimation of pack density in grey wolf (Canis lupus) by applying spatially explicit capture-recapture models to camera trap data supported by genetic monitoring. *Frontiers in Zoology* 15:38.

Reich, B.J. and B. Gardner (2014). A spatial capture-recapture model for territorial species. *Environmetrics* 25: 630-637.

Royle, J.A., M. Kéry and J. Guélat 2011. Spatial capture-recapture models for search-encounter data. *Methods in Ecology and Evolution*, 2, 602–611.

Royle, J.A., R. Chandler, R. Sollmann and B. Gardner (2014). Spatial Capture-Recapture, Elsevier, USA.

Russell, R.E., J.A. Royle, R. Desimone, M.K. Schwartz, V.L. Edwards, K.P. Pilgrim and K.S. Mckelvey (2012). Estimating Abundance of Mountain Lions From Unstructured Spatial Sampling. *Journal of Wildlife Management* 76: 1551-1561.

Sarmento, P., J. Cruz, C. Eira and C. Fonseca (2014). A spatially explicit approach for estimating space use and density of common genets. *Animal Biodiversity and Conservation* 37.1: 23–33.

Sollmann, R., B. Gardner and J. Belant (2012). How does spatial study design influence density estimates from spatial capture-recapture models? *PLoS ONE* 7(4):e34575.

Sun, C.C., A.K. Fuller and J.A. Royle (2014). Trap Configuration and Spacing Influences Parameter Estimates in Spatial Capture-Recapture Models. *PLoS ONE* 9(2): e88025.

Whittington, J. and M.A. Sawaya (2015). A Comparison of Grizzly Bear Demographic Parameters Estimated from Non-Spatial and Spatial Open Population Capture-Recapture Models. *PLoS ONE* 10(7): e0134446.

Williams, B.K., J.D. Nichols J.D., and M.J. Conroy (2002). Analysis and management of animal populations, San Diego: Academic Press.

Modèles intégrés de population pour des espèces sociales – Un cas d'étude avec les éléphants de mer

3.1 ARTICLE 2. Integrated population modeling for social species: a case study with elephants seals

Résumé

L'organisation sociale, la structure sociale et le système de reproduction sont des composants clés des systèmes sociaux qui influencent fortement la dynamique de la population. Ignorer le système social dans la modélisation démographique peut conduire à une fausse inférence sur la dynamique de la population et, à son tour, à des actions de gestion erronées. Ici, nous nous appuyons sur les travaux d'autres auteurs et proposons un cadre statistique pour évaluer formellement l'importance de la structure sociale dans une population de phoques de l'éléphant du sud (*Mirounga leonina*) pour en déduire la dynamique de sa population. Nous avons utilisé des modèles intégrés de population (IPM) en combinant des données à long terme de capture-recapture sur la reproduction des femelles et le dénombrement des éléphanteaux sur l'île de Marion, dans le sud de l'océan Indien, au cours de la période 1978-2016.

En partageant des informations sur les paramètres communs entre les deux sources de données, nous avons mis en évidence un effet de socialité sur la dynamique de la population de phoques éléphants, qui ne pouvait pas être démontré lorsque les dénombrements étaient analysés séparément.

Bien que ces modèles soient de plus en plus utilisés en écologie de population, les IPM n'ont été étendus que récemment aux espèces sociales. Ainsi, nous espérons que notre proposition encouragera l'application des IPMs pour une meilleure compréhension de la démographie des espèces sociales.

Mots-clés: Détection imparfaite, modèles intégrés de population, capture-recapture, modèles matriciels, espèce sociale.

INTEGRATED POPULATION MODELING FOR SOCIAL SPECIES: A CASE STUDY WITH ELEPHANT SEALS

Lorena Mansilla[1,2], W. Chris Oosthuizen[3,4], Roger Pradel[1,5], P. J. Nico de Bruyn[3,6], Marthán N. Bester[3,7], and Olivier Gimenez[1,8]

[1]*Centre d'Ecologie Fonctionnelle et Evolutive (UMR 5175), CNRS – Université de Montpellier – Université Paul-Valéry Montpellier – EPHE, campus CNRS, Montpellier cedex 5, France*

[2]E-mail: lorena.rociomansilla@gmail.com

[3] Mammal Research Institute, Department of Zoology and Entomology, University of Pretoria, Private Bag X20, Hatfield 0028, South Africa

[4]E-mail: wcoosthuizen@zoology.up.ac.za

[5]E-mail: roger.pradel@cefe.cnrs.fr

[6]E-mail: pjndebruyn@zoology.up.ac.za

[7]E-mail: mnbester@zoology.up.ac.za

[8]E-mail: olivier.gimenez@cefe.cnrs.fr

Abstract.— Social organization, social structure and mating system are key components of social systems that strongly influence population dynamics. Ignoring the social system in demographic modelling can lead to false inference about population dynamics and, in turn, to erroneous management actions. Here, we build on previous work and propose a statistical framework to formally assess the importance of social structure in infering population dynamics of social species. We used integrated population models (IPMs) that are increasingly used in population ecology but have only recently been extended to social species. As a case study, we estimated and tested the effect of the social structure on population dynamics of southern elephant seals (Mirounga leonina) by combining long-term capture-recapture data on females breeding and pup counts at Marion Island, in the southern Indian Ocean, during the period 1978-2016. By sharing information on parameters that are in common between the two sources of data, we demonstrated an effect of sociality on population dynamics of elephant seals that could not be showed when the counts were analyzed in isolation. Overall, we hope that our proposal will foster the application of integrated population models for a better understanding of the demography of social species.

Key words.— imperfect detection, integrated population models, mark-recapture, matrix models, *Mirounga leonina*, social species

INTRODUCTION

Social species occur in functional units like colonies, groups or harems. The social system of these species is usually described by their social organization, social structure and mating system (e.g., Kappeler and van Schaik 2002). Several studies showed that these key components of social systems strongly influence the dynamics of populations (Gerber 2006; González-Suárez and Gerber 2008; Ferrari et al. 2009; Hickey and Sollmann 2018). Besides,

ignoring the social system in demographic modelling can lead to false inference about population dynamics and, in turn, to erroneous management actions (Vucetich et al. 1997; Zeigler and Walters 2014; Gerber and White 2014).

To infer population dynamics, integrated population models (IPMs) are increasingly used in population ecology (Schaub and Abadi 2011; Zipkin and Saunders 2018). These models allow the integration of several types of information, such as capture-recapture, age-at-harvest, telemetry, and count data into a single statistical analysis (Besbeas et al. 2002). IPMs combine a matrix population model at their core to capture the species demography with relevant statistical models for the different sources of data. By sharing information on parameters that are in common between these models, IPMs yield estimates that are more precise than when the different sources of data are analyzed separately (Besbeas et al. 2002).

Until recently, IPMs have been restricted to monogamous species, which limited their application to social species. Tenan et al. (2016) extended classical IPMs to nonmonogamous species by using a two-sex matrix population model (e.g., (Jenouvrier et al. 2010)). The authors illustrated their approach using a brown bear (*Ursus arctos*) population. Here, we build on the work of Tenan et al. (2016) and develop a proper statistical framework to formally assess the importance of social structure in infering population dynamics of social species.

In this paper, we develop an IPM to extend the population model that Ferrari et al. (2009) used to quantify the effect of the social structure on population dynamics of southern elephant seals (*Mirounga leonina*). As a case study we used long-term data on female southern elephant seals breeding at Marion Island, in the southern Indian Ocean (Bester et al. 2011). Southern elephant seals are the largest living pinnipeds, and among the most sexually dimorphic and polygynous extant mammals (Le Boeuf and Laws 1994). Females aggregate in

harems during the synchronous breeding season with territorial males fighing for dominance status. Aggregation and territoriality make southern elephant seals a relevant candidate model for testing IPMs for social species.

METHODS

Elephant seal biology

Southern elephant seals are wide-ranging marine predators that breed annually on numerous Southern Ocean islands as well as at Peninsula Valdés in Argentina. Southern elephant seals are extreme capital breeders and both males and females fast while hauled out at breeding colonies, relying on catabolism of blubber lipids and body protein for metabolic energy (Boyd 2000). Socially mature males arrive ashore first at the start of breeding seasons (in mid-August) and establish territories before females arrive (Galimberti et al. 2002). Male dominance hierarchies are initially formed through antagonistic interactions (fighting), and the social hierarchy is subsequently maintained through the breeding season by way of acoustic cues (Casey et al. 2015). The mating system is extreme polygyny (Fabiani et al. 2004; de Bruyn et al. 2011), and males compete for access to females which aggregate in groups known as harems. Females arrive at breeding colonies in September and October. Nearly all females ashore during a breeding season give birth to a single pup, and females remain ashore for the entire lactation period of approximately 23 days. Females are in estrus during the last few days of lactation, at which time they will mate.

At breeding sites such as Marion Island, where harems are relatively small (< 60 females) and spatially segregated, most harems are under the near exclusive control of a single dominant male, the alpha male (Fabiani et al. 2004). Subordinate males typically linger at the periphery of harems and will only mate opportunistically with females on the harem-boundary, or with those females which moved away from harems, if at all (Wilkinson and van

91 Aarde 1999). The large size of elephant seal harems, up to one order of magnitude larger than
92 harems of other polygynous mammals (Clutton-Brock 1989), and the persistent attempts of
93 subordinate males to interact with females, produce a complex social network (Galimberti et
94 al. 2002).

95 **Data collection**

96 *Population counts data*

97 The number of female elephant seals ashore over the course of a breeding season closely
98 approximates a normal distribution with a peak around 15 October each year (Authier et al.
99 2011, Fig. S1). Every year from 1973 to 2016, direct counts of elephant seals were made
100 during the peak of the breeding season at beaches along the north-eastern coastline of Marion
101 Island.

102 Approximately 25% of the population breed within the area between Ship's Cove and
103 Archway Bay, and trends observed here are similar to that of the total population. We used 15
104 October counts of breeding females and breeding males (alpha males and subordinate males)
105 as an index of abundance and the operational sex ratio (OSR) of the adult population. The
106 annual mean harem size, defined as the average number of females per harem, was also
107 estimated using 15 October counts. Here, a harem refers to a group of two or more females,
108 with or without a male, formed on the six beaches within the study area. Accessibility of
109 breeding beaches and the relative ease with which breeding elephant seals can be approached
110 means that direct counts contain minimal observation error. Counts are nonetheless subject to
111 a degree of spatial and temporal sampling variance, as only a portion of the breeding
112 population was counted, and because the staggered arrival and departure date of females mean
113 that even the peak breeding season census can miss females that may have come ashore to
114 breed (Authier et al. 2011). The total number of pups born over the course of the breeding

season was estimated as the sum of the number of breeding females, weaned pups and dead pups counted on 15 October (e.g., Lewis et al. 2004; Ferrari et al. 2009).

Capture-recapture data

From 1983 to 2009, 6,439 recently weaned female elephant seal pups born at Marion Island were marked with two unique hind-flipper tags (Pistorius et al. 2011). Capture-recapture resight effort occurred in all years on a systematic 7- or 10-day cycle (Oosthuizen et al. 2019b) on all beaches on Marion Island where female elephant seals hauled out for breeding, moulting and resting (Mulaudzi et al. 2008). A total of 65,602 resightings of marked female elephant seals were made between 1983 and 2014.

Integrated population model

In this section, we describe the two components of the IPM we developed based on the Southern elephant seal life cycle (Figure 1). Our IPM is built as the product of the likehood for the population counts model and the likehood for the capture-recapture model (Figure 2). We describe these two components below.

[FIGURE 1 AROUND HERE]

Population dynamics model

We follow (Ferrari et al. 2009) and define N_t the number of pups in breeding season t as a function of fertility F and N_f the number of adult females. We have:

$$N(t) = \alpha F(t-1) N_f(t) \quad (1)$$

where α is a fertility constant and the function F is defined over the breeding season $t-1$ (whenever they were pregnant) as:

$$F(t) = (1 + R(t)^a)^{1/a} \quad (2)$$

where R represents the social structure and is the mean harem size times the number of adult males per adult female. Parameter a determines the strength of this variable on the function value (Ferrari et al. 2009). More precisely, whenever $a \rightarrow$ +/-∞, we have $F(t) = 1$ and there is no influence of the social structure whereas whenever $a \rightarrow 0$, we have $F(t) = \infty$ and there is a strong influence of social structure.

Assuming breeding starts not before two years,, and that most females reproduce at 3 and 4 years old, we also have:

$$N_f(t) = \phi N_f(t-1) + \pi \rho r N(t-3) + (1-\pi)\rho r \phi_{a3} N(t-4) \quad (3)$$

where ϕ is the adult female survival, π is the proportion of females breeding at age 3 (and $1-\pi$ the proportion of females breeding at age 4), ρ is a constant corresponding to the mean sex ratio (proportion of females) at birth recorded from 1983 to 2009 (0.506), r the recruitment rate of adult females and ϕ_{a3} the female survival from age 3 to 4. The first term in equation (3) represents surviving breeders of $t-1$, the second term is a proportion π of 3-year old females and third term is a proportion $1-\pi$ of 4-year females that did not breed at age 3.

Replacing $N_f(t)$ of equation (3) in equation (1) and writing $N_f(t-1) = N(t-1)/\alpha F(t-2)$, we get:

$$N(t) = \phi \frac{F(t)}{F(t-1)} N(t-1) + qF(t)[(1-\pi)\phi_{a3} N(t-4) + \pi N(t-3)] \quad (4)$$

where $q = \alpha\rho r$. We assume a multiplicative sampling error V_t, so that observed pup counts y_t in breeding season t is:

$$y_t = N_t \, V_t \quad (5)$$

With $V_t \sim Lognormal(0, \sigma^2)$, we get the likelihood for the pup counts L_{counts} as:

$$-2\ln L_{counts} = \exp(-0.5\ln(2\pi) - \ln(\sigma) - \frac{1}{2\sigma^2} \Sigma(\ln y_t - \ln N_t)^2) \quad (6)$$

Capture-recapture model

We built a multievent capture-recapture model (Pradel 2005) to estimate demographic parameters with likelihood $L_{capture-recapture}$. Female elephant seals were assumed to occupy one of the following states each year: pre-breeder PB (has not previously pupped), breeder B (pupped in the current year); non-breeder NB (pupped previously, but not in the current year); and D dead. All individuals entered the marked population as weaned pups (thus in the pre-breeder state). Encounter histories summarised multiple sightings of an individual between two consecutive breeding seasons (September in year t to August in year $t+1$) as a single encounter: 0 for non-observed, 1 for non-breeding and 2 for breeding. Pre-breeding and non-breeding elephant seals typically do not attend breeding colonies in the breeding season but are observed at other times of the year (e.g., during the moult and winter haulout) (Oosthuizen et al. 2019b).

171 The transition probabilities between states correspond to apparent annual survival
172 (hereafter survival) and breeding probability. We assumed age-specific pre-breeder survival
173 (Pistorius and Bester 2002) and constant adult survival. We denoted ϕ_{a0} as the survival
174 probability of newborn females, $\phi_{a1}, \phi_{a2}, \phi_{a3}, \phi_{a4}$ the survival probability of 1-year old, 2-
175 year old, 3-year old and 4-year old females and ϕ the survival probability of older adult
176 females.

177 In elephant seals, there is no recruitment to the breeding population on the beachers
178 prior to age 3 and in our dataset, most surviving females recruited at age 3 or age 4 years
179 (Oosthuizen et al. In review). The transition probability from pre-breeder to breeder was
180 therefore assumed to depend on age, with ψ_{B2}, ψ_{B3} and ψ_{B4} the probability of breeding in the
181 next year for 2-year old, 3-year old and 4-year old females, ψ_B the probability of a
182 reproductive female to remain a reproductive female.

183 Because attendance behaviour differs between breeding states, we allowed capture
184 probabilities to vary with state, with p_{PB} the probability of observing a pre-breeding female
185 outside the breeding season, p_B the probability of observing a breeding female in the breeding
186 season, and p_{NB} the probability of observing a non-breeding female outside of the breeding
187 season.

188

189 [FIGURE 2 AROUND HERE]

190

191 **Parameter estimation**

192 We used maximum likelihood theory to estimate the parameters of the IPM model and to
193 derive confidence intervals. To maximize the IPM likelihood, we used the quasi-Newton

194 algorithm as implemented in the optim function from program R (R Code Team 2019). We
195 expected a better precision for parameters that were in common between the two likelihoods
196 L_{counts} and $L_{capture-recapture}$, namely ϕ and ϕ_{a3}. We also obtained confidence intervals for
197 the number of pups observed using the parametric boostrap method (Davison and Hinkley
198 1997).

199

200 **Test of the influence of sociality**

201 To formally test the effect of sociality on population dynamics, we considered the null
202 hypothesis of no influence of social structure where *a* reached infinity (*a* = 1,000) in the IPM
203 likelihood and tested it with a likelihood ratio test (LRT) against the alternative hypothesis in
204 which *a* was estimated (representing nonlinear fertility dependence on social structure). We
205 also considered this comparison using models with pup counts only to determine whether
206 combining sources of data in an IPM increased our ability to detect the influence of social
207 structure.

208

209 **RESULTS**

210 When comparing models in which parameter *a* was fixed vs. estimated with count data only,
211 the null hypothesis of no effect of sociality on demography could not be rejected (Table 1). In
212 contrast, when count and capture-recapture data were combined in the IPM, the LRT was
213 significant (p = 0.05). The effect of sociality was confirmed by the estimate of parameter *a*
214 which was far from infinity in both the IPM (-0.99 [-1.18; -0.83]) and the model for count
215 data only (-2.08 [-5.47; -0.88]).

216

[TABLE 1 AROUND HERE]

The survival of newborn females was low (0.60 [0.59; 0.61]) while that of pre-breeders and adults varied between 0.71 ([0.68; 0.74]) for 4-year old females and 0.79 ([0.77; 0.81]) for 3-year old females (Table 1). The probability of breeding for the first time varied substantially with age with a peak for 4-year old females. Regarding the detection process, the probability of observing a breeding female in the breeding season was higher than that of observing a pre-breeder or non-breeder female outside the breeding season (Table 1). The demographic parameter estimates were indistinguishable whether we let parameter *a* be estimated or we fixed it.

When inspecting the predictions of number of pups born annually from the IPM, the fit of the model to the observed counts was satisfactory from 1998 onwards, while it captured poorly the observed decreasing trend from 1981 to 1995 (Figure 3).

[FIGURE 3 AROUND HERE]

DISCUSSION

The inclusion of social structure (e.g., operational sex ratios) in population models can produce different dynamics to female-only models that excludes behavioral data, even in polygynous species where female numbers are thought to limit reproduction (Gerber 2006; Gerber and White 2014). We illustrated the relevance of integrated population models (IPMs) for modeling the demography of polygynous species and provide a statistical framework to formally assess the effect of sociality on population dynamics in such species.

241 Identifying whether behavioral attributes influence demographic parameters can
242 enhance our understanding of population dynamics. A shortage of breeding males, resulting in
243 low insemination rates, is one mechanism previously suggested to contribute to the southern
244 elephant seal population decline at Marion Island (Skinner and van Aarde 1983). This
245 hypothesis was later refuted as dominant bulls are capable of mating multiple times with all
246 females in harems (Wilkinson and van Aarde 1999). However, the role of males in the
247 dynamics of populations is not limited to active mechanisms, such as sexual activity, by
248 which they may influence the breeding rates of females and so population dynamics
249 (Mysterud et al. 2002). Males also have a more indirect influence on population dynamics and
250 female demographic parameters simply by being a component of population density
251 (Mysterud et al. 2002), through sexual harassment of females, or by modifying female
252 behavior (e.g., Milner-Gulland et al. 2003; Galliard et al. 2005). Single-sex population matrix
253 models incorporating sex-ratios may therefore account partly for male influence on
254 population dynamics, although they do not incorporate sex-specific vital rates. Two-sex
255 matrix population models are becoming more common in demographic studies of species with
256 unbalanced sex ratios or unique social structures (e.g., Tongen et al. 2016; Shyu and Caswell
257 2018) and their use in the IPM framework is encouraged (see Tenan et al. 2016 for an
258 illustration of two-sex IPMs).

259 In IPMs, the single model likelihoods of several datasets (population count data and
260 demographic data in this study) are combined to create a joint likelihood model upon which
261 inference is based (Schaub and Abadi 2011). Typically, this approach enhances statistical
262 power to increase parameter estimate precision. We expected a better precision for parameters
263 that were in common between the two likelihoods L_{counts} and $L_{capture-recapture}$, namely ϕ
264 and ϕ_{a3}. However, demographic parameters of the combined capture-recapture and count
265 data IPM did not have better precision in this study, probably because the capture-recapture

266 data are informative enough (recapture probabilities are high) so that these parameters are
267 already very well estimated. The IPM and count model differed, however, in their estimates
268 of parameter a, which determines the strength of social structure on the fertlility function. The
269 IPM estimate of a was -0.99, which approximates the harmonic mean fertility function
270 (Gerber 2006). The effect of social structure was weaker in the count model.

271 Ferrari et al. (2009) previously used a deterministic population model, similar to our
272 count model, to investigate the relationship between social structure and population dynamics
273 of southern elephant seals breeding at Peninsula Valdés in Argentina. Their results suggested
274 a better fit of predicted values to observed data when social structure was included in the
275 fertility function of the model. One advantage of formulating this model as an IPM is that we
276 could independently estimate parameters ρ , r and α (Equations 2 and 3) which was part of a
277 composite recruitment parameter in Ferrari et al. (2009). Also, by combining with capture-
278 recapture data, we could relax the assumption of known demographic parameters (survival
279 and transitions between reproductive states) that was made in Ferrari et al. (2009) and
280 estimate them directly. Overall, our estimates of survival and breeding probabilities were
281 comparable to previous estimates obtained for this population (e.g., Pistorius et al. 1999a,
282 2011; Pistorius and Bester 2002, Oosthuizen et al. 2018).

283 Although testing it directly would be difficult, the most plausible hypothesis
284 explaining the decline in pup counts we observed and predicted (Figure 2) is a reduction in
285 food resources and/or quality through environmental change (McMahon et al. 2005). An
286 alternative hypothesis based on historical fish extraction (Ainley and Blight 2009), again
287 suggests that alteration in prey availability was key to population declines. Investigating the
288 effect of environmental stochasticity in southern elephant seals breeding at Marion Island is
289 the object of ongoing research. Life table response experiment analyses (e.g., Koons et al.
290 2016) and their extension to IPMs (Koons et al. 2017) will aid our ecological understanding

of the observed changes in the population trajectory by revealing the contribution of different demographic parameters to variation in realized population growth rates.

Overall, we hope that our proposal will foster the application of integrated population models to polygynous species for a better understanding of the demography of social species.

ACKNOWLEDGMENTS

This research is part of a doctoral thesis of the first author, funded by CONICYT, PFCHA/DOCTORADO BECAS CHILE/2016-72170563. We thank Marion Island Marine Mammal Programme field personnel and the South African Department of Environmental Affairs for field support. The Department of Science and Technology of South Africa provided funding for elephant seal research at Marion Island through the National Research Foundation (NRF). Opinions expressed and conclusions arrived at, are those of the authors and are not necessarily to be attributed to the NRF.

LITERATURE CITED

Ainley DG, Blight LK (2009) Ecological repercussions of historical fish extraction from the Southern Ocean. Fish and Fisheries 10:13–38. doi: 10.1111/j.1467-2979.2008.00293.x

Authier M, Delord K, Guinet C (2011) Population trends of female Elephant Seals breeding on the Courbet Peninsula, îles Kerguelen. Polar Biology 34:319–328. doi: 10.1007/s00300-010-0881-1

Besbeas P, Freeman SN, Morgan BJT, Catchpole EA (2002) Integrating mark-recapture-recovery and census data to estimate animal abundance and demographic parameters. Biometrics 58:540–547

314 Bester M, de Bruyn P, Oosthuizen W, et al (2011) The Marine Mammal Programme at the
315 Prince Edward Islands: 38 years of research. African Journal of Marine Science 33:511–521.
316 doi: 10.2989/1814232X.2011.637356

317 Boyd IL (2000) State-dependent fertility in pinnipeds: contrasting capital and income
318 breeders. Functional Ecology 14:623–630. doi: 10.1046/j.1365-2435.2000.t01-1-00463.x

319 Casey C, Charrier I, Mathevon N, Reichmuth C (2015) Rival assessment among northern
320 elephant seals: evidence of associative learning during male–male contests. Royal Society
321 Open Science 2:150228. doi: 10.1098/rsos.150228

322 Clutton-Brock TH (1989) Review Lecture: Mammalian mating systems. Proceedings of the
323 Royal Society of London B Biological Sciences 236:339–372. doi: 10.1098/rspb.1989.0027

324 Davison AC, Hinkley DV (1997) Bootstrap Methods and Their Application. Cambridge
325 University Press

326 de Bruyn PJN, Tosh CA, Bester MN, et al (2011) Sex at sea: alternative mating system in an
327 extremely polygynous mammal. Animal Behaviour 82:445–451. doi:
328 10.1016/j.anbehav.2011.06.006

329 Fabiani A, Galimberti F, Sanvito S, Hoelzel AR (2004) Extreme polygyny among southern
330 elephant seals on Sea Lion Island, Falkland Islands. Behav Ecol 15:961–969. doi:
331 10.1093/beheco/arh112

332 Ferrari MA, Lewis MN, Pascual MA, Campagna C (2009) Interdependence of social structure
333 and demography in the southern elephant seal colony of Península Valdés, Argentina. Marine
334 Mammal Science 25:681–692. doi: 10.1111/j.1748-7692.2008.00268.x

335 Galimberti F, Fabiani A, Sanvito S (2002) Measures of breeding inequality: a case study in

336 southern elephant seals. Can J Zool 80:1240–1249. doi: 10.1139/z02-117

337 Galliard J-FL, Fitze PS, Ferrière R, Clobert J (2005) Sex ratio bias, male aggression, and
338 population collapse in lizards. PNAS 102:18231–18236. doi: 10.1073/pnas.0505172102

339 Gerber LR (2006) Including behavioral data in demographic models improves estimates of
340 population viability. Frontiers in Ecology and the Environment 4:419–427. doi:
341 10.1890/1540-9295(2006)4[419:IBDIDM]2.0.CO;2

342 Gerber LR, White ER (2014) Two-sex matrix models in assessing population viability: when
343 do male dynamics matter? Journal of Applied Ecology 51:270–278. doi: 10.1111/1365-
344 2664.12177

345 González-Suárez M, Gerber LR (2008) A Behaviorally Explicit Demographic Model
346 Integrating Habitat Selection and Population Dynamics in California Sea Lions. Conservation
347 Biology 22:1608–1618. doi: 10.1111/j.1523-1739.2008.00995.x

348 Hickey JR, Sollmann R (2018) A new mark-recapture approach for abundance estimation of
349 social species. PLOS ONE 13:e0208726. doi: 10.1371/journal.pone.0208726

350 Jenouvrier S, Caswell H, Barbraud C, Weimerskirch H (2010) Mating Behavior, Population
351 Growth, and the Operational Sex Ratio: A Periodic Two-Sex Model Approach. The American
352 Naturalist 175:739–752. doi: 10.1086/652436

353 Kappeler PM, van Schaik CP (2002) Evolution of Primate Social Systems. International
354 Journal of Primatology 23:707–740. doi: 10.1023/A:1015520830318

355 Koons DN, Arnold TW, Schaub M (2017) Understanding the demographic drivers of realized
356 population growth rates. Ecological Applications 27:2102–2115. doi: 10.1002/eap.1594

357 Koons DN, Iles DT, Schaub M, Caswell H (2016) A life-history perspective on the

358 demographic drivers of structured population dynamics in changing environments. Ecology
359 Letters 19:1023–1031. doi: 10.1111/ele.12628

360 Le Boeuf BJ, Laws RM (eds) (1994) Elephant seals: population ecology, behavior, and
361 physiology. University of California Press, Berkeley

362 Lewis M, Campagna C, Zavatti J (2004) Annual cycle and inter-annual variation in the haul-
363 out pattern of an increasing southern elephant seal colony. Antarctic Science 16:219–226. doi:
364 10.1017/S0954102004002020

365 McMahon CR, Bester MN, Hindell MA, et al (2009) Shifting trends: detecting
366 environmentally mediated regulation in long-lived marine vertebrates using time-series data.
367 Oecologia 159:69–82. doi: 10.1007/s00442-008-1205-9

368 Milner-Gulland EJ, Bukreeva OM, Coulson T, et al (2003) Reproductive collapse in saiga
369 antelope harems. Nature 422:135. doi: 10.1038/422135a

370 Mulaudzi TW, Hofmeyr GJG, Bester MN, et al (2008) Haulout site selection by southern
371 elephant seals at Marion Island. African Zoology 43:25–33. doi:
372 10.1080/15627020.2008.11407403

373 Mysterud A, Coulson T, Stenseth NC (2002) The role of males in the dynamics of ungulate
374 populations. Journal of Animal Ecology 71:907–915. doi: 10.1046/j.1365-2656.2002.00655.x

375 Oosthuizen WC, Postma M, Altwegg R, et al (2019a) Individual heterogeneity in life-history
376 trade-offs with age at first reproduction in capital breeding elephant seals. In review in
377 Population Ecology.

378 Oosthuizen WC, Pradel R, Bester MN, de Bruyn PJN (2019b) Making use of multiple
379 surveys: Estimating breeding probability using a multievent-robust design capture–recapture

model. Ecology and Evolution 9:836–848. doi: 10.1002/ece3.4828

Pistorius PA, Bester MN (2002) Juvenile survival and population regulation in southern elephant seals at Marion Island. African Zoology 37:35–41. doi: 10.1080/15627020.2002.11657152

Pistorius PA, Bester MN, Kirkman SP (1999) Survivorship of a declining population of southern elephant seals, *Mirounga leonina*, in relation to age, sex and cohort. Oecologia 121:201–211. doi: 10.1007/s004420050922

Pistorius PA, Bruyn P de, Bester MN (2011) Population dynamics of southern elephant seals: a synthesis of three decades of demographic research at Marion Island. African Journal of Marine Science 33:523–534. doi: 10.2989/1814232X.2011.637357

Pradel R (2005) Multievent: an extension of multistate capture-recapture models to uncertain states. Biometrics 61:442–7. doi: 10.1111/j.1541-0420.2005.00318.x

Schaub M, Abadi F (2011) Integrated population models: a novel analysis framework for deeper insights into population dynamics. J Ornithol 152:227–237. doi: 10.1007/s10336-010-0632-7

Shyu E, Caswell H (2018) Mating, births, and transitions: a flexible two-sex matrix model for evolutionary demography. Popul Ecol 60:21–36. doi: 10.1007/s10144-018-0615-8

Skinner JD, van Aarde RJ (1983) Observations on the Trend of the Breeding Population of Southern Elephant Seals, *Mirounga leonina*, at Marion Island. Journal of Applied Ecology 20:707–712. doi: 10.2307/2403121

Tenan S, Iemma A, Bragalanti N, et al (2016) Evaluating mortality rates with a novel integrated framework for nonmonogamous species: Mortality in Nonmonogamous Species.

402 Conservation Biology 30:1307–1319. doi: 10.1111/cobi.12736

403 Tongen A, Zubillaga M, Rabinovich J (2016) A two-sex matrix population model to represent
404 harem structure. Mathematical Biosciences and Engineering 13:1077–1092. doi:
405 10.3934/mbe.2016031

406 Vucetich JA, Peterson RO, Waite TA (1997) Effects of Social Structure and Prey Dynamics
407 on Extinction Risk in Gray Wolves. Conservation Biology 11:957–965. doi: 10.1046/j.1523-
408 1739.1997.95366.x

409 Wilkinson IS, van Aarde RJ (1999) Marion Island elephant seals: the paucity-of-males
410 hypothesis tested. Can J Zool 77:1547–1554. doi: 10.1139/z99-127

411 Zeigler SL, Walters JR (2014) Population models for social species: lessons learned from
412 models of Red-cockaded Woodpeckers (*Picoides borealis*). Ecological Applications 24:2144–
413 2154. doi: 10.1890/13-1275.1

414 Zipkin EF, Saunders SP (2018) Synthesizing multiple data types for biological conservation
415 using integrated population models. Biological Conservation 217:240–250. doi:
416 10.1016/j.biocon.2017.10.017

417

418 TABLE 1: Model comparison and parameter estimates for the southern elephant seal analysis.
419 We provide estimates with 95% confidence intervals for the parameters of the integrated
420 population model (IPM) and a model with count data only in which parameter *a* is either fixed
421 to infinity (*a* = 1,000) or estimated. The p-value of a likelihood-ratio test (LRT) for the null
422 hypothesis that *a* is infinite is given.

	IPM	**IPM *a* fixed**	**Count model**	**Count model *a* fixed**
deviance	43166.99	43170.68	1.96	2.04
LRT p-value	0.05		0.79	
a	-0.99 (-1.18; -0.83)	-	-2.08 (-5.47; -0.88)	-
σ	1.63 (0.61; 4.35)	10.29 (3.85; 28.50)	1.62 (0.61; 4.31)	1.61 (0.63; 4.48)
ϕ_{a0}	0.60 (0.59; 0.61)	0.60 (0.59; 0.61)	-	-
ϕ_{a1}	0.76 (0.75; 0.78)	0.76 (0.75; 0.78)	-	-
ϕ_{a2}	0.78 (0.77; 0.79)	0.78 (0.77; 0.79)	-	-
ϕ_{a3}	0.79 (0.77; 0.81)	0.79 (0.77; 0.81)	-	-
ϕ_{a4}	0.71 (0.68; 0.74)	0.71 (0.68; 0.74)	-	-
ϕ	0.76 (0.75; 0.77)	0.76 (0.75; 0.77)	-	-
ψ_{B2}	0.31 (0.29; 0.32)	0.31 (0.29; 0.32)	-	-
ψ_{B3}	0.68 (0.65; 0.70)	0.67 (0.65; 0.70)	-	-
ψ_{B4}	0.56 (0.52; 0.61)	0.56 (0.52; 0.61)	-	-
ψ_{B}	0.82 (0.80; 0.83)	0.82 (0.80; 0.83)	-	-
ψ_{NB}	0.73 (0.68; 0.76)	0.73 (0.68; 0.76)	-	-
p_{PB}	0.78 (0.77; 0.78)	0.78 (0.77; 0.78)	-	-
p_{B}	0.91 (0.89; 0.93)	0.91 (0.89; 0.93)	-	-
p_{NB}	0.87 (0.77; 0.93)	0.87 (0.77; 0.93)	-	-

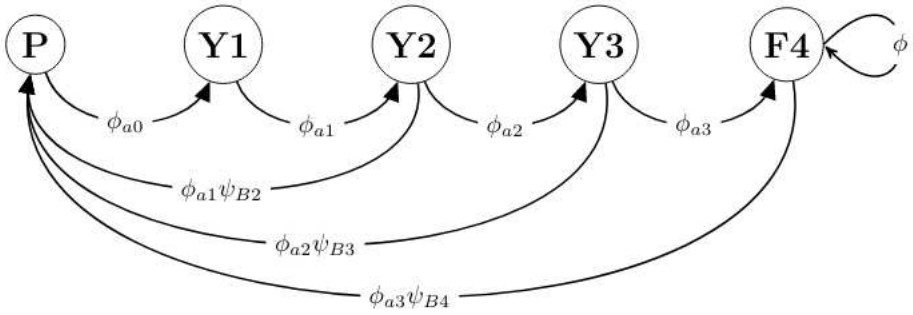

423

424 FIGURE 1: Southern elephant seal life cycle diagram. The states of development of females are
425 represented by P: pups, Y1: 1-year old females, Y2: 2-year old females, Y3: 3-year old
426 females and F4: females ≥ 4-years old.

427

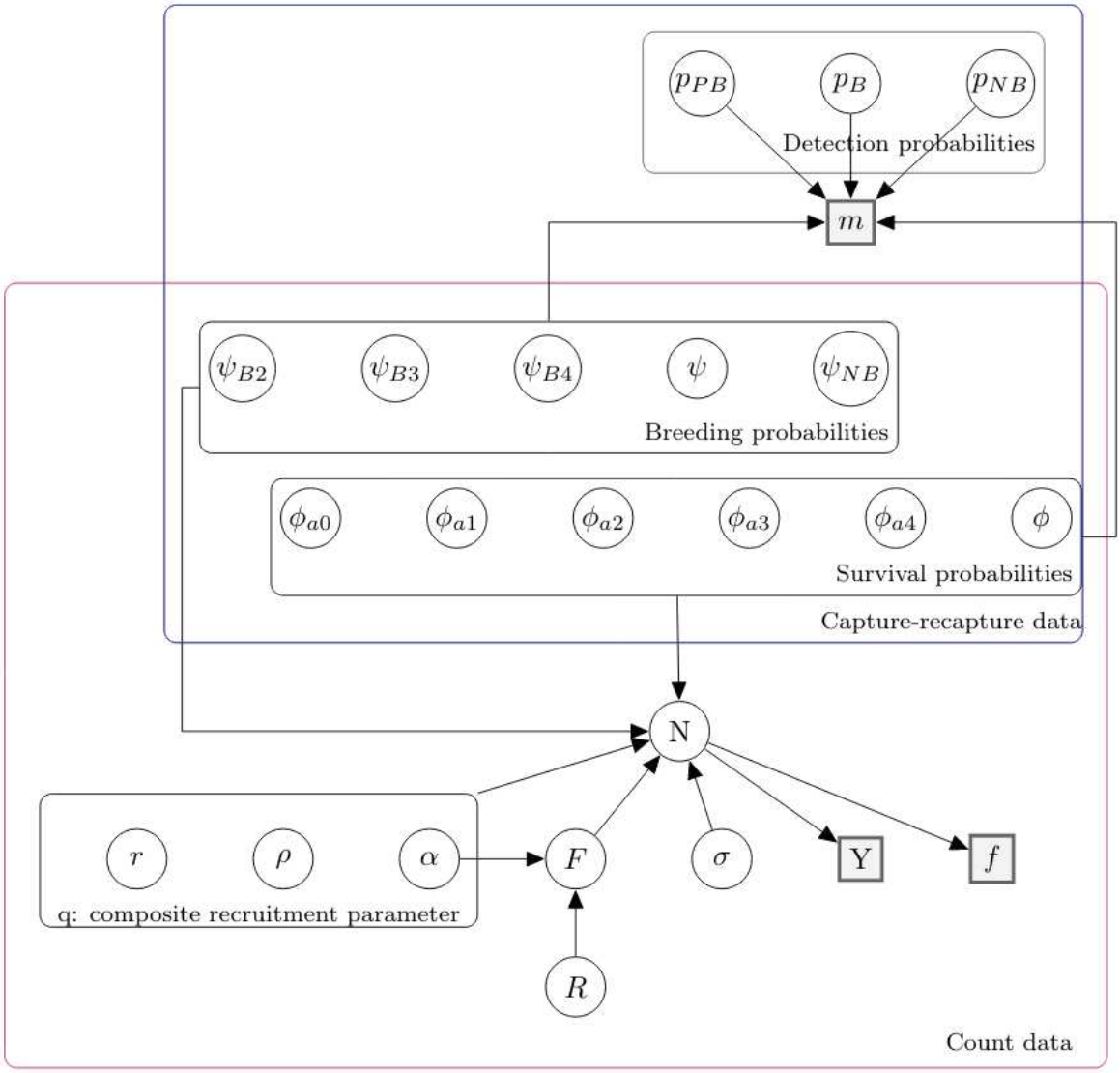

428

429 FIGURE 2: Directed Acyclic Graph (DAG) displaying the parameters and data used in the
430 IPM. *m* stands for the capture-recapture data, *Y* is for the pup counts data, *f* is for female
431 counts data. The notation for the model parameters are given in the main text.

432

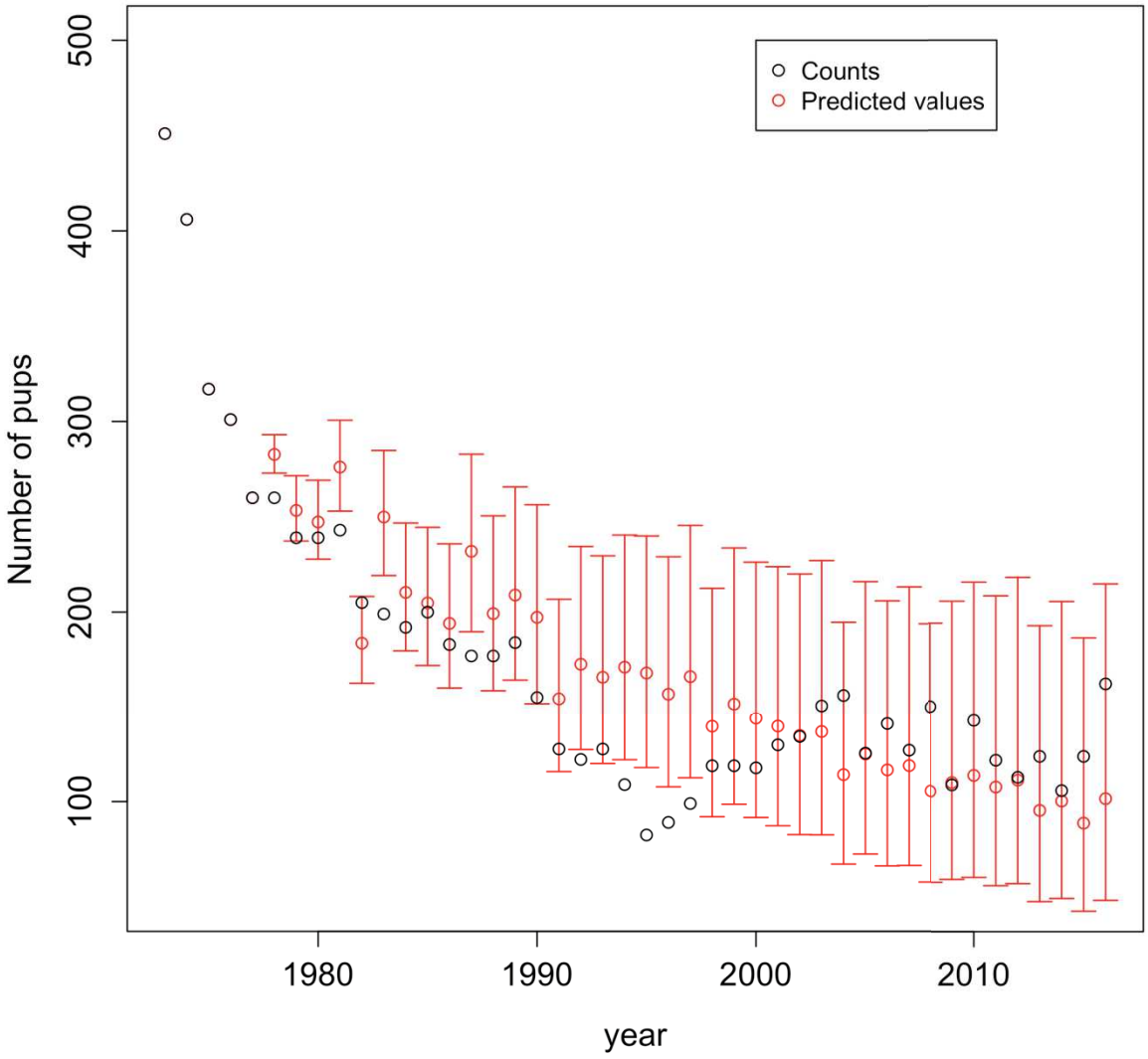

FIGURE 3: The number of southern elephants seal pups born at Marion Island from 1973 to 2016. We compare the observed counts (in black) vs. the predicted counts (in red) with 95% confidence intervals from the IPM combining both count and capture-recapture data. Note that there are no estimates for the first five years – see equation (4).

Chapter 4: OBJECTIF 3

Décrire et quantifier les réseaux sociaux animaux quand la détectabilité est imparfaite

4.1 ARTICLE 3. Inferring animal social networks with imperfect detection

Résumé

L'analyse de réseau social fournit un outil puissant pour comprendre l'organisation sociale des animaux. Cependant, dans les populations en liberté, il est presque impossible de surveiller de manière exhaustive les individus d'une population et de suivre leurs associations. Ignorer le problème de la détection individuelle imparfaite et éventuellement hétérogène peut conduire à un biais substantiel dans les mesures standards des caractéristiques d'un réseau social. Ici nous proposons un modèle à espace d'états pour analyser des données de capture-recapture et décrire un réseau social. Nous réalisons une étude de simulation pour valider notre approche. En outre, nous montrons comment la visualisation des réseaux et le calcul de métriques standards peuvent bénéficier de la prise en compte les probabilités de détection. La méthode est illustrée par les données d'une population de dauphins de Commerson (*Cephalorynchus commersonii*) en Patagonie Argentine. Notre approche constitue un pas en avant vers un cadre statistique général pour l'analyse des réseaux sociaux de populations d'animaux sauvages.

Mots-clés: Inférence bayésienne, Capture-recapture, modèles multiétats, réseau social.

Ecological Modelling 401 (2019) 69–74

Contents lists available at ScienceDirect

Ecological Modelling

journal homepage: www.elsevier.com/locate/ecolmodel

Inferring animal social networks with imperfect detection

Olivier Gimenez[a,*], Lorena Mansilla[a], M. Javier Klaich[b], Mariano A. Coscarella[b,c], Susana N. Pedraza[c], Enrique A. Crespo[b,c]

[a] CEFE, CNRS, Univ Montpellier, Univ Paul Valéry Montpellier 3, EPHE, IRD, Montpellier, France
[b] Facultad de Ciencias Naturales y de la Salud, Universidad Nacional de la Patagonia San Juan Bosco, Blvd. Brown 3051, 9120, Puerto Madryn, Chubut, Argentina
[c] Laboratorio de Mamíferos Marinos, CESIMAR, CONICET, Blvd. Brown 2915, 9120 Puerto Madryn, Chubut, Argentina

ARTICLE INFO

Keywords:
Bayesian inference
Capture-recapture
Multistate models
Social networks

ABSTRACT

Social network analysis provides a powerful tool for understanding social organisation of animals. However, in free-ranging populations, it is almost impossible to monitor exhaustively the individuals of a population and to track their associations. Ignoring the issue of imperfect and possibly heterogeneous individual detection can lead to substantial bias in standard network measures. Here, we develop capture-recapture models to analyse network data while accounting for imperfect and heterogeneous detection. We carry out a simulation study to validate our approach. In addition, we show how the visualisation of networks and the calculation of standard metrics can account for detection probabilities. The method is illustrated with data from a population of Commerson's dolphin (*Cephalorhynchus commersonii*) in Patagonia Argentina. Our approach provides a step towards a general statistical framework for the analysis of social networks of wild animal populations.

1. Introduction

Knowledge of the social organisation of animal populations is essential to develop sound conservation and management strategies as social structure affects habitat use, information diffusion, as well as the genetic composition and the spread of information and diseases within these populations (Krause and Ruxton, 2002).

Social network analysis (SNA; Croft et al., 2008; Whitehead, 2008) has recently known an increasing number of applications to characterize in particular the social structure of animal populations. SNA allows the study of social networks through their visualisation and the calculation of several descriptive statistics, with important applications in ecology, evolution, epidemiology and behavioural ecology (Craft and Caillaud, 2011; Farine and Whitehead, 2015; Krause et al., 2007; Sih et al., 2009; Wey et al., 2008).

In free-ranging populations however, individuals may or may not be seen (or recaptured) at various times over a study period. This raises the issue of detectability less than one that makes it difficult to track associations between individuals. In other words, when one or two individuals of a dyad are missed, were they associated or not? Besides being imperfect, detection is often heterogeneous due to variation in individual traits such as, e.g., sex (Tavecchia et al., 2001), social status (Cubaynes et al., 2010; Hickey and Sollmann, 2019), infection status (Marescot et al., 2018) or pair-bond status (Choquet and Gimenez, 2012; Culina et al., 2013). Overall, ignoring the issue of imperfect and heterogeneous individual detection can lead to substantial bias in estimating the probability of association between individuals (Hoppitt and Farine, 2018; Lusseau et al., 2008; Weko, 2018).

To address these issues, Klaich et al. (2011) developed a capture-recapture model where detection probabilities of individuals in dyads varied between individuals that are associated and those that are not. Their approach requires complex probabilistic calculations that make it specific to their case study, and therefore difficult to extend to other situations. Here, we use a state-space modelling (SSM) approach (e.g., Buckland et al., 2004) to acknowledge that data on associations between individuals derived from field studies are imperfect observations of the underlying social structure. Specifically, the SSM approach makes the two-component process underlying network structure explicit: i) the temporal dynamic of associations between individuals and ii) the observations generated from the underlying process in i).

We apply the SSM framework to capture-recapture (CR) data (Gimenez et al., 2007) to analyse network data while accounting for imperfect and heterogeneous detection of individuals. We estimate dyad association probability and distinguish the dynamic of associated vs. non-associated states from their partial observation. We carry out a simulation study to assess bias in the association probability. Last, we show how the visualisation and the calculation of standard network metrics can account for detection probabilities. The approach is

* Corresponding author at: CEFE, 1919 route de Mende, 34293, Montpellier, France.
E-mail address: olivier.gimenez@cefe.cnrs.fr (O. Gimenez).

https://doi.org/10.1016/j.ecolmodel.2019.04.001
Received 11 January 2019; Received in revised form 30 March 2019; Accepted 1 April 2019

illustrated with data from a population of Commerson's dolphin (*Cephalorhynchus commersonii*) in Patagonia Argentina.

2. Model development

2.1. State-space modelling of capture-recapture data

Following Klaich et al. (2011), we derived dyad association histories from individual captures and non-captures. For example, let us assume a 4-occasion CR experiment in which two individuals have capture histories '1011' and '1001' where a '1' stands for an individual detection and '0' for a non-detection. We considered that behavioural interactions between individuals occurred within groups ('gambit of the group' *sensu* Whitehead and Dufault, 1999). Let us assume that these two individuals were both detected in the same group at the first occasion but in a different group at the last one, then the association history for this particular dyad is '2013' where '0' stands for none of the two individuals of a dyad are seen, '1' for one individual only of the dyad is seen, '2′ for the two individuals of a dyad are seen associated and '3' for the two individuals of a dyad are seen non-associated.

To analyse these dyadic data, we implemented a SSM formulation (Gimenez et al., 2007) of multistate CR models (Lebreton et al., 2009) for closed populations. We considered two states A and B for 'dyad associated' and 'dyad non-associated' respectively. We denoted x_t^i, a multinomial trial taking values (1,0) or (0,1) if, at time t, dyad i is in state A or B respectively. Given the underlying states, a dyad may be recaptured in the observations 0, 1, 2 or 3 defined above considering imperfect detection. We denoted y_t^i, a multinomial trial taking values (1,0,0,0), (0,1,0,0), (0,0,1,0), (0,0,0,1) if, at time t, dyad i is observed as a 0, 1, 2 or 3. The state–space model relies on a combination of two equations. First, the state equation specifies the state of dyad i at time t given its state at time $t-1$:

$$x_t^i \sim \text{Multinomial}(1, \Psi x_{t-1}^i)$$

where Ψ gathers the probabilities for a dyad of staying associated and non-associated between two successive occasions (Table 1a). We also defined the probability π for a dyad of being in initial state associated. Second, the observation equation specifies the observation of dyad i at time t given its state at time t:

$$y_t^i \sim \text{Multinomial}(1, Px_t^i)$$

where P gathers the detection probabilities and of an individual being associated and non-associated in a dyad (Table 1b).

Table 1
Transition matrices used in the state and observation equations of the state-space CR network model. States A and B are for associated and non-associated. Parameters p and ψ are the detection and transition probabilities.

a) State matrix

Previous occasion	Current occasion	
	A	B
A	ψ^{AA}	$1-\psi^{AA}$
B	$1-\psi^{BB}$	ψ^{BB}

b) Observation matrix P

Current occasion	Current occasion			
	0	1	2	3
A	$(1-p^A)(1-p^A)$	$2p^A(1-p^A)$	p^Ap^A	0
B	$(1-p^B)(1-p^B)$	$2p^B(1-p^B)$	0	p^Bp^B

Table 2
Bias in parameter estimates for the homogeneous scenarios.

scenario	p	π	ψ^{AA}	ψ^{BB}	bias p	bias π	bias ψ^{AA}	bias ψ^{BB}
1	0.3	0.2	0.1	0.1	0.50	26.49	120.98	58.77
2	0.8	0.2	0.1	0.1	0.08	9.46	4.37	1.36
3	0.3	0.7	0.1	0.1	−0.33	−1.23	142.04	22.83
4	0.8	0.7	0.1	0.1	−0.21	−3.23	8.91	−0.04
5	0.3	0.2	0.4	0.1	0.07	14.73	27.30	53.03
6	0.8	0.2	0.4	0.1	−0.04	1.02	−1.65	4.74
7	0.3	0.7	0.4	0.1	0.60	−10.96	65.19	26.16
8	0.8	0.7	0.4	0.1	−0.04	−0.37	−8.88	0.79
9	0.3	0.2	0.9	0.1	0.29	4.46	−23.10	37.30
10	0.8	0.2	0.9	0.1	0.11	2.29	−5.57	7.26
11	0.3	0.7	0.9	0.1	−0.25	0.30	−14.44	28.57
12	0.8	0.7	0.9	0.1	0.07	−0.55	−7.99	3.91
13	0.3	0.2	0.1	0.4	−0.74	54.58	45.20	24.95
14	0.8	0.2	0.1	0.4	−0.08	6.23	2.19	4.71
15	0.3	0.7	0.1	0.4	0.27	−25.83	29.36	7.66
16	0.8	0.7	0.1	0.4	−0.11	−11.71	3.05	1.72
17	0.3	0.2	0.4	0.4	0.45	14.96	10.59	21.80
18	0.8	0.2	0.4	0.4	−0.09	3.22	−1.45	−0.27
19	0.3	0.7	0.4	0.4	0.64	−13.37	5.67	5.96
20	0.8	0.7	0.4	0.4	0.02	0.24	−1.44	−0.71
21	0.3	0.2	0.9	0.4	−0.26	8.35	−17.84	−28.74
22	0.8	0.2	0.9	0.4	0.01	1.28	−1.62	−1.72
23	0.3	0.7	0.9	0.4	0.45	−1.59	−10.12	−5.75
24	0.8	0.7	0.9	0.4	−0.08	−0.52	−2.47	−0.54
25	0.3	0.2	0.1	0.9	0.94	38.86	21.21	−1.08
26	0.8	0.2	0.1	0.9	0.08	8.48	2.90	0.87
27	0.3	0.7	0.1	0.9	0.11	−47.67	10.35	−2.45
28	0.8	0.7	0.1	0.9	−0.34	2.48	1.29	−0.87
29	0.3	0.2	0.4	0.9	−0.46	11.66	−4.68	−16.83
30	0.8	0.2	0.4	0.9	−0.22	2.55	−0.36	−1.68
31	0.3	0.7	0.4	0.9	−0.27	−6.82	−7.96	−7.75
32	0.8	0.7	0.4	0.9	0.04	−1.00	−0.86	−1.29
33	0.3	0.2	0.9	0.9	1.18	3.33	−30.90	−55.94
34	0.8	0.2	0.9	0.9	0.12	0.47	−1.45	−2.53
35	0.3	0.7	0.9	0.9	−0.74	−3.30	−20.09	−38.39
36	0.8	0.7	0.9	0.9	−0.16	−1.19	−0.85	−1.26

2.2. Bayesian fitting using MCMC methods

We used Bayesian theory in conjunction with Markov Chain Monte Carlo (MCMC) methods to carry out inference. Inference was based on empirical medians and credible intervals. As a by-product of the MCMC simulations, we also obtained numerical summaries for any function of the parameters, in particular the metrics describing the network structure.

2.3. Calculating network measures while accounting for imperfect detection

In SNA, a wide range of descriptive statistics can be used to characterize the properties of the structure of a network. Here, we focused on four of them. We used for each animal in the network the number of other animals with which it was associated – *degree* – and the number of shortest paths between pairs of animals that passed through it – *betweeness*. In addition, we quantified the degree to which an animal's immediate neighbours were associated – *cluster coefficient* – and the average of all path lengths between all pairs of animals in the network – *average path length* (Croft et al., 2008). These measures are useful to characterize the properties of a network regarding the spread of disease or information (Craft and Caillaud, 2011; Watts and Strogatz, 1998).

A feature of MCMC algorithms is that the dyad states x_t^i's are treated as parameters to be estimated, just like the transition and detection probabilities. We generated values from the posterior distributions of the dyads' states, which, in turn, were used to visualize the network and characterize its structure over time. Specifically, for each MCMC iteration, we calculated the degree and betweeness for each individual (R package sna; Butts, 2008), as well as the clustering coefficient and the average path length (R package igraph; Csardi and Nepusz, 2006),

Table 3
Bias in parameter estimates for the heterogeneous scenarios.

scenario	p^A	p^B	π	ψ^{AA}	ψ^{BB}	bias p^A	bias p_B	bias π	bias ψ^{AA}	bias ψ^{BB}
1	0.3	0.8	0.2	0.1	0.1	0.59	−0.24	4.67	5.86	5.61
2	0.3	0.8	0.7	0.1	0.1	0.18	−0.39	−6.01	1.17	12.27
3	0.3	0.8	0.2	0.4	0.1	−0.16	−0.65	−2.13	−6.94	2.94
4	0.3	0.8	0.7	0.4	0.1	0.84	−0.49	−25.65	−2.16	4.77
5	0.3	0.8	0.2	0.9	0.1	−0.02	−2.53	−15.23	−6.76	1.87
6	0.3	0.8	0.7	0.9	0.1	0.67	−14.33	−131.51	−8.99	8.40
7	0.3	0.8	0.2	0.1	0.4	−0.11	0.34	2.82	9.96	6.86
8	0.3	0.8	0.7	0.1	0.4	1.55	0.30	−0.32	2.34	0.53
9	0.3	0.8	0.2	0.4	0.4	−0.65	−0.69	0.88	−2.29	2.30
10	0.3	0.8	0.7	0.4	0.4	1.41	−1.75	−3.50	−2.06	7.67
11	0.3	0.8	0.2	0.9	0.4	0.49	−0.06	2.86	−3.88	−0.25
12	0.3	0.8	0.7	0.9	0.4	0.81	−4.39	−11.31	−1.57	2.71
13	0.3	0.8	0.2	0.1	0.9	4.24	−0.21	0.26	27.14	−1.08
14	0.3	0.8	0.7	0.1	0.9	1.63	−0.22	−0.49	1.94	−2.15
15	0.3	0.8	0.2	0.4	0.9	7.33	−0.96	−1.02	−1.77	0.34
16	0.3	0.8	0.7	0.4	0.9	−0.05	−0.38	−1.43	−1.41	−0.78
17	0.3	0.8	0.2	0.9	0.9	−1.53	−0.24	0.43	−8.22	−0.36
18	0.3	0.8	0.7	0.9	0.9	0.84	−0.48	0.53	−1.08	−1.45
19	0.8	0.3	0.2	0.1	0.1	−0.39	−0.01	11.75	4.63	3.82
20	0.8	0.3	0.7	0.1	0.1	0.03	−0.63	4.72	1.48	7.67
21	0.8	0.3	0.2	0.4	0.1	0.47	0.73	16.29	3.33	3.73
22	0.8	0.3	0.7	0.4	0.1	0.52	−1.16	−0.14	1.50	5.51
23	0.8	0.3	0.2	0.9	0.1	0.00	0.04	17.21	−2.35	2.46
24	0.8	0.3	0.7	0.9	0.1	−0.13	1.98	−8.68	0.17	4.71
25	0.8	0.3	0.2	0.1	0.4	−0.94	0.38	2.54	11.96	−26.02
26	0.8	0.3	0.7	0.1	0.4	−0.79	−0.64	−0.89	1.91	−11.83
27	0.8	0.3	0.2	0.4	0.4	−0.91	−0.14	5.53	8.95	−3.96
28	0.8	0.3	0.7	0.4	0.4	−0.52	0.57	−0.87	1.32	−3.13
29	0.8	0.3	0.2	0.9	0.4	−0.48	1.01	2.13	−3.45	0.13
30	0.8	0.3	0.7	0.9	0.4	−0.48	0.58	−1.17	0.17	−1.46
31	0.8	0.3	0.2	0.1	0.9	−30.02	21.00	27.86	112.23	−196.71
32	0.8	0.3	0.7	0.1	0.9	−1.90	0.23	2.38	1.93	−8.34
33	0.8	0.3	0.2	0.4	0.9	−9.87	2.22	7.98	27.76	−6.73
34	0.8	0.3	0.7	0.4	0.9	−1.40	0.28	0.70	1.65	−1.85
35	0.8	0.3	0.2	0.9	0.9	0.14	−0.29	0.86	−8.69	−1.06
36	0.8	0.3	0.7	0.9	0.9	0.22	0.16	−0.41	−0.32	−1.45

Table 4
Parameters estimates (posterior medians) with 95% credible intervals for the Commerson's dolphin case study.

Parameter	Estimate with 95% credible interval				
	Occasion 1	Occasion 2	Occasion 3	Occasion 4	Occasion 5
Average path length	1.31 [1.25; 1.38]	1.65 [1.54; 1.79]	1.61 [1.57; 1.66]	1.60 [1.55; 1.65]	1.61 [1.56; 1.66]
Clustering coefficient	0.68 [0.61; 0.74]	0.36 [0.27; 0.45]	0.42 [0.39; 0.45]	0.39 [0.35; 0.43]	0.40 [0.36; 0.43]
Individual detection	0.27 [0.26; 0.28]	0.11 [0.10; 0.12]	0.44 [0.42; 0.45]	0.17 [0.16; 0.18]	0.20 [0.19; 0.21]
Staying associated			0.33 [0.17; 0.50]		
Staying non-associated			0.57 [0.48; 0.69]		

hence obtaining the posterior distribution for each of these metrics. Data and codes are available on GitHub https://github.com/oliviergimenez/social_networks_capture_recapture.

3. Simulation study

We conducted a simulation study to assess the bias in parameter estimates. We considered a scenario where detection probabilities were homogeneous. We simulated 100 CR datasets with $\pi = 0.2, 0.7$, $\psi^{AA} = 0.1, 0.4, 0.9$ and $\psi^{BB} = 0.1, 0.4, 0.9$ and $p^A = p^B = 0.3, 0.8$ (in total, 36 different configurations) and to each simulated dataset we fitted a CR model with homogeneous detection probabilities. We also considered a heterogeneous scenario where all parameters were set to the same values as in the homogeneous scenarios, except the detection probabilities which we set to $p^A = 0.3$, $p^B = 0.8$ and $p^A = 0.8$, $p^B = 0.3$ (in total, 36 different configurations). We fitted a model with heterogeneous detection probabilities to these simulated datasets. For both the homogeneous and the heterogeneous scenarios, we calculated the relative bias of all parameters.

For the homogeneous scenarios, the bias decreased when detection increased (Table 2). Bias was negligible on detection, around +5% on the transition probabilities and around -13% on π in scenario 19 with $\psi^{BB} = 0.4$. When $\psi^{BB} = 0.9$ in scenario 31, the bias in π decreased by a factor 2. For the heterogeneous scenarios, the bias was negligible, except for scenario 31 in which the proportion of associated dyads was low and all dyads tended to remain non-associated (Table 3).

4. Case study

To illustrate our methodological approach, we used a real-world example as a case study. We used photo-identification data on a population of Commerson's dolphin (*C. commersonii*) that was monitored in the coastal waters near the Chubut River mouth (43∘20`_S, 65∘00`_W) in the Patagonian coast (Coscarella et al., 2003). Commerson's dolphins are particularly abundant in the area during the austral spring (Coscarella et al., 2010). The mean residence time in the sampling area was 15 days (SE = 6.4), therefore we sampled 5 times in October 2007 to unravel which individual was associated with which,

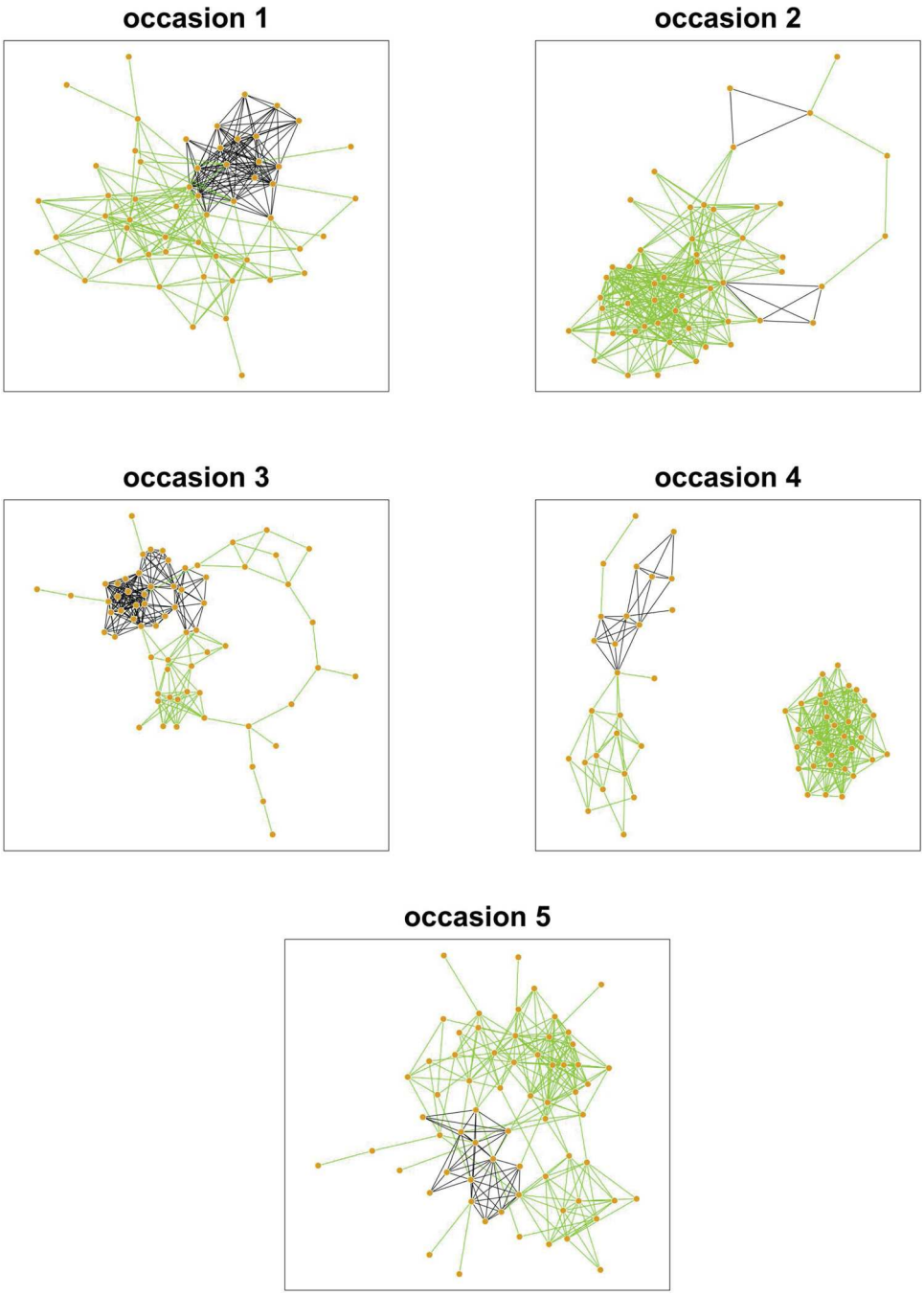

Fig. 1. Visualisation of the network for the Commerson's dolphin population, over five sampling occasions, for the year 2007, showing associations (lines) between individuals (orange circles). For each edge, we calculated the average number of times the corresponding dyad was estimated as being associated ($x = 1$) over the total number of MCMC simulations. Then, we displayed only the edges for which this number was larger than the 0.90 quantile of the distribution of x. Black edges are for observed dyads (also corresponding to $x = 1$ for simulations) while green edges are for dyads that are estimated to be associated (with probability 0.69, 0.39, 0.42, 0.42 and 0.40 for capture occasion 1, 2, 3, 4 and 5 respectively) but for which one or the two individuals were not detected. (For interpretation of the references to colour in this figure legend, the reader is referred to the web version of this article.).

while arriving and leaving the area together (Coscarella et al., 2011). Two individuals were considered associated when they were photo-identified during the same encounter, while they were considered not associated otherwise (Coscarella et al., 2011).

Over the study, a total of 71 dolphins were detected which led to 71*(71-1)/2 = 2485 association histories. Based on previous analyses (Klaich et al., 2011), we considered time-dependent state-independent individual detection probabilities. Individual detections varied between 11% and 44% (Table 4). The probability of staying associated was 33% while that of staying non-associated was 57% with very little overlap in the credible intervals (Table 4), suggesting a high turnover in the dynamic of associations and a fission-fusion social organization.

Along the five sampling occasions, the estimated network showed changes in its structure (Fig. 1). At occasions 1, 2, 3 and 5, the estimated network had a single component with a higher number of associated dyads at occasion 1 than at occasions 2, 3 and 5. Although the number of dyads was higher at occasion 1, all networks were fully connected (i.e. none individual or group of individuals were isolated from other individuals). At occasion 4, the network estimated had two components, isolated from each other (i.e. none of the individuals from one component was associated with any of the individuals in the other component). This suggests that at least two groups might exist having preferential associations between individuals inside each group.

Average path length was lower on the first sampling occasion than in the subsequent ones, while the reverse pattern was observed for the clustering coefficient (Table 4). These estimated values also suggest high individual connectivity and that the estimated social network has features related to a small-world type network. At the individual level, degree was heterogeneous (Fig. 2), with individuals spreading all over the range of its distribution (Fig. 2). In contrast, betweeness appeared relatively homogeneous, despite some dolphins with low betweeness and a single animal with very high betweeness (Fig. 2).

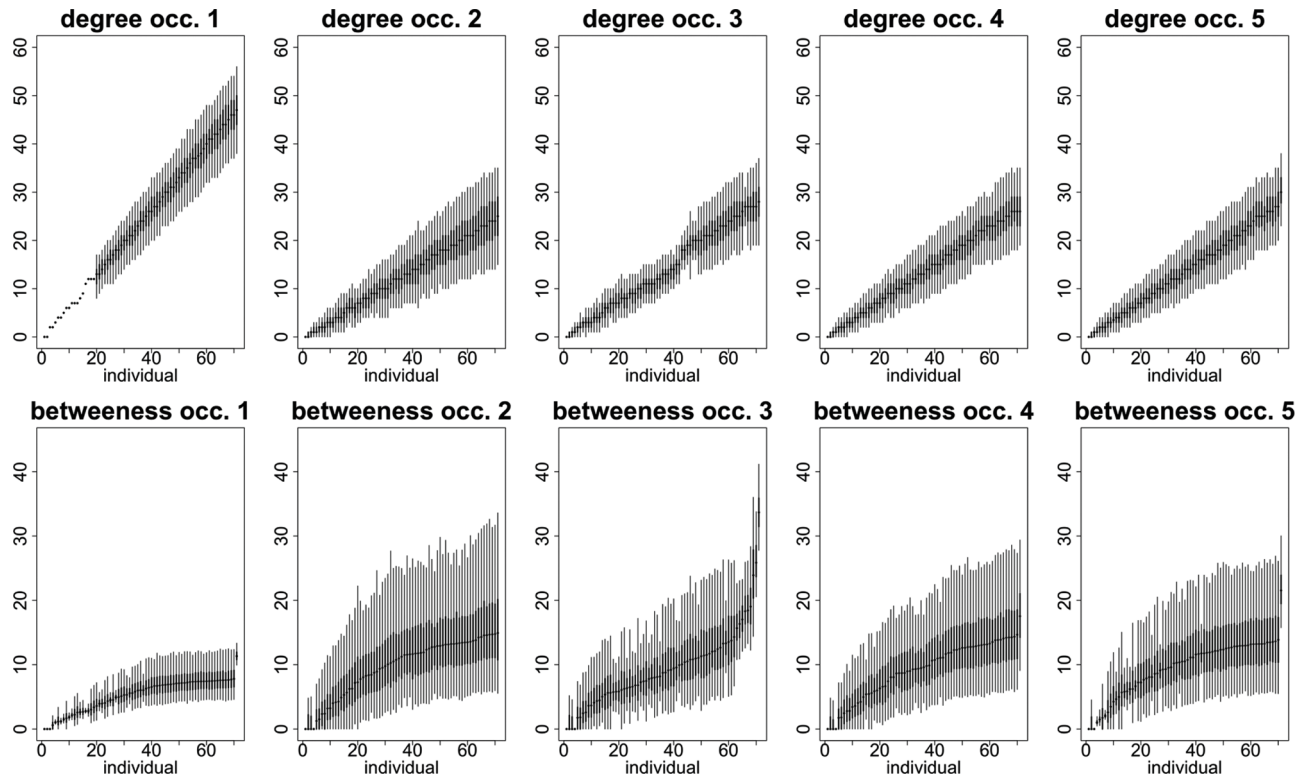

Fig. 2. Local properties of the Commerson's dolphin network. For each individual and for each of the 5 capture occasions, degree (top panels) and betweeness (bottom panels) are summarized with the posterior mean (circle), the 50% (thick line) and 95% (thin line) credible intervals.

5. Discussion

We have proposed a new statistical approach combining network analyses with CR models formulated as state-space models. Our framework has several appealing advantages. First and most importantly, ignoring imperfect and possibly heterogeneous detection may lead to biased results about the structure and dynamics of associations (see Fig. 1). Our CR model provides a robust method to estimate social networks. Second, in addition to social status, our model can easily incorporate individual-level traits such as age or sex through regression-like functions. This opens an avenue towards investigating the relationships between the phenotype and social position of individuals. Third, our method provides unbiased and precise estimates of relevant metrics to characterise the properties of social networks (see the Simulation study section), the whole process being controlled for imperfect and heterogeneous detection. Another appealing feature of our approach is the quantification of uncertainty associated to network measures under the form of Bayesian credible intervals (Table 2 and Fig. 2). Last, the social organisation can be visualised over time while accounting for imperfect detection, providing the opportunity for testing socio-ecological hypotheses in free-ranging animal populations. For example, the rapid turnover of the free ranging Commerson's dolphin groups has been previously proposed (Coscarella et al., 2011), and here we could identify this turnover within the fission-fusion society model.

When inspecting the results of the dolphin case study, there are advantages in adopting a CR approach to infer social networks. First, when it comes to visualizing the network, we illustrate in Fig. 1 what we would obtain with a standard approach with in black edges, while the green edges correspond to the dyads that are estimated to be associated with the new approach by correcting for imperfect detection. Clearly, the structure and dynamics of the network are different depending on whether we ignore imperfect detection (black edges only) or we consider the model-based estimated network (edges of both colors). Second, regarding network metrics, the only way to estimate degree and betweenness for all occasions when non-detections occur (Fig. 2) is to resort to a CR approach to account for missing values.

Our CR model requires data on individuals that can be uniquely identifiable. Identifying individuals can be achieved using non-invasive marking (such as coat patterns, body scars, or genetic profiling for mammals; e.g., Cubaynes et al., 2010; Marescot et al., 2018; Santostasi et al., 2016) or invasive marking (such as rings for birds, colouring for insects or passive integrated transponders for fishes; e.g., Băncilă et al., 2018; Buoro et al., 2010; Lagrange et al., 2014). The model also needs data on interactions or associations. Here, we rely on the 'gambit of the group' method which states that all individuals within a group of animals observed at a point in time are associated (Farine and Whitehead, 2015).

Our model relies on several assumptions. First, we have considered closed populations while demographic process might occur in animal populations. The extension of our model to open populations is feasible (Lebreton et al., 2009) to incorporate survival and dispersal, therefore allowing to assess the influence of social structure on fitness. Second, we assumed that association states were correctly assigned while some uncertainty might occur due to incomplete information. In the SSM framework, incorporating uncertainty in state assignment is relatively straightforward (Gimenez et al., 2012; Pradel, 2005). Third, we assumed independence of the association histories to form the SSM likelihood. To account for an individual effect, random effects can be incorporated in CR models (Choquet et al., 2013; Choquet and Gimenez, 2012; Gimenez and Choquet, 2010), which opens a promising avenue towards a general statistical framework for the analysis of animal social networks (Cross et al., 2012; Van Duijn et al., 2004).

Overall, we hope our proposal will foster applications of social network analysis to free-ranging animal population in behavioural ecology to describe social behaviour and social dynamics, in evolution ecology to explore the fitness consequences of the social positions of individuals and in epidemiological ecology to determine the

implications of network structure and dynamics in the spread of diseases.

Competing interests

The authors declare no competing interests.

Acknowledgements

This paper is dedicated to our colleague Dr. Susana N. Pedraza, who passed away while this work was being conducted. Logistic support was provided by Centro Nacional Patagónico (CONICET). This study was partially funded by the National Research Council of Argentina (CONICET-PIP 0742/98), Agencia Nacional de Promoción Científica y Tecnológica (01-04030A, 11679, and 33934), Fundación BBVA (BIOCON 04) and GEF Project CNP-BB 27. This work is part of the second author's doctoral thesis funded by CONICYT, PFCHA/DOCTORADO BECAS CHILE/2016-72170563. Fieldwork was authorised by the Dirección de Áreas Protegidas de la Provincia del Chubut.

References

Băncilă, R.I., Pradel, R., Choquet, R., Plăiaşu, R., Gimenez, O., 2018. Using temporary emigration to inform movement behaviour of cave-dwelling invertebrates: a case study of a cave harvestman species. Ecol. Entomol. 43, 551–559. https://doi.org/10.1111/een.12645.

Buckland, S.T., Newman, K.B., Thomas, L., Koesters, N.B., 2004. State-space models for the dynamics of wild animal populations. Ecol. Modell. 171, 157–175. https://doi.org/10.1016/j.ecolmodel.2003.08.002.

Buoro, M., Prévost, E., Gimenez, O., 2010. Investigating evolutionary trade-offs in wild populations of atlantic salmon (salmo salar): incorporating detection probabilities and individual heterogeneity. Evolution 64, 2629–2642. https://doi.org/10.1111/j.1558-5646.2010.01029.x.

Butts, C.T., 2008. Social network analysis with sna. J. Stat. Softw. 24. https://doi.org/10.18637/jss.v024.i06.

Choquet, R., Gimenez, O., 2012. Towards built-in capture-recapture mixed models in program E-SURGE. J. Ornithol. 152, 625–639.

Choquet, R., Sanz-Aguilar, A., Doligez, B., Nogué, E., Pradel, R., Gustafsson, L., Gimenez, O., 2013. Estimating demographic parameters from capture-recapture data with dependence among individuals within clusters. Methods Ecol. Evol. 4, 474–482. https://doi.org/10.1111/2041-210X.12030.

Coscarella, M.A., Dans, S.L., Crespo, E.A., Pedraza, S.N., 2003. Potential impact of unregulated dolphin watching activities in Patagonia. J. Cetacean Res. Manag. 77–84.

Coscarella, M.A., Pedraza, S.N., Crespo, E.A., 2010. Behavior and seasonal variation in the relative abundance of Commerson's dolphin (Cephalorhynchus commersonii) in northern Patagonia, Argentina. J. Ethol. 28, 463–470. https://doi.org/10.1007/s10164-010-0206-4.

Coscarella, M.A., Gowans, S., Pedraza, S.N., Crespo, E.A., 2011. Influence of body size and ranging patterns on delphinid sociality: associations among Commerson's dolphins. J. Mammal. 92, 544–551. https://doi.org/10.1644/10-MAMM-A-029.1.

Craft, M.E., Caillaud, D., 2011. network models: an underutilized tool in wildlife epidemiology? Interdiscip. Perspect. Infect. Dis. 2011, 1–12. https://doi.org/10.1155/2011/676949.

Croft, D.P., James, R., Krause, J., 2008. Exploring Animal Social Networks. Princeton University Press, Princeton, NJ.

Cross, P.C., Creech, T.G., Ebinger, M.R., Heisey, D.M., Irvine, K.M., Creel, S., 2012. Wildlife contact analysis: emerging methods, questions, and challenges. Behav. Ecol. Sociobiol. 66, 1437–1447. https://doi.org/10.1007/s00265-012-1376-6.

Csardi, G., Nepusz, T., 2006. The igraph software package for complex network research. InterJ. Complex Syst. 9.

Cubaynes, S., Pradel, R., Choquet, R., Duchamp, C., Gaillard, J.-M., Lebreton, J.-D., Marboutin, E., Miquel, C., Reboulet, A.-M., Poillot, C., Taberlet, P., Gimenez, O., 2010. Importance of accounting for detection heterogeneity when estimating abundance: the case of French wolves. Conserv. Biol. 24, 621–626. https://doi.org/10.1111/j.1523-1739.2009.01431.x.

Culina, A., Lachish, S., Pradel, R., Choquet, R., Sheldon, B.C., 2013. A multievent approach to estimating pair fidelity and heterogeneity in state transitions. Ecol. Evol. 3, 4326–4338. https://doi.org/10.1002/ece3.729.

Farine, D.R., Whitehead, H., 2015. Constructing, conducting and interpreting animal social network analysis. J. Anim. Ecol. 84, 1144–1163. https://doi.org/10.1111/1365-2656.12418.

Gimenez, O., Choquet, R., 2010. Incorporating individual heterogeneity in studies on marked animals using numerical integration: capture-recapture mixed models. Ecology 91, 951–957. https://doi.org/10.1007/s10336-010-0613-x.

Gimenez, O., Rossi, V., Choquet, R., Dehais, C., Doris, B., Varella, H., Vila, J.-P., Pradel, R., 2007. State-space modelling of data on marked individuals. Ecol. Modell. 206, 431–438. https://doi.org/10.1016/j.ecolmodel.2007.03.040.

Gimenez, O., Lebreton, J.-D., Gaillard, J.-M., Choquet, R., Pradel, R., 2012. Estimating demographic parameters using hidden process dynamic models. Theor. Popul. Biol. 82, 307–316.

Hickey, J.R., Sollmann, R., 2019. A new mark-recapture approach for abundance estimation of social species. PLoS One 14.

Hoppitt, W.J.E., Farine, D.R., 2018. Association indices for quantifying social relationships: how to deal with missing observations of individuals or groups. Anim. Behav. 136, 227–238. https://doi.org/10.1016/j.anbehav.2017.08.029.

Klaich, M.J., Kinas, P.G., Pedraza, S.N., Coscarella, M.A., Crespo, E.A., 2011. Estimating dyad association probability under imperfect and heterogeneous detection. Ecol. Modell. 222, 2642–2650. https://doi.org/10.1016/j.ecolmodel.2011.03.027.

Krause, J., Ruxton, G.D., 2002. Living in Groups. Oxford University Press, Oxford, UK.

Krause, J., Croft, D.P., James, R., 2007. Social network theory in the behavioural sciences: potential applications. Behav. Ecol. Sociobiol. 62, 15–27. https://doi.org/10.1007/s00265-007-0445-8.

Lagrange, P., Pradel, R., B??lisle, M., Gimenez, O., 2014. Estimating dispersal among numerous sites using capture-recapture data. Ecology 95, 2316–2323.

Lebreton, J.-D., Nichols, J.D., Barker, R.J., Pradel, R., Spendelow, J.A., 2009. Modeling individual animal histories with multistate capture-recapture models. Adv. Ecol. Res. 41, 87–173. https://doi.org/10.1016/S0065-2504(09)00403-6.

Lusseau, D., Whitehead, H., Gero, S., 2008. Incorporating uncertainty into the study of animal social networks. Anim. Behav. 75, 1809–1815. https://doi.org/10.1016/j.anbehav.2007.10.029.

Marescot, L., Benhaiem, S., Gimenez, O., Hofer, H., Lebreton, J.-D., Olarte-Castillo, X.A., Kramer-Schadt, S., East, M.L., 2018. Social status mediates the fitness costs of infection with canine distemper virus in Serengeti spotted hyenas. Funct. Ecol. 32, 1237–1250. https://doi.org/10.1111/1365-2435.13059.

Pradel, R., 2005. Multievent: an extension of multistate capture-recapture models to uncertain states. Biometrics 61, 442–447. https://doi.org/10.1111/j.1541-0420.2005.00318.x.

Santostasi, N.L., Bonizzoni, S., Bearzi, G., Eddy, L., Gimenez, O., 2016. A robust design capture-recapture analysis of abundance, survival and temporary emigration of three odontocete species in the gulf of Corinth, Greece. PLoS One 11, e0166650. https://doi.org/10.1371/journal.pone.0166650. https://doi.org/10.1371/journal.pone.0166650.

Sih, A., Hanser, S.F., McHugh, K.A., 2009. Social network theory: new insights and issues for behavioral ecologists. Behav. Ecol. Sociobiol. 63, 975–988. https://doi.org/10.1007/s00265-009-0725-6.

Tavecchia, G., Pradel, R., Boy, V., Johnson, A.R., Zilly, F.C., 2001. Sex- and age-related variation in survival and cost of first reproduction in Greater Flamingos. Ecology 82, 165–174.

Van Duijn, M.A.J., Snijders, T.A.B., Zijlstra, B.J.H., 2004. p2: a random effects model with covariates for directed graphs. Stat. Neerl. 234–254.

Watts, D.J., Strogatz, S.H., 1998. Collective dynamics of 'small-world' networks. Nature 393, 3.

Weko, C.W., 2018. Isolating bias in association indices. Anim. Behav. 139, 147–159. https://doi.org/10.1016/j.anbehav.2018.03.011.

Wey, T., Blumstein, D.T., Shen, W., Jordán, F., 2008. Social network analysis of animal behaviour: a promising tool for the study of sociality. Anim. Behav. 75, 333–344. https://doi.org/10.1016/j.anbehav.2007.06.020.

Whitehead, H., 2008. Analyzing Animal Societies: Quantitative Methods for Vertebrate Social Analysis. University of Chicago Press.

Whitehead, H., Dufault, S., 1999. Techniques for analyzing vertebrate social structure using identified individuals: review and recommendations. Advances in the Study of Behavior. Elsevier, pp. 33–74. https://doi.org/10.1016/S0065-3454(08)60215-6.

Chapter 5: Discussion

Le comportement des individus est lié à leur survie et constitue une composante essentielle à la compréhension de la persistance des espèces. L'on s'intéresse entre autres à savoir si un individu peut survivre jusqu'à assurer la survie de ses descendants, quelle est son espérance de vie et comment les caractéristiques de socialité mesurées à l'échelle individuelle impactent les populations. En effet, l'individu est lié à la population dont il fait partie au travers de son cycle de vie (Caswell 2001). Souvent, le cycle de vie d'un individu est structuré par l'âge, mais l'âge ne détermine pas complètement le devenir d'une population, et d'autres facteurs comme la socialité y contribuent. Dans cette thèse, nous avons présenté trois modèles démographiques pour trois espèces sociales, en utilisant des données de capture-recapture, avec pour objectif de quantifier les caractéristiques sociales de ces espèces.

Dans le premier chapitre, nous avons combiné un modèle de capture-recapture spatialement explicite et une méthode de partitionnement pour estimer le nombre et la taille des meutes. Il y a peu de travaux dans la littérature qui se sont intéressés au problème (Caniglia et al. 2014 ; López-Bao et al. 2018; Mattioli et al. 2018). Notre approche permet, à partir des estimations de centres d'activité individuels, d'extraire l'information contenue dans les données de capture-recapture sur certaines composantes de la structure sociale des loups, y compris les tailles et emplacements probables des groupes. Cette information pourrait être utile pour déterminer les caractéristiques structurelles qui incitent les groupes à se déplacer, les individus à se disperser ou ce qui fait que les groupes disparaissent. Les modèles de capture-recapture spatialement explicites permettent de lier le type et l'amplitude des espaces que certains groupes occupent en fonction des membres qui composent ces groupes, leurs schémas de déplacement, les types d'habitats requis et leur succès et patrons de dispersion (Royle et al. 2017). Par conséquent, au travers de notre méthodologie, on pourrait aussi considérer l'hétérogénéité dans la détection (Pledger et al. 2003, Pledger et al. 2010, Royle 2008) en fonction de changements potentiels des états sociaux pendant le cycle de vie des individus (subordonné ou dominant par exemple) ce qui pourrait nous aider à mieux comprendre la dynamique de ces populations.

Dans notre deuxième chapitre, on développe un modèle intégré de population, en combinant des données de capture-recapture de femelles reproductrices d'éléphants de mer avec des données de comptage des petits, pour expliquer les variations temporelles dans les effectifs de petits. On estime aussi les probabilités de survie selon les états de cycle de vie et les probabilités de transition entre les états reproductifs. Nous montrons comment incorporer la structure sociale (sex-ratio) dans un modèle intégré, et comment la combinaison de données permet d'estimer des paramètres autrement non estimables (Ferrari et al. 2009). Notre approche généralise le travail de Ferrari et al. (2009) en proposant la modélisation intégrée et celui de Tenan et al. (2016) en permettant de tester formellement l'influence de la structure sociale sur la dynamique de la population. Une extension possible de notre approche consiste à intégrer explicitement les mâles, car pour certaines populations, leur comportement agressif via la compétition pour le territoire et les événements d'accouplement affecte la fécondité des femelles (Kvarnemo & Ahnesjö 1996). Techniquement, cela consisterait à incorporer des proportions de chaque sexe (Ferrari et al. 2009; Gerber et al.

2010) ou de considérer des matrices de projection de population à deux sexes (Gonzalez-Suarez & Gerber 2008, Gonzalez-Suarez 2014). Ces développements permettraient de déterminer l'impact des mâles sur la dynamique de la population.

Dans le troisième chapitre, nous proposons une nouvelle approche pour quantifier les réseaux sociaux grâce à des données de capture-recapture et l'illustrons sur une population de dauphins. Notre modèle d'inférence peut être facilement appliqué à d'autres espèces pour peu que l'on dispose des bases de données de capture-recapture et d'association des individus. L'approche permet d'améliorer notre connaissance des structures et dynamiques sociales, et du temps que les individus investissent dans ces relations sociales. Les relations possibles entre la structure sociale et la démographie des espèces ont été peu étudiées, les animaux marins ne faisant pas exception.

Dans les groupes sociaux d'épaulards, le rôle de certains individus dans les réseaux a été étudié (Wiliams & Lusseau 2006) et il a été constaté que, pour la même espèce, de fortes associations sont corrélées positivement à la survie apparente : les individus en groupes perturbés par plusieurs événements de mortalité ont des associations plus faibles avec une diminution conséquente des performances individuelles (Busson et al. 2018). Des réseaux sociaux ont également été développés pour étudier les comportements d'association des hyènes tachetées entre parents et non parents en liant ces comportements à la disponibilité des ressources (Holekamp et al. 2011), ou encore pour étudier la dynamique de contagion des agents pathogènes chez les macaques (Lehmann et al. 2016). Notre approche permet d'aborder ces questions en conditions naturelles en prenant en compte le défaut de détection. Une possibilité d'extension de l'approche consisterait à différentier les raisons de l'agrégation des individus; en effet, le ré-seau social peut changer de caractéristiques si l'on considère le fait que les individus sont en activité d'alimentation, de jeu, d'accouplement, etc.

L'inclusion du statut social a été récemment incorporé dans les analyses de viabilité des populations. Par exemple, Marescot et al. (2016) et Benhaiem et al. (2018) ont étudié les effets de la structure sociale sur l'épidémie de la maladie de Carré dans une population de hyènes tachetées en discrétisant les états sociaux. Une piste de recherche serait d'inclure le réseau social directement dans l'analyse de viabilité.

En conclusion, la méthodologie développée dans cette thèse repose sur l'analyse de trois modèles de population, chacun incluant différents aspects de la structure sociale des espèces, à savoir le domaine vital, le cycle de vie individuel et les associations dyadiques. L'originalité du travail consiste à avoir combiné plusieurs types de modèles pour analyser des bases de données imparfaites, avec l'objectif de prendre en compte tous les individus, y compris ceux qui ne peuvent pas être observés de manière exhaustive. Nous espérons que ces développements encourageront l'étude de la démographie des espèces sociales dans leur milieu naturel.

References

[1] Apollonio M, Mattioli L, Scandura M, Mauri L, Gazzola A, Avanzinelli E. 2004. Wolves in the Casentinesi Forests: insights for wolf conservation in Italy from a protected area with a rich wild prey community. Biol Conserv 120:249–260

[2] Benhaiem S. Marescot, L. East m., Kramer-Schadt, S, Gimenez O., Lebreton J-D., and Hofer Heribert. 2018. Slow recovery from a disease epidemic in the spotted hyena, a keystone social carnivore. Communications biology. 1:201

[3] Buckland, S.T., Newman, K.B., Thomas, L., Koesters, N.B. 2004. State-space models for the dynamics of wild animal populations. Ecological Modelling 171:157–175.

[4] Busson, M., Authier, M., Barbraud, C., Tixier, P., Reisinger, R., Janc, A., et Guinet C. 2019. Role of sociality in the response of killer whales to an additive mortality event. PNAS. 116(24): 11812-11817.

[5] Caniglia R., Fabbri E., Cubaynes S., Gimenez O., Lebreton J.D., Randi E. 2012. An improved procedure to estimate wolf abundance using non-invasive genetic sampling and capture–recapture mixture models. Conservation Genetics. 13(1):53-64.

[6] Caniglia, R., Fabbri, E., Galaverni, M., Milanesi, P., and Randi, E. 2014. Noninvasive sampling and genetic variability, pack structure, and dynamics in an expanding wolf population. J. Mamm. 95(1): 41-59.

[7] Caro, T. 1998. Behavioral Ecology and conservation. Oxford University Press.

[8] Daneri, G., R. Carlini. A and Rodhouse, P. 2000. Cephalopod diet of the southern elephant seal, Mirounga leonina, at King George Island, South Shetland Islands. Antarctic Science. 12(1):16-19.

[9] Daneri, G. and Carlini, A. 2002. Fish prey of southern elephant seals, Mirounga leonina, at King George Island. Polar Biol 25(10):739–743.

[10] Ferrari M., Lewis M., Pascual M., and Campagna C. 2009. Interdependence of social structure and demography in the southern elephant seal colony of Península Valdés, Argentina. Marine mammal science. 25(3): 681–692.

[11] Gerber L., González-Suárez M., Hernandez- C. and Young J., Sabo J. 2010. The cost of male aggression and polygyny in California Sea Lions (Zalophus californianus). Plos One. 5(8):1-8.

[12] Gonzalez-Suarez M. 2014. ¿Es relevante la ecología del comportamiento para entender y predecir la dinámica de las poblaciones? Ecosistemas. 23(4):93-97.

[13] Gerber, L. 2006. Including behavioral data in demographic models improves estimates of population viability. Front Ecol Environ. 4(8): 419-427.

[14] Gimenez, O., Lebreton, J-D., Gaillard, J-M., Choquet, R., and Pradel, R. 2012. Estimating demographic parameters using hidden process dynamic models. Theoretical Population Biology. 82:307–316.

[15] Goodall, R.N.P., Galeazzi, A.R., Leatherwood, S., Miller, K.W., Cameron, I.S., Kastelein, R., and Sobral, A.P. 1988. Studies of Commerson's dolphins, Cephalorhynchus commersonii, off Tierra del Fuego, 1976-1984, with a review of information on the species in the South Atlantic. Biology of the Genus Cephalorhynchus. 9: 3-70.

[16] González-Suárez, M., and Gerber, L. 2008. A Behaviorally Explicit Demographic Model Integrating Habitat Selection and Population Dynamics in California Sea Lions. Conservation Biology 22(6):1608-18.

[17] González-Suárez, M. 2014. ¿Es relevante la ecología del comportamiento para entender y predecir la dinámica de las poblaciones? Ecosistemas. 23(4):93-97.

[18] Hindell. M. A., Bradshaw. C. J. A., Sumner. M.D., Kelvin. J.M., and Burton. H.R. 2003. Dispersal of female southern elephant seals and their prey consumption during the austral summer: relevance to management and oceanographic zones. Journal of Applied Ecology. 40: 703–715.

[19] Holekamp K., Smith J., Strelioff C, Van Horn R., and Watts H. 2011. Society, demography and genetic structure in the spotted hyena. Molecular Ecology. 1-20.

[20] Iñíguez, M.A. and Tossenberger. V.P. 2010. Commerson's Dolphins (Cephalorhynchus commersonii) off Ría Deseado, Patagonia, Argentina. Aquatic Mammals Journal. 33(3): 276-285.

[21] Kappeler, P., and van Schaik, C. 2002. Evolution of Primate Social systems. International Journal of Primatology. 23(4):707-740.

[22] Kruschke, J. 2010. Doing Bayesian Data Analysis: A Introduction with R and BUGS. Academic Press.

[23] Kvarnemo C. and Ahnesjö I. 1996. The dynamics of operational sex ratios and competition for mates. Tree. 11(10):404-408.

[24] Laws, R.M. 1953. The Elephant Seal (Mirounga leonina, Linn.): I. Growth and age. London, HMSO, 62pp. (Falkland Islands Dependencies Survey Scientific Reports, 8).

[25] Laws R.M. 1994. History and present status of elephant seal populations. In: Elephant seals: population ecology, behavior, and physiology, Le Boeuf BJ, Laws RM (eds), pp. 49-65, University of California Press, Berkeley. USA.

[26] Le Boeuf, B.J., and Laws, R.M. 1994. Elephant seals:an introduction to the genus. In lE boeuf, B.J. and R.M. Laws (Eds.) Elephant seals: population ecology, behavior, and physiology. pp. 1-26, University of California Press, Berkeley, USA.

[27] Lee, P.M. 2012. Bayesian statistics an introduction. Wiley and Sons, Ltd. Fourth edition. Pp: 462.

[28] Lehmann, J., Majolo, B., and Mcfarland, R. 2016. The effects of social network posi-tion on the survival of wild Barbary macaques, Macaca sylvanus. Behavioral Ecology, 27 (1): 20-28.

[29] López-Bao J.v., Godinho R., Pacheco C., Lema F. J., García E., Llaneza L., Palacios V. and Jiménez J. 2018. Toward reliable population estimates of wolves by combining spatial capture-recapture models and non-invasive DNA monitoring. Scientific Reports.8: 2177.

[30] Marescot, L., Benhaiem, S., Gimenez O., Hofer, H., Lebreton, J-D., Olarte-Castillo, X., Kramer-Schadt, S., East, M. 2018. Social status mediates the fitness costs of infection with canine distemper virus in Serengeti spotted hyenas. Functional Ecolog. 32(5):1237-1250.

[31] Mattioli L, Canu A, Passilongo D, Scandura M, and Apollonio M. 2018. Estimation of pack density in grey wolf (Canis lupus) by applying spatially explicit capture-recapture models to camera trap data supported by genetic monitoring. Frontiers in Zoology.15:38.

[32] Mech, L.D. 1999. Alpha status, dominance, and division of labor in wolf packs. Can. J. Zool. 77:1196-1203.

[33] Mech, L.D., et Boitani, L. 2003. Wolves: behavior, ecology, and conservation. University of Chicago Press. Pp. 472.

[34] Oosthuizen C., Postma M., Altwegg R., Nevoux M., Pradel R., Bester M., de Bruyn P.J.N. 2019. Individual heterogeneity in life-history trade-offs with age at first reproduction in capital breeding elephant seals. Population Ecology. 1-15.

[35] Oosthuizen, C. W., Pradel, R., Bester, M., and de Bruyn, P.J.N. 2019. Making use of multi- ple surveys: Estimating breeding probability using a multievent-robust design capture–recapture model. Ecology and Evolution, 9(2):836-848.

[36] Pistorius, P.A., de Bruyn, P. and Bester M.N. 2011. Population dynamics of southern elephant seals: a synthesis of three decades of demographic research at Marion Island. African Journal of Marine Science 33:523–534.

[37] Pledger S, Pollock K, Norris J. 2003. Open Capture-Recapture Models with Heterogeneity: I. Cormack-Jolly-Seber Model. Biometrics. 59(4):786-794.

[38] Pledger, S., Pollock, K.H. and Norris, J.L. 2010. Open Capture–Recapture Models with Heterogeneity: II. Jolly–Seber Model. Biometrics 66, 883–890.

[39] Sutherland, W. 1998. The importance of behavioural studies in conservation biology. Animal Behaviour. 56:801-809.

[40] Rabiner, L.R. 1989. A tutorial on Hidden Markov Models and Selected Applications in Speech Recognition. Proceedings of the IEE, 77(2):257-286.

[41] Royle J.A., Kuller A, and Sutherland C. 2017. Unifying population and lanscape ecology with spatial capture-recapture. Ecography 40:1-12.

[42] Royle, J.A. 2008. Modeling Individual Effects in the Cormack–Jolly–Seber Model: A State–Space Formulation. Biometrics 64, 364–370.

[43] UICN. Page WEB: https://www.iucnredlist.org/species (visité: 22/08/2019).

[44] Tenan S., Iemma A., Bragalanti N., Pedrini P, De Barba M., Randi E., Groff C. and Genovart. 2016. Evaluating mortality rates with a novel integrated framework for nonmonogamous species. Conservation Biology, 30(6):1307-1319.

[45] Vucetich, J., Peterson, R., and Waite, T. 1997. Effects of social structure and prey dynamics on extinction risk in gray wolves. Conservation Biology. 11(4): 957-965.

[46] Wilson, E. O. 1998. Sociobiology: the new synthesis. Cambridge, MA: Belknap Press. 8° edition. Schaub, M. and F. Abadi. 2011. Integrated population models: a novel analysis framework for deeper insights into population dynamics. J Ornithol. 152(1):S227-S237.

[47] Wiliams R., and Lusseau D. 2006. A killer whale social network is vulnerable to targeted remov-als. Biol. Lett. 2(4):497–500.

[48] Withehead, H. 2008. Analyzing Animal Societies, Quantitative Methods for Vertebrate Social Analysis. The University of Chicago Press.

[49] Zeigler, S. and Walters, J. 2014. Population models for social species: lessons learned from models of Red-cockaded Woodpeckers (*Picoides borealis*). Ecological Applications. 24(8): 2144-2154.

Annexe A: A propos du Chapitre 2

```
#.....................................................................#
# Estimating the number of packs in wolf populations using spatially-
# explicit capture-recapture models and clustering methods
# (Section: Analyses wolf data set)
# Authors: Gimenez O., Mansilla L. & Pradel R.
# Date last modification: August 2019.
# Objective: Identify individuals' activity centers, number of
# individuals and packs in a population sample of Italian wolves.
#.....................................................................#

# GENERAL CONSTANTS:
radius95=17000    # home range diameter (from Caniglia et al. J
                  # Mammalogy 2014)
cs <- c(13000, 13000) # spacing of traps in both direction
scale_par=10000   # scaling applied to coordinates in SCR model for
                  # numerical reasons
J=30              # A constant in the SCR model
Madd=100          # number of empty CH added to observed CH (data
                  # augmentation)
h_wolf = 40000    # cutting point used to identify clusters (i.e.
                  # packs)
# derived constants:
sigma=17000/sqrt(qchisq(.95,2))
# end general constants

# load packages
#install.packages("remotes")
#remotes::install_github("mikemeredith/makeJAGSmask")
library(makeJAGSmask)
library(scrbook)
library(rgdal)
library(rgeos)
library(maptools)
library(lattice)
library(cluster)
library(Rcapture)
library(rjags)
library(fpc)
library(mixtools)
library(stringi)
library(lubridate)
library(tidyverse)
library(raster)
library(ggplot2)

#.....................................................................#
# BASE DATA.
# Transformation to spatial points and creation of trap grid
#.....................................................................#
#setwd("C:/DATA/students/LORENA MANSILLA/loups")
italian <- read.csv("wolves_fd_lm.csv", sep=",", dec=".")
italian <- italian %>%  # the pipe command comes with package dplyr
                        #(imported from magrittr)
  mutate(fecha2 = dmy(fecha)) %>%  # convert fecha to day-month-year format
                        # for further manipulation
  filter(fecha2 >= as.Date('2006-10-01'),
         fecha2 <= as.Date('2007-03-31')) # filter data to keep only
                        # data from oct 2006 to mar 2007
italian$X_ID <- droplevels(italian$X_ID) # only observed individual tags
                        # are retained
```

```
italian$month <- factor(italian$month,levels =
c('10','11','12','1','2','3'),ordered = T) # month as ordered factor
                        # create a grid that bounds the study area
xy <- cbind(italian$EST_UTM32WGS84,italian$NORD_UTM32WGS84)
S <- SpatialPoints(xy, proj4string = CRS("+init=epsg:27572"))
# http://forums.cirad.fr/logiciel-R/viewtopic.php?t=3049
bb <- bbox(S)# contains min and max latitudes and longitudes of
# observations
# maximum numbers of territories contained in the range of
# latitudinal and longitudinal observations respectively
ratiorangeterritory <- (bb[,2]-bb[,1])/cs
# max numbers of territories rounded up
cd <- ceiling(ratiorangeterritory)
# the shift below is to better center the grid with respect to
# observations
shift <- (cd-ratiorangeterritory)*cs/2
# the grid for traps an individual may move outside of this grid but adding
# 1 to cd ensures that its center of activity cannot be outside i.e. a
# buffer zone is added
grd <- GridTopology(cellcentre.offset=bb[,1]-shift, cellsize=cs,
cells.dim=cd+1)
sg_study_area <- SpatialGrid(grd)
# convert the grid into a polygon
polys <- as.SpatialPolygons.GridTopology(grd)
proj4string(polys) <- CRS("+init=epsg:27572")
# get center of grid pixels (i.e. the coordinates of our fake traps)
centers = coordinates(polys)
# for each detection, get associated trap (the closest one)
trap_of_det <- over(S,polys)
#.....................................................................#
#.............................. SOME FIGURES.........................#
#.....................................................................#
# plots location of traps (red points) and observations on same
# figure
# 1. observations labeled by name (a number) of activated trap
par(mfrow=c(1,2))
plot(centers, col="red", pch="", cex=0.7, xlab='Easting',ylab='Northing',
main = 'Activated traps')
text(centers, label=row.names(centers), col="red", cex = 0.5, adj =
c(0.5,0.5))
text(coordinates(S), label=trap_of_det, cex=0.45, adj=c(0.5,0.5))
# 2. observations labeled by name (a number) of detected individual
plot(centers, col="red", pch="", cex=0.7, xlab='Easting', ylab='Northing',
main = 'Detected individuals')
text(centers, label=row.names(centers),col="red",cex=0.5,adj=c(0.5,0.5))
text(coordinates(S),label=as.numeric(italian$X_ID),cex=0.45,adj=c(0.5,0.5))
#.....................................................................#
#.......................HISTORIES OF ENCOUNTERS .....................#
#.....................................................................#
# Create capture histories for standard CR model
CHmakeup <- list(individual = levels(italian$X_ID),occasion =
levels(italian$month))
CHmatrix <- matrix(0,nrow = length(CHmakeup[[1]]),ncol =
length(CHmakeup[[2]]),dimnames = CHmakeup)
for (i in 1:dim(italian)[1]) {CHmatrix[italian$X_ID[i],italian$month[i]] <-
1}
#.....................................................................#
# ..................... MATRIX OF CAPTURES BY TRAPS.....................#
#.....................................................................#
# Create capture locations for spatially-explicit model
SCRmakeup <- list(individual = levels(italian$X_ID),trap = 1:length(polys))
```

```
SCRmatrix <- matrix(0,nrow = length(SCRmakeup[[1]]),ncol =
length(polys),dimnames = SCRmakeup)
for (i in 1:dim(italian)[1]) {SCRmatrix[italian$X_ID[i],trap_of_det[i]] <-
SCRmatrix[italian$X_ID[i],trap_of_det[i]]+1}
#.....................................................................#
#.....................Spatially-Explicit Model.....................#
#.....................................................................#

#.....................................................................#
#.............................. JAGS MODEL.............................#
#.....................................................................#
subs <- radius95/scale_par # scaled buffering
y <- rbind(SCRmatrix,matrix(0,Madd,dim(SCRmatrix)[2])) # data
# augmentation
Nobsd <- dim(SCRmatrix)[1] # number actually observed
M <- dim(y)[1] # total number of candidate individuals after data
# augmentation
scaled_centers <- centers/scale_par # trap positionning is scaled
# for better numerical performance
# scaled coordinates of buffer zone (i.e. where centers of activity
# are allowed)
xl <- min(scaled_centers[,1])-subs
xu <- max(scaled_centers[,1])+subs
yl <- min(scaled_centers[,2])-subs
yu <- max(scaled_centers[,2])+subs
dataless<-list(y=y,trapmat=scaled_centers,J=J,xu=xu,xl=xl,yu=yu,yl=yl)

sink("SECRmodel.txt")
cat("
data {
  dimy <- dim(y)
  dimtrapmat <- dim(trapmat)
  M <- dimy[1] # number of candidate individuals is first dimension of y
  ntrap <- dimtrapmat[1] # number of traps is first dimension of trapmat
}
model {
# priors
  sigma2 ~ dunif(0, 20) # movement parameter
  lam0 ~ dgamma(0.1,0.1)
  psi ~ dunif(0, 1) # probability of belonging to the population
# likelihood
  for (i in 1:M){
    z[i]~dbern(psi) # latent variable to indicate whether the
    # individual belongs to the population (1) or not (O)
    # activity center somewhere in buffer zone
    SX[i]~dunif(xl, xu)
    SY[i]~dunif(yl, yu)
    for(j in 1:ntrap) {
      D2[i,j] <- pow(SX[i]-trapmat[j,1], 2) + pow(SY[i]-trapmat[j,2],2)
      g[i,j] <- exp(-D2[i,j]/sigma2)
      lambda[i,j] <- J * g[i,j] * lam0 * z[i]
      y[i,j] ~ dpois(lambda[i,j])
    }
  }
# number of individuals
  N <- sum(z[])
}
",fill=TRUE)
sink()
```

```
# Parameters to estimate
params = c("lam0","sigma2","N","psi","SX","SY")

# Initial values
sigma2 = 5
psi = .6
SX = as.vector(runif(M,bb[1,1], bb[1,2])/scale_par)
SY = as.vector(runif(M,bb[2,1], bb[2,2])/scale_par)
init1 =  list(psi=psi, lam0=.2, SX=SX, SY=SY, sigma2=sigma2)
init2 =  list(psi=psi, lam0=.2, SX=SX, SY=SY, sigma2=sigma2)
inits<-list(init1,init2)

# call JAGS from R
library(jagsUI) # jagsUI is supposed to be more verbose than R2jags.

# mcmc options
ni <- 6000
na <- 1000
nc <- 2
nb <- 1000
nt <- 3

start<-as.POSIXlt(Sys.time())
out1_caniglia_6mesesless <- jagsUI::jags(data = dataless, # 9 min 19 sec to
run
           inits = inits,
           parameters.to.save = params,
           model.file = "SECRmodel.txt",
           n.chains = nc,
           n.adapt = na,
           n.iter = ni,
           n.burnin = nb,
           n.thin = nt,
           DIC = TRUE,
           parallel=TRUE,
           n.cores=2)
end <-as.POSIXlt(Sys.time())
duration = end-start
print(out1_caniglia_6mesesless)
save(out1_caniglia_6mesesless, file = 'reswolf.RData')

# numerical summaries
library(MCMCvis)
round(MCMCsummary(out1_caniglia_6mesesless,
          params = c('lam0','sigma2','N'),
          Rhat = TRUE,
          n.eff = TRUE),2)

# posterior distributions
library(ggmcmc)
mcmc_df <- as.data.frame(as.matrix(out1_caniglia_6mesesless $samples))
par_mcmc <- as.matrix(mcmc_df[,c('lam0','sigma2','N')])
par_mcmc <- as.mcmc(par_mcmc)
par <- ggs(par_mcmc)
p <- ggplot(par, aes(x = value))  +
  geom_density(aes(fill = Parameter), alpha = 0.5) +
# geom_line(aes(y = density), data = par, colour = "red") +
  facet_wrap(~ Parameter, scales='free')
ggsave('dens.jpg',dpi=600, width = 30, height = 20, units = "cm")
```

```
# retrieve activity centers for each individual and iteration
ACa<-
simplify2array(out1_caniglia_6mesesless$sims.list[c("SX","SY")])*scale_par
# an array (descaled)
ACa <- ACa[,1:Nobsd,] # retain only observed individuals
nsample <- dim(ACa)[1]

# JAGS model summary statistics from 4000 samples (thin = 3; chains = 2;
adapt+burnin = 2000):
#
#        Lower95  Median Upper95    Mean     SD Mode  MCerr MC%ofSD SSeff   AC.30   psrf
# lam0     0.092   0.118   0.150   0.119  0.015   --      0     2.9  1160   0.014      1
# sigma2   0.307   0.368   0.431    0.37  0.032   --  0.001       3  1098   0.023      1
# N          115     130     144  130.47  7.647   132  0.19     2.5  1619  -0.001      1
# psi      0.574   0.669   0.774   0.669  0.051   --  0.001     2.2  2035   0.014      1
#.....................................................................#
#          IDENTIFICATION OF PACKS, clustering by distance
# Individuals separated by > h_wolf =40000 are assumed to belong to
# distinct packs.
# The distance 40000 was determined by examining the histogram of
# distances.
# It corresponds to the lower gap in the histogram.
# Clustering is done for each sample iteration separately.
# The composition of packs at each iteration is the basic information for
# studying interactions.
#.....................................................................#
# pack.composition will save the details of identified packs at each
# iteration
pack.composition <- vector("list", nsample)
# matrix of interactions between pairs to be filled in (interaction
# = same group membership)
interact <- matrix(0, nrow = Nobsd, ncol = Nobsd)
for (i in 1:nsample){   # loop over MCMC samples
  clust <- hclust(dist(ACa[i,,])^2 , method = "ward.D") # clustering
            # for current sample
  contar<- cutree(clust,h = (h_wolf)^2) # application of cutting
            # distance
  current_nb_cluster <- length(unique(contar)) # nb of packs
            #identified in current MCMC sample
  individuos.clus<- lapply(1:current_nb_cluster,function(eso)
                        which(contar==eso)) # packs composition
  # interaction matrix incremented according to current packs
  # composition
  for (cl in 1:current_nb_cluster) {
    interact[individuos.clus[[cl]],individuos.clus[[cl]]] <-
    interact[individuos.clus[[cl]],individuos.clus[[cl]]]+1
  }
  pack.composition[[i]] <- individuos.clus ## current pack
  # composition saved
}
# proportion of times each pair has been assigned to same pack over
# samples
interact <- interact/nsample

# estimated number of packs
pack.number <- as.numeric(lapply(pack.composition,length))
mean(pack.number) # 11.20, min=8, max=14
sd(pack.number) # 0.98
hist(pack.number)
table(pack.number)
```

```
# pack.number
# 8    9   10   11   12   13   14
# 4  104  647 1371  920  249   37

pn <- enframe(pack.number)
ggplot(pn, aes(x = value)) + geom_histogram() + scale_color_grey() +
scale_fill_grey() + labs(title="",x="Number of packs", y="Density") +
theme_classic()ggsave('histpacks.jpg',dpi=600)
# list of pack sizes per iteration (note: the biggest pack over the # whole
sample has 27 individuals)
pack.size <- lapply(pack.composition, function(cluster)
as.numeric(lapply(cluster,length)))
# mean pack size per iteration
mean.pack.size <- as.numeric(lapply(pack.size,mean)) # ranges from
# 6.71 to 11.75
mean(mean.pack.size) # 8.46
sd(mean.pack.size) # 0.75

library(reshape2)
library(igraph)

# matrix of frequencies of dyads
freq_matrix <- interact
freq_matrix[upper.tri(freq_matrix)] <- prod(dim(freq_matrix))
freq_df <- melt(freq_matrix)
# filter out the upper matrix values
freq_df <- filter(freq_df, value != nrow(freq_df)) %>% filter(Var1 != Var2)
hist(freq_df$value)

# create adjacency list with frequences > 0.9
adj_list <- freq_df %>% filter(value > 0.9)
names(adj_list) <- c('from', 'to', 'weight') # Frequency of dyads

dim(adj_list)

# create igraph S3 object
net <- graph.data.frame(adj_list, directed = FALSE)

# store original margins
orig_mar <- par()$mar

plot(net, layout = layout_components(net), edge.width = E(net)$weight,
vertex.size=1.5, vertex.color="blue")

# how many packs in the wolf real data
library(lubridate)
read_csv2('DB_ISPRA_23032017_filtered_Olivier.csv') %>%
select(month,Year,Pack) %>%
filter(Year %in% c(2006,2007)) %>%
mutate(date = paste0(month,'/',Year)) %>%
mutate(date = zoo::as.yearmon(date, "%m/%Y")) %>%
filter(date > 'sep 2006', date < 'avr 2007') %>%
filter(!is.na(Pack)) %>%
pull(Pack) %>%
unique()
```

```
#.....................................................................#
# Estimating the number of packs in wolf populations using spatially-
# explicit capture-recapture models and clustering methods
# (Section: Simulation)
# Authors: Mansilla L., Gimenez O., Pradel R.
# Date last modification: August 2019.
# Objective: objective: simulate populations of positions of grouped
# individuals and then generate capture-recapture samples and estimate the
# number of groups (packs).
#.....................................................................#

# Required libraries
library(MASS)
library(spatstat)
library(spatial)
library(scrbook)
library(raster)
library(rgdal)
library(rgeos)
library(maptools)
library(sp)
library(lattice)
library(cluster)
library(rjags)
library(jagsUI)
library(graphics)
library(stats)
library(Rcapture)
library(nortest)
library(SimDesign)
library(tmvtnorm)
library(mixtools)

setwd("C:/Users/mansilla/Desktop/11 groups 12092019") # Where you save the archive of results,
I use the editor of text EmEditor
sink("out_sim_11grupos_12092019.txt")

sim_CRgroups2 <- function(r){

#                     PART I : GENERATION OF POPULATIONS AND SAMPLES
#.....................................................................
# ..................................... PACKS.....................................
#.....................................................................
# We think in packs of animals in an area represented as disc.
# This disc has an center, an area and radius.
# Gived that the animals that inhabit the disc area of group are in movement,
# the center of pack are moving equally.
# We think this as Wiener process in five times, for five occasion of sampling.
#.....................................................................
# Variables for groups
#.....................................................................
# A : Rectangular area of 19,171 km^2, this correspond to area of our case real about wolves
# r : Number of groups obtained from Poisson distribution with parameters
#    of intensity 11. This r points will be used as mean of Wiener process.
# P : r values with distribution Uniform in the space
#.....................................................................
#..................... Numbers of groups and mean position of pakcs.................
#.....................................................................

# patterns points per unit area
AX <- sqrt(19171)*sqrt(1000)   # The space in exe X,
AY <- sqrt(19171)*sqrt(1000)   # The space in exe Y,
A <- AX*AY # Area of unit square, 1 unit :19171 km^2 (Caniglia et al. 2014)

#............ Number of groups
# Uniform spatial distribution of groups
plot(P <- cbind(runif(r,10200,AX+9800), runif(r,10200,AY+9800)))
row.names(P)<-paste("Group", 1:r, sep="")
label<-row.names(P)

#............ Motions of packs
K=5            # 5 occasions of sampling
dt=153.47      # dt is sigma for Brownian motion
# The Brownian for X
bmx=matrix(0,nrow=r,ncol=K)
bbmx=NULL
for(i in 1:r){
```

```
for(k in 1:K)
bmx[i,k]= cumsum((rnorm(1,P[i,1],dt))/sqrt(K))}
#The Brownian for Y
bmy=matrix(0,nrow=r,ncol=K)
bbmy=NULL
for(i in 1:r){
for(k in 1:K)
bmy[i,k]= cumsum((rnorm(1,P[i,2],dt))/sqrt(K))}
# The befores results are tabulated with the name "w"
w1<-matrix(t(bmx),ncol=1,nrow=r*K)
w2<-matrix(t(bmy),ncol=1,nrow=r*K)
w<-cbind(w1,w2)
row.names(w)<-paste("group", rep(1:r, each=K), sep="")

# Means of movements tabulated as SE
mbmx=vector(mode="numeric", length=r)
for(i in 1:length(mbmx)){ mbmx[i]<-mean(bmx[i,])}
mbmy=vector(mode="numeric", length=r)
for(i in 1:length(mbmy)){ mbmy[i]<-mean(bmy[i,])}
SE<-cbind(mbmx,mbmy)
row.names(SE)<-paste("group_", 1:r, sep="")
etiquetas<-row.names(SE)
plot(w1,w2)

name <- unique(etiquetas)     # I take the groups without repeat him
dist<-list()                  # I create one object in which I will save the distances
max <- list()                 # between position of groups
for(i in 1:length(name)){
    dist[[i]] <- dist(SE)
    max[[i]] <- max(abs(dist[[i]]))
} #i

#............ Trajectories of Pakcs
matmax <-as.matrix(max[which(max>0)])
dist_mean = mean(as.numeric(matmax[,1]))# mean distance maximum of packs
print(dist_mean)
m.dist.SE<-mean(dist(SE))
print(m.dist.SE)

#.....................................................................................
# ..........................SIMULATION OF INDIVIDUALS ..............................
#.....................................................................................
# Here I simulate the number of individuals presents in the inhabited circular areas (I will
# assume that the area is circular) as a variable with Poisson distribution of mean 9 (*)
# (average obtained from our results of the wolf data analysis)

r0=107.04      # value of path in the Wiener process, derived from individual hra 36000km^2
               # (Caniglia et al. 2014)

lambda.h = 6   # (*)
n.i <- rpois(r,lambda.h)
n.i <- n.i+3   # (*)

N.i = rep(n.i,K) #sequence of size of packs
pcor = 0       # parameter of correlation for the truncated bivariate Gaussian (**)
Sigma = matrix(c((r0**2), (pcor*r0^2), (pcor*r0^2), (r0**2)), 2,2)

i <-seq(1,nrow(w)-4,by=5); OC1<-w[i,]
i <-seq(2,nrow(w)-3,by=5); OC2<-w[i,]
i <-seq(3,nrow(w)-2,by=5); OC3<-w[i,]
i <-seq(4,nrow(w)-1,by=5); OC4<-w[i,]
i <-seq(5,nrow(w),by=5); OC5<-w[i,]
tablareor <- rbind(OC1,OC2,OC3,OC4,OC5)
matriz.mu <- cbind(tablareor[,1],tablareor[,2])
matriz.mu <- as.matrix(matriz.mu)

# (**) Here the truncated bivariate Gaussian is generated for represent the positions of
# individuals for different positions of packs in five occasions

packs <- NULL
for (i in 1:length(N.i)){
  sim = rtmvnorm(n=N.i[i], mean=as.vector(matriz.mu[i,]), sigma=Sigma, lower=matriz.mu[i,]-r0,
     upper=matriz.mu[i,]+r0)
     packs <- rbind(packs,sim)
}

IDs = rep(paste("Ind", 1:sum(n.i), sep=""),K)
```

```
oc <- c(rep(1:K,each=sum(n.i)))
midata <- data.frame(IDs,packs,oc)   # all simulated position data, it contains the variables
                                     # of names of simulated individuals coordinates of
                                     # simulated individuals and occasions of detections.
XY<-midata[,2:3]
#.............................................................
# Conversion of data frames in Spatial points and polygons
# as correspond for the generating of grid of traps
#.............................................................
S <- SpatialPoints(XY)
plot(S)
hra=74000 # hra of packs (Caniglia et al. 2014)
sigma=sqrt(hra/pi)/sqrt(qchisq(.95,2)) ; print(sigma);print(2*sigma)
radius95= sigma*sqrt(qchisq(.95,2)); print(radius95)
cs <- c(124,124) # (***)
bb <- bbox(S)
# (***) Sollmann et al. (2012) recommended trap distances be less than 2sigma.
# http://forums.cirad.fr/logiciel-R/viewtopic.php?t=3049#

bb <- bbox(S)  # contains min and max latitudes and longitudes of observations
               # maximum numbers of territories contained in the range of latitudinal and
               # longitudinal observations respectively
ratiorangeterritory <- (bb[,2]-bb[,1])/cs
# max numbers of territories rounded up
cd <- ceiling(ratiorangeterritory)
# the shift below is to better center the grid with respect to observations
shift <- (cd-ratiorangeterritory)*cs/2
# The grid for traps
# Un individual may move outside of this grid but adding 1 to cd ensures that its center of
# activity cannot be outside
# i.e. a buffer zone is added
grd <- GridTopology(cellcentre.offset=bb[,1]-shift, cellsize=cs, cells.dim=cd+1)
sg_study_area <- SpatialGrid(grd)

# convert the grid into a polygon
polys <- as.SpatialPolygons.GridTopology(grd)
class(polys)

# get center of the pixels of the grid (the coordinates of our fake traps)
centers = coordinates(polys)

#.............................................................................
#.............. PROCCES OF OBSERVATION AND GENERATION OF SAMPLE .....................
#.............................................................................
# Here a sample is generated from a probability of encounter Poisson based in the
# distance between the coordinates of simulated points and coordinates of traps (this
# follows the method in the Royle's book 2014, chapter 11).

N = sum(n.i); print(N)
J=5
lambda0 = 0.02 #basal encounter

y = array(NA,c(N,nrow(centers),J))
row.names(y) = paste("Ind", 1:N, sep="")
colnames(y) = paste("Site", 1:nrow(centers), sep="")
lambda = array(NA,dim = c(N,J,nrow(centers)))
d = NULL
XY3 <- array(data = as.matrix(XY), dim = c(N,5,2))
# RP25082019: added loop over years. XY3 used instead of XY below
for (k in 1:J) { # loop over years
  for (i in 1:N){ # RP: loop over individuals
    for(j in 1:nrow(centers)) { # RP: loop over traps
       d <-(XY3[i,k,1]-centers[j,1])^2 + (XY3[i,k,2]-centers[j,2])^2
       lambda[i,k,j] <- exp(-d/(2*sigma^2)) * lambda0 * J
       y[i,j,k] <- rpois(1,lambda[i,k,j]) # RP: this was not correct because it did not
account for the movements between occasions.
}}
} # end loop over years (k)
ydetectK <- which(y[,,1:J]!=0,1)     # Which, where and when were detected?
mean(lambda)
y2d <- apply(y,c(1,2),sum)           # I sum detections for occasions of captures
ncaps <- apply(y2d,1,sum)            # How times each individual has been captured
y <- y2d[ncaps>0,]                   # I keep the individuals detected at least once

ynom <- factor(row.names(ydetectK))
ydetectK <- data.frame(ynom,ydetectK)
```

```
midata <- cbind(as.character(midata[,1]), midata[,2:4])
ynew <- cbind(as.character(ynom),ydetectK[,2:4])
colnames(midata) <- c("IDs","X1", "X2", "oc")
colnames(ynew) <- c("IDs","nb_id", "Site_trap", "oc")
prob.det <- ifelse(paste(midata[,1], midata[,4]) %in% paste(ynew[,1], ynew[,4])==1,1,0)
midata <- cbind(midata[,1], midata[,2:4],prob.det)
submidata <- subset(midata, prob.det==1)
colnames(submidata) <- c("IDs","X1", "X2", "oc","prob.det")
# Previous section give a "Warning message". This advertence is caused because "ydetectK"
# contains repeated row, no problem with that, because some individuals are detected more than
# once, that's possible.
IDs <- submidata[,1]
XY <- submidata[,2:3]
oc <- submidata[,4]

# Convertion of data to spatial points for generate the grid of traps
S <- SpatialPoints(XY)
#.....................................................................................
# for each detection, get associated trap
trap_of_det = NULL
for (i in 1:length(S)){
  mask = over(S[i],polys)
  trap_of_det = c(trap_of_det,mask)
}
length(trap_of_det)
length(S)
#.....................................................................................
# Fix the detection data in different dataframes to create the capture histories
# and detection matrix
#.....................................................................................
data <- data.frame(
ID=IDs,
site=trap_of_det,
oc=oc)

coord <- data.frame(
Site=1:nrow(centers),
X = centers[,1],
Y = centers[,2])

site = trap_of_det
nbsites <- dim(coord)[1]

# ........ Here the structure of detection is tabulated
detections <- data.frame(IDs,site,oc)
nbocc <- length(unique(oc))
detections2 <- detections[,-c(2)]

#......... Matrix of detection histories
mat.prob.det <- ifelse(midata$prob.det==1,1,0)
# Following line triggers a warning when not all individuals are captured
hist.p1 <- matrix(mat.prob.det, nrow=length(unique(IDs)),ncol=nbocc)# hist.p1
sim.closedp <- closedp.t(hist.p1); print(sim.closedp)
#.....................................................................................
# Here the generation of sampling and start the estimation of population parameters
# is finished.
#.....................................................................................
#                     PARTE II: ESTIMATION OF POPULATION PARAMETERS
# .........Create capture histories for spatially-explicit closed model.............
detections3 <- detections # is table with columns: IDs, site, occasion.
IDs <- detections3[,1] # extract the Ids of detected individuals
traps <- coord
ntraps <- nrow(traps)
names.traps <- traps$Site
detections4 <- detections3[order(detections3[,1]),]
detections5 <- detections4[!duplicated(detections4),]

# Create matrix of individuals (rows) by traps (columns)
temp <- NULL
histoires2 <- matrix(0,nrow=length(unique(IDs)),ncol=ntraps)
compteur <- 1
for (i in unique(IDs)){
  mask = (detections3[,1]==i) # indiv courant
  mask2 = detections3[mask,2] # site where the ind is detected
  tempo <- 1:ntraps
  tempo2 <- NULL
  for (j in mask2){
```

```
    mask3 <- levels(names.traps)==j
    tempo2 <- c(tempo2,tempo[mask3])
    tempo2 <- unique(tempo2)
    rownames(histoires2) <- unique(IDs)
    colnames(histoires2) <- levels(names.traps)
    histoires2[i,j]  <- length(detections5[which(detections5[,1]==i & detections5[,2]==j),3])
  }
  compteur <- compteur + 1 }# increase the index of individual



#.....................................................................................
#.............. transformation of coordinates in SpatialPointDataFrame .............
#.....................................................................................
traps <- coord
dfr <- data.frame(x = traps$X, y = traps$Y)
spdfr <- dfr
## transformation en SpatialPointDataFrame
coordinates(spdfr) <- ~ x + y

## sistema de ccordenadas de referencia grados decimales WGS84
spdfr <- SpatialPointsDataFrame(coords = dfr, data = dfr,
    proj4string = CRS("+proj=longlat +datum=WGS84 +ellps=WGS84 +towgs84=0,0,0"))
spdfr
str(spdfr)
traps <- coordinates(spdfr)
scale_par = 1000
traps <- traps/scale_par   # Change the scale to make the computing easier
ntraps = nrow(traps)
trapmat = as.matrix(traps)

#.....................................................................................
# Then the variables that will be used in the txt file of the SCR model for JAGS are
# defined.
#.....................................................................................
subs <- (radius95*7)/scale_par
llx = (min(traps[,1])-subs)
upx = (max(traps[,1])+subs)
lly = (min(traps[,2])-subs)
upy = (max(traps[,2])+subs)

xl = llx
yl = lly
yu = upy
xu = upx

plot(traps,xlim=c(llx,upx),ylim=c(lly,upy))
rect(xl, yl, xu, yu, border = "black")
nbindobs <- nrow(hist.p1)
Madd = 50
M = Madd+nbindobs
aug = matrix(0, nrow=Madd, ncol=ntraps)
J = 5
Yarray = as.matrix(rbind(histoires2, aug))
data1 <- list(y=as.matrix(Yarray),M=M,trapmat=trapmat,J=J,ntraps=ntraps,xu=xu,
               xl=xl,yu=yu,yl=yl)
#.....................................................................................
# Model. The txt file of the SCR model for JAGS is defined.
#.....................................................................................
               sink("SCRmodel.txt")
               cat("
               model {
               # priors
               sigma2 ~ dunif(0,10)
               sigma <- sqrt(sigma2 / 2)
               lam0 ~ dgamma(0.1,0.1)
               psi ~ dunif(0, 1) # probability to belong to the population
               #Likelihood
               for (i in 1:M){
               z[i]~dbern(psi) # latent variable to indicate whether the
                               # individual belongs to the population (1) or not (O)
               SX[i]~dunif(xl, xu)
               SY[i]~dunif(yl, yu)
               for(j in 1:ntraps) {
                   D2[i,j] <- pow(pow(SX[i]-trapmat[j,1], 2) + pow(SY[i]-trapmat[j,2],2),0.5)
                   g[i,j] <- exp(-(D2[i,j]*D2[i,j])/sigma2)
                   lambda[i,j] <- J * g[i,j] * lam0 * z[i]
```

```
                    y[i,j] ~ dpois(lambda[i,j])
                    } #j
                } #i
                #Derived quantities
                N <- sum(z[1:M])
                }
                ",fill=TRUE)
                sink()

# Parameters monitored (to estimate)
params = c("lam0","sigma2","N","psi","SX","SY","z")
# Initial values
sigma2 = 5
psi = .8
SX = as.vector(runif(M,bb[1,1], bb[1,2])/scale_par)
SY = as.vector(runif(M,bb[2,1], bb[2,2])/scale_par)
z = as.vector(rbinom(M, 1, .8))
init1 =  list(psi=psi, lam0=.004, SX=SX, SY=SY, sigma2=sigma2)
init2 =  list(psi=psi, lam0=.004, SX=SX, SY=SY, sigma2=sigma2)
init1 =  list(psi=psi, lam0=.004, sigma2=sigma2)
init2 =  list(psi=psi, lam0=.004, sigma2=sigma2)
inits <- list(init1,init2)

#.....................................................................................
# call JAGS from R
#.....................................................................................
# MCMC settings
ni <- 2000
na <- 1000
nc <- 2
nb <- 1000
nt <- 1

# run jags
start <- as.POSIXlt(Sys.time())
out <- jags(data = data1,
            inits = inits,
            parameters.to.save = params,
            model.file = "SCRmodel.txt",
            n.chains = nc,
            n.adapt = na,
            n.iter = ni,
            n.burnin = nb,
            n.thin = nt)
end <- as.POSIXlt(Sys.time())
duration = end-start
#print(out, dig=2); out
#setwd("C:/Users/mansilla/Desktop/11 groups 12092019") # Where will it be saved
save(out, file="out_sim_11groups_12092019.RData")

# PART III
#.....................................................................................
#...... Estimating of centrals points of groups from estimated activity centers
#.....................................................................................
#load("out_sim_11groups_12092019.RData")
out <- rbind(out$samples[[1]],out$samples[[2]])

print(quantile(out[,1],probs=c(2.5/100,50/100,97.5/100)))# estimated lambda0
print(mean(out[,1])) # mean of lam0 estimated
print(sd(out[,1])) # sd of lam0 estimated

print(quantile(out[,2],probs=c(2.5/100,50/100,97.5/100)))# estimated sigma2
print(mean(out[,2]))# mean sigma2 estimated
print(sd(out[,2])) # sd of sigma2 estimated

print(quantile(out[,3],probs=c(2.5/100,50/100,97.5/100)))# estimated N
print(mean(out[,3]))# mean of N estimated
print(sd(out[,3])) # sd of N estimated

print(quantile(out[,4],probs=c(2.5/100,50/100,97.5/100)))# estimated psi
print(mean(out[,4]))# mean of psi estimated
print(mean(out[,4]))# sd of psi estimated

# get coordinates of activity centers
# x coord
Sx <- out[,5:(M+5-1)]
dim(Sx)
```

```
# y coord
Sy <- out[,(M+5):(2*M+5-1)]
dim(Sy)
# ind variable: z is 1 if ind belongs to the pop, 0 otherwise
z <- out[,(2*M+5):(3*M+5-1)]
dim(z)

# get rid of individuals that are not in the pop
Sx[z==0]<-NA
Sy[z==0]<-NA

# array of estimated activity centers coordinates
AC <- array(NA,c(nrow(Sx),ncol(Sx),2))
AC[,,1] <- Sx
AC[,,2] <- Sy

# list of everything
obj <- list(Sx=Sx,Sy=Sy,z=z)

# individuals that do belong to the pop
mask = which(apply(z,2,mean)==1) # I keep only the individuals with z = 1 for all iterations
mask # It have the labels of the individuals we keep here

# estimated activity centers
plot(S)
plot(sg_study_area, add=TRUE)
points(centers, col="blue", pch=19,cex=0.7)

matrix_AC = NULL
for (i in mask){
                current_AC <- AC[, i, ]
                average_AC <- apply(current_AC,2,mean)*scale_par
                matrix_AC <- rbind(matrix_AC,average_AC)
                points(average_AC[1],average_AC[2], pch=19,col='red')
                name = paste("Ind", i, sep="")
                text(average_AC[1],average_AC[2], name,cex = 0.8)
}

distance<-c(dist(matrix_AC, method="euclidean"),replace=TRUE)
print(mean(distance))
obs_75qt <- quantile(distance,probs=75/100);print(obs_75qt)

load("out_sim_11groups_12092019.RData")
# retrieve activity centers for each individual and iteration
ACa <- simplify2array(out$sims.list[c("SX","SY")])*scale_par # an array (descaled)
ACa <- ACa[,1:nrow(histoires2),] # retain only observed individuals
nsample <- dim(ACa)[1]

h_wolf=obs_75qt
## pack.composition will save the details of identified packs at each iteration
pack.composition <- vector("list", nsample)
for (i in 1:nsample){         # loop over MCMC samples
  clust <- hclust(dist(ACa[i,,])^2 , method = "ward.D") # clustering for current sample
  contar<- cutree(clust,h = (h_wolf)^2) # application of cutting distance
  current_nb_cluster <- length(unique(contar)) # nb of packs identified in current MCMC sample
  individuos.clus<- lapply(1:current_nb_cluster,function(eso) which(contar==eso)) # packs
composition
  pack.composition[[i]] <- individuos.clus ## current pack composition saved
}

# estimated number of packs
pack.number <- as.numeric(lapply(pack.composition,length))
print(mean(pack.number)); print(min(pack.number)); print(max(pack.number))#
print(sd(pack.number))
qt.pack.number <- as.numeric(quantile(pack.number,probs=c(2.5/100,50/100,97.5/100)))
print(qt.pack.number)

# list of pack sizes per iteration (note: the biggest pack over the whole sample has 27
# individuals)
pack.size <- lapply(pack.composition, function(cluster) as.numeric(lapply(cluster,length)))
# mean pack size per iteration
mean.pack.size <- as.numeric(lapply(pack.size,mean)); print(mean(mean.pack.size));
print(sd(mean.pack.size))
min.pack.size <- as.numeric(lapply(pack.size,min)); print(mean(min.pack.size))
max.pack.size <- as.numeric(lapply(pack.size,max)); print(mean(max.pack.size))
grupos_kmean <- kmeans(current_AC, mean(pack.number)); print(grupos_kmean)
```

```
#positions of packs
contar_kmean <- grupos_kmean$cluster; print(contar_kmean)
print(table(contar_kmean))# sizes of groups
print(mean(dist(grupos_kmean$centers, method="euclidean")))# mean distance of estimated packs
return(mean(pack.number))
}

set.seed(50)
nb_sim=100
r <- rpois(nb_sim,11)
allres<-matrix(NA, nrow=nb_sim, ncol=2)
colnames(allres)=c('r','mean.pack.number')
allres[,1] <- r
for(i in 51:length(allres[,1])){
allres[i,2]=sim_CRgroups2(allres[i,1])
}
allres
save.image(file = "out_end_sim_11groups_12092019.RData")
```

Annexe B: A propos du Chapitre 3

```
#.....................................................................
# Count model for elephant seals in R
# October 2018
# Authors: Gimenez O., Oosthuizen C., Pradel R., Mansilla L.
#.....................................................................
set.seed(8888)

# Read in Marion Island data
nb_females_all <- read.table('C:/Users/mansilla/Desktop/Des elephantes de
la mer/ipm/nb_females_all_MSA.txt',header=T)
nb_pups <- read.table('C:/Users/mansilla/Desktop/Des elephantes de la
mer/ipm/nb_pups_MSA.txt',header=T)
N <- nb_pups$number_pups
# Nb of females per males
nb_females_per_males <-
nb_females_all$nb_females[nb_females_all$component=='females_per_adult_male
']
# Adult sex ratio (males per female)
adult_sexratio <- 1 / nb_females_per_males
# Harem size
harem_size <-
nb_females_all$nb_females[nb_females_all$component=='harem_size']
# R2 variable
R2 <- harem_size * adult_sexratio
# alpha = psiB_B
alpha <- 0.81
# phiPB0
phi0 <- 0.6
# birth sex ratio
bsr <- read.table('C:/Users/mansilla/Desktop/Des elephantes de la
mer/ipm/birth_sexratio_MSA.txt',header=T)
bsr <- bsr / 2
# dataset
dat <- data.frame(year = 1973:2016, N, R2, rho = mean(as.matrix(bsr)))
dat

# build the function S to minimize, see Eq 7
dev_seals <- function(theta,dat) {
# theta is the vector of parameter (q,a) with
# - q = rho * r * alpha
# - F = (1+R2^a)^(1/a)
## dat is a data.frame containing the data
# - N the number of pups
# - R2 the social structure variable that is used to calculate the
# fertility function
# - bsr birth sex ratio

# we use data from 1973 to 1977 to initialize
# we predict pop size from 1978-2016

# get parameters
t_start <- 1978
qq <- 1/(1+exp(-theta[1]))
aa <- -exp(theta[2])
sigma <- exp(theta[3])
pp <- 0.76
pi <- 0.3

dat$Npredict <- dat$N

# first year
```

```
Ft1 <- (1 + dat$R2[dat$year==(t_start)]^aa)^(1/aa)
Ft2 <- (1 + dat$R2[dat$year==(t_start-1)]^aa)^(1/aa)
# RP: modified to pi starting at 3 and 1-pi starting at 4
rho <- dat$rho[1]
dat$Npredict[dat$year==t_start] <- qq * rho * Ft1 * (pp*(1-
pi)*dat$Npredict[dat$year==(t_start-4)] +
pi*dat$Npredict[dat$year==(t_start-3)]) + pp * Ft1/Ft2 *
dat$Npredict[dat$year==(t_start-1)]
# then subsequent years
for (t in (t_start+1):2016){
      Ft1 <- (1 + dat$R2[dat$year==(t)]^aa)^(1/aa)
      Ft2 <- (1 + dat$R2[dat$year==(t-1)]^aa)^(1/aa)
      dat$Npredict[dat$year==t] <- qq * rho * Ft1 * (pp*(1-
pi)*dat$Npredict[dat$year==(t-4)] + pi*dat$Npredict[dat$year==(t-3)]) + pp
* Ft1/Ft2 * dat$Npredict[dat$year==(t-1)]
}
sum((log(dat$N[dat$year>=t_start])-
log(dat$Npredict[dat$year>=t_start]))^2)/(sigma*sigma) + 2 * log(sigma)
}

# initial values
theta_init <- c(runif(1,0,1),runif(1,-5,0),runif(1,0,1)) # qq, a, sigma
#[1]  0.5775979 -2.7058086  0.8354707

# evaluate deviance
dev_seals(theta_init,dat)
#[1] 255.7823

# minimization
tmpmin <- optim(par = theta_init, fn = dev_seals,gr = NULL, dat = dat,
hessian=TRUE, method="BFGS", control=list(trace=1, REPORT=1, maxit =
10000))

# get parameter estimates
(qq <- 1/(1+exp(-tmpmin$par[1]))) # 0.5336822
(aa <- -exp(tmpmin$par[2])) #  -2.076718
(sigma <- exp(tmpmin$par[3])) #  1.620012

# standard errors on the link scale
SE_l <- sqrt(diag(solve(tmpmin$hessian)))
# 2.2247467 3.9986898 0.5000032

# confidence intervals
plogis(c(tmpmin$par[1] - 1.96 * SE_l[1],tmpmin$par[1] + 1.96 * SE_l[1]))
# 0.01440642 0.98896336
-exp(c(tmpmin$par[2] - 1.96 * SE_l[2],tmpmin$par[2] + 1.96 * SE_l[2]))
#  -8.196419e-04 -5.261760e+03
exp(c(tmpmin$par[3] - 1.96 * SE_l[3],tmpmin$par[3] + 1.96 * SE_l[3]))
# 0.6080047 4.3164791

# deviance is
tmpmin$value # 1.964853

# AIC is
tmpmin$value + 2*3 # 7.964853

# now predict pups abundance using estimated parameters
t_start <- 1978
dat$Npredict <- dat$N
pp <- 0.76
pi <- 0.3
```

```
rho <- dat$rho[1] #0.5062727
a <- -exp(tmpmin$par[2]) # -2.076718
Ft1 <- (1 + dat$R2[dat$year==(t_start)]^a)^(1/a)
Ft2 <- (1 + dat$R2[dat$year==(t_start-1)]^a)^(1/a)
dat$Npredict[dat$year==t_start] <- qq * rho * Ft1 * (pp*(1-
pi)*dat$Npredict[dat$year==(t_start-4)] +
pi*dat$Npredict[dat$year==(t_start-3)]) + pp * Ft1/Ft2 *
dat$Npredict[dat$year==(t_start-1)]
# then subsequent years
for (t in (t_start+1):2016){
      Ft1 <- (1 + dat$R2[dat$year==(t)]^aa)^(1/aa)
      Ft2 <- (1 + dat$R2[dat$year==(t-1)]^aa)^(1/aa)
dat$Npredict[dat$year==t] <- qq * rho * Ft1 * (pp*(1-
pi)*dat$Npredict[dat$year==(t-4)] + pi*dat$Npredict[dat$year==(t-3)]) + pp
* Ft1/Ft2 * dat$Npredict[dat$year==(t-1)]
}
dat
mean(dat$Npredict)
#[1] 184.1097

# compare predictions to observed values
plot(1973:2016,dat$N,xlab='year',ylab='Number of pups',ylim=c(50,800))
points(1973:2016,dat$Npredict,col='red')
legend(1990,800,c('Counts','Predicted values'), pch = c(1,1),
col=c('black','red'))
```

```
#.....................................................................#
# Estimating the number of packs in wolf populations using spatially-
# explicit capture-recapture models and clustering methods
# (Section: Simulation)
# Authors: Mansilla L., Gimenez O., Pradel R.
# Date last modification: August 2019.
# Objective: objective: simulate populations of positions of grouped
# individuals and then generate capture-recapture samples and estimate the
# number of groups (packs).
#.....................................................................#

# Required libraries
library(MASS)
library(spatstat)
library(spatial)
library(scrbook)
library(raster)
library(rgdal)
library(rgeos)
library(maptools)
library(sp)
library(lattice)
library(cluster)
library(rjags)
library(jagsUI)
library(graphics)
library(stats)
library(Rcapture)
library(nortest)
library(SimDesign)
library(tmvtnorm)
library(mixtools)

setwd("C:/Users/mansilla/Desktop/11 groups 12092019") # Where you save the archive of results,
I use the editor of text EmEditor
sink("out_sim_11grupos_12092019.txt")

sim_CRgroups2 <- function(r){

#                     PART I : GENERATION OF POPULATIONS AND SAMPLES
#.....................................................................
# ..................................... PACKS.....................................
#.....................................................................
# We think in packs of animals in an area represented as disc.
# This disc has an center, an area and radius.
# Gived that the animals that inhabit the disc area of group are in movement,
# the center of pack are moving equally.
# We think this as Wiener process in five times, for five occasion of sampling.
#.....................................................................
# Variables for groups
#.....................................................................
# A : Rectangular area of 19,171 km^2, this correspond to area of our case real about wolves
# r : Number of groups obtained from Poisson distribution with parameters
#    of intensity 11. This r points will be used as mean of Wiener process.
# P : r values with distribution Uniform in the space
#.....................................................................
#..................... Numbers of groups and mean position of pakcs.................
#.....................................................................

# patterns points per unit area
AX <- sqrt(19171)*sqrt(1000)   # The space in exe X,
AY <- sqrt(19171)*sqrt(1000)   # The space in exe Y,
A <- AX*AY # Area of unit square, 1 unit :19171 km^2 (Caniglia et al. 2014)

#............ Number of groups
# Uniform spatial distribution of groups
plot(P <- cbind(runif(r,10200,AX+9800), runif(r,10200,AY+9800)))
row.names(P)<-paste("Group", 1:r, sep="")
label<-row.names(P)

#............ Motions of packs
K=5            # 5 occasions of sampling
dt=153.47      # dt is sigma for Brownian motion
# The Brownian for X
bmx=matrix(0,nrow=r,ncol=K)
bbmx=NULL
for(i in 1:r){
```

```
for(k in 1:K)
bmx[i,k]= cumsum((rnorm(1,P[i,1],dt))/sqrt(K))}
#The Brownian for Y
bmy=matrix(0,nrow=r,ncol=K)
bbmy=NULL
for(i in 1:r){
for(k in 1:K)
bmy[i,k]= cumsum((rnorm(1,P[i,2],dt))/sqrt(K))}
# The befores results are tabulated with the name "w"
w1<-matrix(t(bmx),ncol=1,nrow=r*K)
w2<-matrix(t(bmy),ncol=1,nrow=r*K)
w<-cbind(w1,w2)
row.names(w)<-paste("group", rep(1:r, each=K), sep="")

# Means of movements tabulated as SE
mbmx=vector(mode="numeric", length=r)
for(i in 1:length(mbmx)){ mbmx[i]<-mean(bmx[i,])}
mbmy=vector(mode="numeric", length=r)
for(i in 1:length(mbmy)){ mbmy[i]<-mean(bmy[i,])}
SE<-cbind(mbmx,mbmy)
row.names(SE)<-paste("group_", 1:r, sep="")
etiquetas<-row.names(SE)
plot(w1,w2)

name <- unique(etiquetas)     # I take the groups without repeat him
dist<-list()                  # I create one object in which I will save the distances
max <- list()                 # between position of groups
for(i in 1:length(name)){
    dist[[i]] <- dist(SE)
    max[[i]] <- max(abs(dist[[i]]))
} #i

#............ Trajectories of Pakcs
matmax <-as.matrix(max[which(max>0)])
dist_mean = mean(as.numeric(matmax[,1]))# mean distance maximum of packs
print(dist_mean)
m.dist.SE<-mean(dist(SE))
print(m.dist.SE)

#.....................................................................................
# ..........................SIMULATION OF INDIVIDUALS ..............................
#.....................................................................................
# Here I simulate the number of individuals presents in the inhabited circular areas (I will
# assume that the area is circular) as a variable with Poisson distribution of mean 9 (*)
# (average obtained from our results of the wolf data analysis)

r0=107.04      # value of path in the Wiener process, derived from individual hra 36000km^2
               # (Caniglia et al. 2014)

lambda.h = 6   # (*)
n.i <- rpois(r,lambda.h)
n.i <- n.i+3   # (*)

N.i = rep(n.i,K) #sequence of size of packs
pcor = 0       # parameter of correlation for the truncated bivariate Gaussian (**)
Sigma = matrix(c((r0**2), (pcor*r0^2), (pcor*r0^2), (r0**2)), 2,2)

i <-seq(1,nrow(w)-4,by=5); OC1<-w[i,]
i <-seq(2,nrow(w)-3,by=5); OC2<-w[i,]
i <-seq(3,nrow(w)-2,by=5); OC3<-w[i,]
i <-seq(4,nrow(w)-1,by=5); OC4<-w[i,]
i <-seq(5,nrow(w),by=5); OC5<-w[i,]
tablareor <- rbind(OC1,OC2,OC3,OC4,OC5)
matriz.mu <- cbind(tablareor[,1],tablareor[,2])
matriz.mu <- as.matrix(matriz.mu)

# (**) Here the truncated bivariate Gaussian is generated for represent the positions of
# individuals for different positions of packs in five occasions

packs <- NULL
for (i in 1:length(N.i)){
  sim = rtmvnorm(n=N.i[i], mean=as.vector(matriz.mu[i,]), sigma=Sigma, lower=matriz.mu[i,]-r0,
     upper=matriz.mu[i,]+r0)
     packs <- rbind(packs,sim)
}

IDs = rep(paste("Ind", 1:sum(n.i), sep=""),K)
```

```
# model integrating capture-recapture data and pup counts
# for elephant seals in R with a maximum likelihood approach
# october 2018
# Authors: Gimenez O., Oosthuizen C., Pradel R., Mansilla L.
#-------------------------------------------------------------------#
#---------- DEVIANCE OF THE INTEGRATED MODEL ----------------------#
#-------------------------------------------------------------------#
dev_integrated_model <- function(b,dat,data,eff,e,garb,nh,km1){

#----------- 1. PARAMETERS
# b[1:14] =
[phiPB0,phiPB1,phiPB2,phiPB3,phiPB4p,phi,psiPB_B2,psiPB_B3,psiPB_B4,psiB_B,
psiNB_B,p1_PB,p2_B,p1_NB]
# b[15] = a in F = (1+R2^a)^(1/a)
# b[16] = sigma observation error on counts

#----------- 2. DATA INPUTS
# dat is a data.frame containing N = number of pups, R2 = social structure.
# variable used to calculate fertility function.
# data contains the encounter histories.
# eff counts.
# e vector of dates of first captures.
# garb vector of initial states.
# km1 nb of recapture occasions (nb of capture occ - 1).
# nh nb ind.

#----------- 3. CAPTURE-RECAPTURE LIKELIHOOD
# OBSERVATIONS (+1)
# 0 : not seen
# 1 : seen outside of breeding
# 2 : seen breeding

# STATES
# PB : pre-breeder
# B : breeder
# NB : non-breeder
# D : dead

# logit link for all parameters
lb <- 1/(1+exp(-b))
phiPB0 <- lb[1]
phiPB1 <- lb[2]
phiPB2 <- lb[3]
phiPB3 <- lb[4]
phiPB4p <- lb[5]
phi <- lb[6]
psiPB_B2 <- lb[7]
psiPB_B3 <- lb[8]
psiPB_B4 <- lb[9]
psiB_B <- lb[10]
psiNB_B <- lb[11]
p1_PB <- lb[12]
p2_B <- lb[13]
p1_NB <- lb[14]

#-- prob of obs (rows) cond on states (col)

# capture
B <- matrix(c(
1-p1_PB,p1_PB,0,
1-p2_B,0,p2_B,
```

```
1-p1_NB,p1_NB,0,
1,0,0),nrow=4,ncol=3,byrow=T)
B <- t(B)

#-- first encounter

BE <- matrix(c(
0,1,0,
0,0,1,
0,1,0,
1,0,0),nrow=4,ncol=3,byrow=T)
BE <- t(BE)

#-- prob of states at t+1 given states at t

# survival
A1_age0 <- matrix(c(
phiPB0,0,0,1-phiPB0,
0,0,0,1,
0,0,0,1,
0,0,0,1),nrow=4,ncol=4,byrow=T)

A1_age1 <- matrix(c(
phiPB1,0,0,1-phiPB1,
0,0,0,1,
0,0,0,1,
0,0,0,1),nrow=4,ncol=4,byrow=T)

A1_age2 <- matrix(c(
phiPB2,0,0,1-phiPB2,
0,0,0,1,
0,0,0,1,
0,0,0,1),nrow=4,ncol=4,byrow=T)

A1_age3 <- matrix(c(
phiPB3,0,0,1-phiPB3,
0,phi,0,1-phi,
0,0,phi,1-phi,
0,0,0,1),nrow=4,ncol=4,byrow=T)

A1_age4p <- matrix(c(
phiPB4p,0,0,1-phiPB4p,
0,phi,0,1-phi,
0,0,phi,1-phi,
0,0,0,1),nrow=4,ncol=4,byrow=T)

# breeding
A2_age0 <- matrix(c(
1,0,0,0,
0,0,1,0,
0,0,1,0,
0,0,0,1),nrow=4,ncol=4,byrow=T)

A2_age1 <- matrix(c(
1,0,0,0,
0,0,1,0,
0,0,1,0,
0,0,0,1),nrow=4,ncol=4,byrow=T)

A2_age2 <- matrix(c(
1-psiPB_B2,psiPB_B2,0,0,
```

```
0,0,1,0,
0,0,1,0,
0,0,0,1),nrow=4,ncol=4,byrow=T)

A2_age3 <- matrix(c(
1-psiPB_B3,psiPB_B3,0,0,
0,psiB_B,1-psiB_B,0,
0,0,1,0,
0,0,0,1),nrow=4,ncol=4,byrow=T)

A2_age4p <- matrix(c(
1-psiPB_B4,psiPB_B4,0,0,
0,psiB_B,1-psiB_B,0,
0,psiNB_B,1-psiNB_B,0,
0,0,0,1),nrow=4,ncol=4,byrow=T)

A_age0 <- A1_age0 %*% A2_age0
A_age1 <- A1_age1 %*% A2_age1
A_age2 <- A1_age2 %*% A2_age2
A_age3 <- A1_age3 %*% A2_age3
A_age4p <- A1_age4p %*% A2_age4p

# init states
PI <- c(1,0,0,0)

# likelihood
   l <- 0
   for (i in 1:nh) # loop on ind
   {
      ei <- e[i] # date of first det
      oe <- garb[i] + 1 # init obs
      evennt <- data[,i] + 1 # add 1 to obs to avoid 0s in indexing
      ALPHA <- PI*BE[oe,]
      for (j in (ei+1):(km1+1)) # cond on first capture
      {
        if (j == (ei+1)) ALPHA <- (ALPHA %*% A_age0)*B[evennt[j],]
        if (j == (ei+2)) ALPHA <- (ALPHA %*% A_age1)*B[evennt[j],]
        if (j == (ei+3)) ALPHA <- (ALPHA %*% A_age2)*B[evennt[j],]
        if (j == (ei+4)) ALPHA <- (ALPHA %*% A_age3)*B[evennt[j],]
        if (j > (ei+4)) ALPHA <- (ALPHA %*% A_age4p)*B[evennt[j],]
     }
      l <- l + log(sum(ALPHA))*eff[i]
   }
dev_capturerecapture <- -2*l

#----------- 4. PUPS COUNTS LIKELIHOOD
# build the deviance function to minimize, see Eq 7 in Ferrari's paper
## we use data from 1973 to 1977 to initialize
# we predict pop size from 1978-2016

# get parameters
t_start <- 1978
aa <- -exp(b[15]) # a in F(t)
sigma <- exp(b[16]) # observation error
pp <- phi
rho <- dat$rho[1]
qq <- 2 * rho * phiPB0 * (phiPB1 * phiPB2) # alpha is what Ferrari calls
                  # fertility constant basically litter size, 1 in our case
dat$Npredict <- dat$N
Ft1 <- (1 + dat$R2[dat$year==(t_start)]^aa)^(1/aa)
Ft2 <- (1 + dat$R2[dat$year==(t_start-1)]^aa)^(1/aa)
```

```
dat$Npredict[dat$year==t_start] <- qq * Ft1 * (phiPB3 * (1-psiPB_B2) *
dat$Npredict[dat$year==(t_start-4)] + psiPB_B2 *
dat$Npredict[dat$year==(t_start-3)]) + pp * Ft1/Ft2 *
dat$Npredict[dat$year==(t_start-1)]
for (t in (t_start+1):2016){
      Ft1 <- (1 + dat$R2[dat$year==(t)]^aa)^(1/aa)
      Ft2 <- (1 + dat$R2[dat$year==(t-1)]^aa)^(1/aa)
      dat$Npredict[dat$year==t] <- qq * Ft1 * (phiPB3 * (1-psiPB_B2) *
dat$Npredict[dat$year==(t-4)] + psiPB_B2 * dat$Npredict[dat$year==(t-3)]) +
pp * Ft1/Ft2 * dat$Npredict[dat$year==(t-1)]
}
dev_pupcounts <- sum((log(dat$N[dat$year>=t_start])-
log(dat$Npredict[dat$year>=t_start]))^2)/(sigma*sigma) + 2 * log(sigma)
dev <- dev_capturerecapture + dev_pupcounts
dev
}

#------------------------------------------------------------------------#
#--------------- MODEL FITTING / PARAMETER ESTIMATION -------------#
#------------------------------------------------------------------------#
# read in capture-recapture data
data <- read.table('C:/Users/mansilla/Desktop/Des elephantes de la
mer/ipm/ES EHM ESURGE headed format.txt')
head(data)
data <- R2ucare::group_data(data[,1:(ncol(data)-1)],rep(1,nrow(data)))
eff <- data[,ncol(data)]
data <- data[,1:(ncol(data)-1)]
# define various quantities
nh <- dim(data)[1]
k <- dim(data)[2]
km1 <- k-1
# compute the date of first capture fc, and state at initial capture
init.state
fc <- NULL
init.state <- NULL
for (i in 1:nh){
temp <- 1:k
fc <- c(fc,min(which(data[i,]!=0)))
init.state <- c(init.state,data[i,fc[i]])
}
# transpose data
data <- t(data)

# read in pups counts data
nb_females_all <- read.table('C:/Users/mansilla/Desktop/Des elephantes de
la mer/ipm/nb_females_all_MSA.txt',header=T)
# Npups
nb_pups <- read.table('C:/Users/mansilla/Desktop/Des elephantes de la
mer/ipm/nb_pups_MSA.txt',header=T)
N <- nb_pups$number_pups
# Nb of females per males
nb_females_per_males <-
nb_females_all$nb_females[nb_females_all$component=='females_per_adult_male
']
# Adult sex ratio (males per female)
adult_sexratio <- 1 / nb_females_per_males
# Harem size
harem_size <-
nb_females_all$nb_females[nb_females_all$component=='harem_size']
# R2 variable
R2 <- harem_size * adult_sexratio
```

```
# birth sex ratio
bsr <- read.table('C:/Users/mansilla/Desktop/Des elephantes de la
mer/ipm/birth_sexratio_MSA.txt',header=T)
bsr <- bsr / 2
# altogether
dat <- data.frame(year=1973:2016,N,R2,rho=mean(as.matrix(bsr)))

# init values
binit <- c(rep(0.5,14), -1, 1.5)

# evaluate the integrated pop model deviance at the initial values, just to
check
dev_integrated_model(binit,dat,data,eff,fc,init.state,nh,km1)

# fit model
deb=Sys.time()
tmpmin <-
optim(binit,dev_integrated_model,NULL,hessian=TRUE,dat,data,eff,fc,init.sta
te,nh,km1,method="BFGS",control=list(trace=1, REPORT=1, maxit = 10000))
fin=Sys.time()
fin-deb

# get estimates and back-transform
b <- tmpmin$par

data.frame(param=c('phiPB0',
'phiPB1',
'phiPB2',
'phiPB3',
'phiPB4p',
'phi',
'psiPB_B2',
'psiPB_B3',
'psiPB_B4',
'psiB_B',
'psiNB_B',
'p1_PB',
'p2_B',
'p1_NB',
'a',
'sigma'), integrated =
c(1/(1+exp(-b[1:14])),-exp(b[15]),exp(b[16])))

#      param integrated
1    phiPB0  0.5984056
2    phiPB1  0.7647213
3    phiPB2  0.7806313
4    phiPB3  0.7910896
5   phiPB4p  0.7113818
6       phi  0.7611661
7  psiPB_B2  0.3077905
8  psiPB_B3  0.6751706
9  psiPB_B4  0.5641837
10   psiB_B  0.8181329
11  psiNB_B  0.7270977
12    p1_PB  0.7764373
13     p2_B  0.9090268
14    p1_NB  0.8731530
15        a -0.9874015
16    sigma  1.6316564
```

```
# deviance is
tmpmin$value # 43166.99

# AIC is
tmpmin$value + 2*16 # 43198.99

#-------------------------------------------------------------------#
#-------------------- PUPS COUNTS PREDICTION -----------------------#
#-------------------------------------------------------------------#

t_start <- 1978

# now predict pups abundance using estimated parameters
pp <- 1/(1+exp(-b[6]))
a <- -exp(b[15])
phiPB0 <- 1/(1+exp(-b[1]))
phiPB1 <- 1/(1+exp(-b[2]))
phiPB2 <- 1/(1+exp(-b[3]))
phiPB3 <- 1/(1+exp(-b[4]))
psiPB_B2 <- 1/(1+exp(-b[7]))

qq <- 2 * mean(as.matrix(bsr)) * phiPB0 * (phiPB1 * phiPB2)

dat$Npredict <- dat$N
Ft1 <- (1 + dat$R2[dat$year==(t_start)]^a)^(1/a)
Ft2 <- (1 + dat$R2[dat$year==(t_start-1)]^a)^(1/a)
dat$Npredict[dat$year==t_start] <- qq * Ft1 * (phiPB3 * (1-psiPB_B2) *
dat$Npredict[dat$year==(t_start-4)] + psiPB_B2 *
dat$Npredict[dat$year==(t_start-3)]) + pp * Ft1/Ft2 *
dat$Npredict[dat$year==(t_start-1)]
for (t in (t_start+1):2016){
      Ft1 <- (1 + dat$R2[dat$year==(t)]^a)^(1/a)
      Ft2 <- (1 + dat$R2[dat$year==(t-1)]^a)^(1/a)
      dat$Npredict[dat$year==t] <- qq * Ft1 * (phiPB3 * (1-psiPB_B2) *
dat$Npredict[dat$year==(t-4)] + psiPB_B2 * dat$Npredict[dat$year==(t-3)]) +
pp * Ft1/Ft2 * dat$Npredict[dat$year==(t-1)]
}
dat
Npredict_point <- dat$Npredict

# compare predictions to observed values
plot(1973:2016,dat$N,xlab='year',ylab='Number of pups',ylim=c(50,800))
points(1973:2016,dat$Npredict,col='red')
legend(1990,800,c('Counts','Predicted values'), pch = c(1,1),
col=c('black','red'))

#-------------------------------------------------------------------#
#-------------------- PUPS COUNTS PREDICTION -----------------------#
#---------------------- WITH CONF INTERVALS ------------------------#
#-------------------------------------------------------------------#

# get confidence intervals
SE_link <- sqrt(diag(solve(tmpmin$hessian)))

# generate boostrap values in conf intervals (use of beta distributions
would be more elegant)
nbboot <- 250
pseudo_p <- 1/(1+exp(-rnorm(nbboot,b[6],SE_link[6])))
pseudo_a <- - exp(rnorm(nbboot,b[15],SE_link[15]))
pseudo_phiPB0 <- 1/(1+exp(-rnorm(nbboot,b[1],SE_link[1])))
pseudo_phiPB1 <- 1/(1+exp(-rnorm(nbboot,b[2],SE_link[2])))
```

```
pseudo_phiPB2 <- 1/(1+exp(-rnorm(nbboot,b[3],SE_link[3])))
pseudo_phiPB3 <- 1/(1+exp(-rnorm(nbboot,b[4],SE_link[4])))
pseudo_psiPB2 <- 1/(1+exp(-rnorm(nbboot,b[7],SE_link[7])))

res <- NULL
for (i in 1:nbboot){
# predict pups abundance using estimated parameters
t_start <- 1978
qq <- 2 * mean(as.matrix(bsr)) * pseudo_phiPB0[i] * (pseudo_phiPB1[i] *
pseudo_phiPB2[i])
dat$Npredict <- dat$N
Ft1 <- (1 + dat$R2[dat$year==(t_start)]^pseudo_a[i])^(1/pseudo_a[i])
Ft2 <- (1 + dat$R2[dat$year==(t_start-1)]^pseudo_a[i])^(1/pseudo_a[i])
dat$Npredict[dat$year==t_start] <- qq * Ft1 * (pseudo_phiPB3[i] * (1-
pseudo_psiPB2[i]) *
dat$Npredict[dat$year==(t_start-4)] + pseudo_psiPB2[i] *
dat$Npredict[dat$year==(t_start-3)]) +
pseudo_p[i] * Ft1/Ft2 * dat$Npredict[dat$year==(t_start-1)]
for (t in (t_start+1):2016){
      Ft1 <- (1 + dat$R2[dat$year==(t)]^pseudo_a[i])^(1/pseudo_a[i])
      Ft2 <- (1 + dat$R2[dat$year==(t-1)]^pseudo_a[i])^(1/pseudo_a[i])
dat$Npredict[dat$year==t] <- qq * Ft1 * (pseudo_phiPB3[i] * (1-
pseudo_psiPB2[i]) *
dat$Npredict[dat$year==(t-4)] + pseudo_psiPB2[i] *
dat$Npredict[dat$year==(t-3)]) +
pseudo_p[i] * Ft1/Ft2 * dat$Npredict[dat$year==(t-1)]
}
res <- cbind(res,dat$Npredict)
}

dim(res)
L <- apply(res,1,quantile,probs=2.5/100) # lower bound boostrap conf
interval on Npredict
U <- apply(res,1,quantile,probs=97.5/100) # upper bound boostrap conf
interval on Npredict

# compare predictions to observed values
plotrix::plotCI(1973:2016, Npredict_point, ui=U,
li=L,col='red',ylim=c(50,500))
points(1973:2016,dat$N,xlab='year',ylab='Number of pups')
legend(1990,400,c('Counts','Predicted values'), pch = c(1,1),
col=c('black','red'))
```

```
# model integrating capture-recapture data and pup counts
# for elephant seals in R with a maximum likelihood approach
# (Fixed social structure parameter "a")
# october 2018
# Authors: Gimenez O., Oosthuizen C., Pradel R., Mansilla L.
#-------------------------------------------------------------------#
#---------- DEVIANCE OF THE INTEGRATED MODEL ----------------------#
#-------------------------------------------------------------------#
dev_integrated_model <- function(b,dat,data,eff,e,garb,nh,km1){

#----------- 1. PARAMETERS
# b[1:14] = [phiPB0,phiPB1,phiPB2,phiPB3,phiPB4p,phi,psiPB_B2,
#           psiPB_B3,psiPB_B4,psiB_B,psiNB_B,p1_PB,p2_B,p1_NB]
# b[15] = sigma observation error on counts

#----------- 2. DATA INPUTS
# dat is a data.frame containing N = number of pups, R2 = social
# structure
# variable used to calculate fertility function
# data contains the encounter histories
# eff counts
# e vector of dates of first captures
# garb vector of initial states
# km1 nb of recapture occasions (nb of capture occ - 1)
# nh nb ind


#----------- 3. CAPTURE-RECAPTURE LIKELIHOOD
# OBSERVATIONS (+1)
# 0Â : not seen
# 1Â : seen outside of breeding
# 2Â : seen breeding

# STATES
# PBÂ : pre-breeder
# BÂ : breeder
# NBÂ : non-breeder
# DÂ : dead

# logit link for all parameters
lb <- 1/(1+exp(-b))
phiPB0 <- lb[1]
phiPB1 <- lb[2]
phiPB2 <- lb[3]
phiPB3 <- lb[4]
phiPB4p <- lb[5]
phi <- lb[6]
psiPB_B2 <- lb[7]
psiPB_B3 <- lb[8]
psiPB_B4 <- lb[9]
psiB_B <- lb[10]
psiNB_B <- lb[11]
p1_PB <- lb[12]
p2_B <- lb[13]
p1_NB <- lb[14]

#-- prob of obs (rows) cond on states (col)
# capture
B <- matrix(c(
1-p1_PB,p1_PB,0,
```

```
1-p2_B,0,p2_B,
1-p1_NB,p1_NB,0,
1,0,0),nrow=4,ncol=3,byrow=T)
B <- t(B)

#-- first encounter
BE <- matrix(c(
0,1,0,
0,0,1,
0,1,0,
1,0,0),nrow=4,ncol=3,byrow=T)
BE <- t(BE)

#-- prob of states at t+1 given states at t
# survival
A1_age0 <- matrix(c(
phiPB0,0,0,1-phiPB0,
0,0,0,1,
0,0,0,1,
0,0,0,1),nrow=4,ncol=4,byrow=T)

A1_age1 <- matrix(c(
phiPB1,0,0,1-phiPB1,
0,0,0,1,
0,0,0,1,
0,0,0,1),nrow=4,ncol=4,byrow=T)

A1_age2 <- matrix(c(
phiPB2,0,0,1-phiPB2,
0,0,0,1,
0,0,0,1,
0,0,0,1),nrow=4,ncol=4,byrow=T)

A1_age3 <- matrix(c(
phiPB3,0,0,1-phiPB3,
0,phi,0,1-phi,
0,0,phi,1-phi,
0,0,0,1),nrow=4,ncol=4,byrow=T)

A1_age4p <- matrix(c(
phiPB4p,0,0,1-phiPB4p,
0,phi,0,1-phi,
0,0,phi,1-phi,
0,0,0,1),nrow=4,ncol=4,byrow=T)

# breeding
A2_age0 <- matrix(c(
1,0,0,0,
0,0,1,0,
0,0,1,0,
0,0,0,1),nrow=4,ncol=4,byrow=T)

A2_age1 <- matrix(c(
1,0,0,0,
0,0,1,0,
0,0,1,0,
0,0,0,1),nrow=4,ncol=4,byrow=T)

A2_age2 <- matrix(c(
1-psiPB_B2,psiPB_B2,0,0,
0,0,1,0,
```

Appendix: Details on the multievent capture-recapture model

I. Notation

ϕ_{a0} survival probability of newborn females
ϕ_{a1} survival probability of 1-year old females
ϕ_{a2} survival probability of 2-year old females
ϕ_{a3} survival probability of 3-year old females
ϕ_{a4} survival probability of 4-year old females
ϕ survival probability of adult females
ψ_{B2} probability of breeding in the next year for 2-year old females
ψ_{B3} probability of breeding in the next year for 3-year old females
ψ_{B4} probability of breeding in the next year for 4-year old females
ψ_B probability of a reproductive female to remain a reproductive female
ψ_{NB} probability of a non-breeding female to remain a non-breeding female
p_{PB} probability of observing a pre-breeding female outside the breeding season
p_B probability of observing a breeding female in the breeding season
p_{NB} probability of observing a non-breeding female outside of the breeding season
a Parameter that determines the strength of the influence of the social structure on the function F,
σ standard deviation of the distribution for sampling error
π is the proportion of adultes females population which breed at 3 years old
$1 - \pi$ proportion of female which are breeders at 4 years of age,
r is the recruitment rate of adult females, ρ is a constant corresponding to the mean sex ratio (proportion of females) at birth
q is a composite recruitment parameter ($q = \alpha\rho r$).
We defined four states: PB for Pre-Breeder, B for Breeder, NB for Non-Breeder and D for Dead. We also had three types of observations: 0 for not seen, 1 for seen outside of breeding and 2 for seen breeding.

II. Matrix of observations or events.

		States			
Obs		PB	B	NB	D
Not seen	0	1-p_{PB}	p_B	p_{NB}	1
Seen outside breeding	1	p_{PB}	0	p_{NB}	0
Seen breeding	2	0	p_B	0	0

Table 1: The matrix B of observations is defined given the states.

		States			
Obs		PB	B	NB	D
Not seen	0	0	0	0	1
Seen outside breeding	1	1	0	1	0
Seen breeding	2	0	1	0	0

Table 2: We fix the matrix B of probability of the first encounter.

III. Matrix of states

IIIa. Survival

	States $t=1$			
States $t=0$	PB	B	NB	D
PB	ϕ_{a0}	0	0	$1-\phi_{a0}$
B	0	0	0	1
NB	0	0	0	1
D	0	0	0	1

Table 3: Matrix of survival of individual of newborn to 1 year old.

	States $t=2$			
States $t=1$	PB	B	NB	D
PB	ϕ_{a1}	0	0	$1-\phi_{a1}$
B	0	0	0	1
NB	0	0	0	1
D	0	0	0	1

Table 4: Matrix of survival of individual of 1 to 2 years old.

	States $t=3$			
States $t=2$	PB	B	NB	D
PB	ϕ_{a2}	0	0	$1-\phi_{a2}$
B	0	0	0	1
NB	0	0	0	1
D	0	0	0	1

Table 5: Matrix of survival of individual of 2 to 3 years old.

	States $t=4$			
States $t=3$	PB	B	NB	D
PB	ϕ_{a3}	0	0	$1-\phi_{a3}$
B	0	ϕ	0	$1-\phi$
NB	0	0	ϕ	$1-\phi$
D	0	0	0	1

Table 6: Matrix of survival of individual of 3 to 4 years old.

	States $t=+4$			
States $t=4$	PB	B	NB	D
PB	ϕ_{a4}	0	0	$1-\phi_{a4}$
B	0	ϕ	0	$1-\phi$
NB	0	0	ϕ	$1-\phi$
D	0	0	0	1

Table 7: Matrix of survival of individual of 4 to more years old.